

**GENERATION OF A SPONTANEOUS HPV16 E6/E7 EXPRESSING
PRE-CLINICAL TUMOR MODEL FOR TESTING THERAPEUTIC
INTERVENTIONS**

**by
Yi-Hsin Lin**

A dissertation submitted to the Johns Hopkins University School of Medicine in
conformity with the requirements for the degree of Doctor of Philosophy

Baltimore, Maryland
December 2016

© Yi-Hsin Lin 2016
All rights reserved

ABSTRACT

Human papillomaviruses (HPV) are a group of non-enveloped DNA viruses, which are notorious for their association with multiple diseases such as genital warts, anogenital and oropharyngeal tumors, and virtually all cervical tumors. It has been known that persistent HPV infection, especially the high-risk types, are a main factor of tumorigenesis. Tumor cell implantation models were traditionally used to study HPV-associated tumor models; however, implantation models display characteristics that are quite different from the tumors that form spontaneously by the expression of HPV oncoproteins. Although a traditional transgenic mouse model does lead to the generation of spontaneous tumor, the formation of tumor is inconsistent and faces the issue of immune tolerance, in which tumor antigens are treated as self-antigens and won't be cleared by the host's immune system. The field of cancer immunotherapy is evolving and has shown great promise. Therefore, we are interested in generating HPV-associated spontaneous tumor models, which can not only recapitulate clinically relevant disease progression but can also overcome immune tolerance issues with a capability for immunotherapy. In the current thesis, I present several relevant HPV+ spontaneous tumor models. In **Chapter 2**, I describe the development of a spontaneous buccal tumor model, arising from plasmid combination including HPV16 E6/E7, NRAS^{G12V} and transposase SB100, which is capable of metastasizing and is useful for testing immunotherapies. In **Chapter 3**, in order to improve the histologic characteristics of the spontaneous tumor described in Chapter 2, I utilize keratinocyte-restricted promoter K14 to drive either HPV16 E6/E7 or transposase SB100 to generate a clinically relevant carcinoma. In

Chapter 4, I replace oncogene NRAS^{G12V} with AKT to generate a clinically relevant carcinoma.

Taken together, my thesis utilized different plasmids combinations to develop spontaneous tumor in either buccal mucosa or lower third vaginal mucosa. The buccal HPV+ models recapitulate the clinical disease progression, while the cervico-vaginal models represent the clinically-relevant squamous cell carcinoma. Although there is room to improve both of these models, they are undoubtedly very useful in future tumor microenvironment, tumor biology and immunotherapy research.

Thesis Advisor:

Mentor:

T.-C. Wu, M.D., Ph.D.

Professor of Pathology, Oncology, OBGYN, and Molecular Microbiology and Immunology, The Johns Hopkins University School of Medicine, Bloomberg School of Public Health

Director of Gynecologic Pathology, The Johns Hopkins University School of Medicine

Pathologist, The Johns Hopkins Hospital

Committee Members:

Kathleen H. Burns, M.D., Ph.D.

James Richard Eshleman, Jr, M.D., Ph.D. #

Chien-Fu Hung, Ph.D.

Richard B.S. Roden, Ph.D.

- Committee Chair

Thesis Readers:

T.-C. Wu, M.D., Ph.D.

Professor of Pathology, Oncology, OBGYN, and Molecular Microbiology and Immunology, The Johns Hopkins University School of Medicine, Bloomberg School of Public Health

Kathleen H. Burns, M.D., Ph.D.

Associate Professor of Pathology and Oncology, Johns Hopkins University School of Medicine.

ACKNOWLEDGEMENTS

As a mom with two kids, a non-native English speaker, and with no prior bench work experience, obtaining a Ph.D. degree seemed an impossible mission for me. The past few years were undoubtedly the most stressful time in my life, but I received a great deal of support from my PI, my lab members, my committee members, my program, my family, my friends and my faith.

First of all, I would like to express my deepest appreciation to my advisor, Dr. T.C. Wu, for allowing me to be a part of his wonderful lab. With his vision and understanding of the most significant issues in the field, his important questions, and his encouraging attitude, Dr. Wu provided an interactive and collaborative research environment. He is extremely kind, and always encouraged me, even when I got negative results or one of my experiments failed. He always stood by me, and provided help and support, especially when I encountered difficulty during my first two years. His dedication to science and education makes him an exceptional physician-scientist and great mentor. I also would like to thank Dr. Hung, who was present in lab every day and always available for immediate help and discussion. He not only helped me solve difficult problems, but even more importantly, he provided me the freedom to ask new questions and develop and conduct my own experiments. He is a perfectionist – creative, enthusiastic, industrious, conscientious and insightful. I am really lucky to have learned from him and sought his guidance during this difficult and exciting scientific adventure. I would also like to thank a member in my lab, Dr. Shiwen Peng. He encouraged me when I almost gave up halfway through my PhD career. He provided brilliant ideas when I was

trouble shooting, and I was never worried about asking him a stupid question. In addition, all other lab members constantly helped me during scientific discussions and created a pleasant and collaborative atmosphere to work in. Some of these lab members include Chih-Ping Mao, Liang-mei He, Ya-Chea Tsai, Yu-Min Chuang, Yu-Pin Su, Ming-chieh Yang, Feng-Woei Tsay, Zuequn Xu, Ssu-Hsueh Tseng, Jinqiu, Andrew Yang, Jessica Jeang, Raymond Soong, Lily Song, Joy Wu, and Sung-Jong Lee. Some of them already left our lab but most are still here and continue to help one another. I would also like to thank our collaborators, Dr. Richard Roden and his lab members, including Joshua Wang, Rosie Jiang, Yung-Nien Chang, and Ravi Anchoori. Each week we have lab meetings together, and I really appreciated their significant questions and informative advice. This cooperative and encouraging environment supported me throughout the years.

I would also like to express much gratitude to the members of my thesis committee, Dr. Richard Roden, Dr. Kathleen H. Burns, and Dr. James Eshelman, for taking time out of their schedules to attend thesis meetings, ask probing questions and provide invaluable input. Their suggestions and comments were thought-provoking and immensely valuable. Furthermore, I am very grateful to Dr. Kathleen H. Burns for her willingness to serve as my thesis reader and her important feedback and suggestions.

I have to thank my dearest family in Taiwan: my mom who suffers from cholangiocarcinoma but tries to maintain her health as much as possible to continuously support me mentally, my brother's and my sister's families who helped take care of my own family so that I could concentrate on my research, my mother-in-law, who stayed

with my family a few times to help out, and of course, my two little girls, who always bring me joy. Finally, I would like to dedicate all my work to my husband, Bo-Yi Sung, who is also my classmate in the Pathobiology program. It's not easy juggling a family and career, especially when both parents are graduate students and under a tremendous amount of stress. He has helped me a lot during my Ph.D. career and his enthusiasm for science, insightful suggestions, and support have kept our family together.

I am grateful to all my friends and colleagues, near and far, who supported me in my work and family life during this time. It would have been impossible to achieve this goal without their help.

I would like to thank the Government Defense Department of Taiwan and Tri-Service Hospital, who offered me a full 4-year scholarship and gave me the opportunity to study in the United States.

Lastly, I give thanks to God and my faith. When I was overwhelmed and lost my confidence, I would tell myself, "He meant to bring you here and you'll be fine." Every time I passed the statue of Christus Consolator in the Johns Hopkins Hospital, I would stop, pray and find peace under his open arms with words "COME unto ME All Ye That Are Weary And Heavy Laden And I Will Give You REST" --from Matthew 11: 28 inscribed on the platform.

TABLE OF CONTENTS

Title	i
Abstract	ii
Acknowledgements	v
Table of Contents	viii
List of Tables	x
List of Figures	xi
Chapter 1. Introduction	1
Chapter 2. Generation of a spontaneous HPV+ oral tumor model by submucosal injection of oncogenic DNA plasmids with electroporation		
a. Introduction	13
b. Materials and Methods	16
c. Results	25
d. Discussion	31
Chapter 3. Attempt to generate a clinically relevant carcinoma with keratinocyte-restricted K14 promoter		
a. Introduction	49
b. Materials and Methods	50
c. Results	53
d. Discussion	57
Chapter 4. Combining HPV16 E6/E7 and AKT induces a clinically relevant carcinoma in a cervico-vaginal tumor model		

a. Introduction	71
b. Materials and Methods	73
c. Results	75
d. Discussion	77
Chapter 5. Summary	85
References	91
Curriculum vitae	111

LIST OF TABLES

Table 1. Summary of animal papillomaviruses models	12
Table 2. Summary of HPV+ preclinical tumor models in	90

LIST OF FIGURES

Chapter 1

- Figure 1. The HPV16 genome. 11

Chapter 2

- Figure 1. Schematic of plasmids used to induce oral tumors by oncogene. 38
- Figure 2. Generation of buccal tumors in immuno-compromised mice. 39
- Figure 3. Immune competent mice suppress tumor formation. 40
- Figure 4. Generation of buccal tumors in immuno-competent mice. 41
- Figure 5. CD3 triple depletion HPV16 oral tumor model. 42
- Figure 6. Characterization of tumors arising from CD3 triple depletion
HPV16 oral tumor model. 43
- Figure 7. Characterization of tumors arising from CD3 triple depletion
HPV16 oral tumor model. 44
- Figure 8. Evaluation of DNA vaccination effect in CD3 triple depletion
spontaneous tumor model. 45
- Figure 9. Evaluation of DNA vaccination effect in CD3 triple depletion
spontaneous tumor model. 46
- Figure 10. Evidence of metastatic capability in a spontaneous tumor model. 47
- Figure 11. Metastatic lymph node sites show primary tumor
Characteristics. 48

Chapter 3

- Figure 1. Schematic of plasmids with K14 promoter. 60
- Figure 2. Buccal tumors arising from K14-driven HPV16 E6/E7. 61

Figure 3. Bioluminescence kinetics of each buccal tumors arising from HPV16 E6/E7 under K14 promoter.	62
Figure 4. Characterization of buccal tumors arising from HPV16 E6/E7 under K14 promoter.	63
Figure 5. Buccal tumors arising from K14-driven transposase SB100.	64
Figure 6. Characterization of buccal tumors arising from SB100 under K14 promoter.	65
Figure 7. Combining K14-driven HPV16 E6/E7 and K14-driven SB100 with different plasmids delivery route.	66
Figure 8. Bioluminescence kinetics of vaginal tumors from different promoters.	67
Figure 9. Bioluminescence kinetics of individual vaginal tumor arising from K14-driven HPV16 E6/E7.	68
Figure 10. Characterization of vaginal tumors arising from K14-driven HPV16 E6/E7.	69
Figure 11. Inconsistent correlation between bioluminescence intensity and tumor growth.	70

Chapter 4

Figure 1. Bioluminescence kinetics of buccal tumors in immunodeficient mice.	79
Figure 2. Buccal tumors arising from HPV16 E6/E7 and AKT oncogenes.	80
Figure 3. Bioluminescence kinetics of vaginal tumors arising from different plasmid combinations in immunodeficient mice.	81

Figure 4. Vaginal tumors arising from HPV16 E6/E7 and AKT oncogenes. 82

Figure 5. Characterization of vaginal tumors arising from HPV16 E6/E7
and AKT oncogenes. 83

CHAPTER 1

Introduction

Malignant disease caused by HPV infection is a global health issue.

The relationships between malignant cancers and certain infectious pathogens, such as Hepatitis B viruses and hepatocellular carcinoma, or *Helicobacter pylori* and stomach cancer, have been well documented. On a global scale, about one in six new diagnosed cancers is associated with a certain type of infection, including viruses, bacteria or parasitic infections. (1,2) There are around 5.5 million new cases of human papillomavirus (HPV) infections globally reported every year (3). In the United States, estimated annual medical cost burden of preventing and treating HPV-associated disease was around \$8.0 billion (2010 U.S. dollars). (4-7). HPV has been identified as the etiological factor of several types of malignancies, and is perhaps best known for being responsible for several ano-genital cancers including, nearly 100% of cervical cancer cases, around 95% of anal cancers, 65% of vaginal cancers, 50% of vulvar cancers and around 35% of penile cancers (8). In addition, HPV is also responsible for nearly 70% of oropharyngeal cancers. Most HPV-associated malignancies are caused by HPV type 16. Only two HPV types, 16 and 18, are responsible for about 70% of all cervical cancers (9). Additionally, in the United States, more than half of cancers diagnosed in the oropharynx are linked to HPV type 16 (10).

In spite of the availability of preventive HPV vaccines, it cannot be used for the

population who already have an existing HPV infection. This population is at risk of getting cancer; therefore, there is a great need for a cancer disease model for HPV infection that researchers can use to evaluate therapeutic intervention to control disease progression.

There is a great need to develop an HPV-infection tumor model.

Nowadays there are a few choices of preventive HPV vaccines, including Gardasil (Merck & Co., FDA approved in 2006), which covers HPV genotypes 6, 11, 16, 18, Cervarix (GlaxoSmithKline, FDA approved in 2009), which covers HPV genotypes 16 & 18, and newly released Gardasil 9 (Merck & Co., FDA approved in 2014), which covers genotypes 6, 11, 16, 18, 31, 33, 45, 52, 58. These vaccines can effectively prevent primary infection, but cannot be used as a therapeutic treatment strategy. For patients with detectable HPV infection, the only available treatment methods involve close follow-up until immune clearance. Previous publications have shown that more than 90% of new HPV infections, including those with high-risk types, can be cleared or become undetectable within two years, with most clearance occurring in the first 6 months after infection (11-14). However, the chance of persistent infection with high-risk HPV types puts infected patients at a greater risk of suffering from cervical cancer precursors and invasive cervical cancer (15-17). Although most HPV infections are temporary and asymptomatic, causing no clinical manifestations, failed control of persistent infection can induce precancerous lesions and invasive cancer. Furthermore, with the uncertainty of viral clearance and the risk of developing cancerous lesions, the psychological burden of patients with HPV infection is enormous. In addition, frequent speculum examination

and colposcopy also cause physical burden, not to mention the expense of time and money. Therefore, my thesis studies have aimed to develop a preclinical spontaneous tumor model, which can be utilized to evaluate therapeutic strategies in clearing HPV infection as well as prevent tumor formation after HPV infection.

Characteristics of HPV infection restrict the development of in vivo models.

HPVs are a large group of non-enveloped DNA viruses with an outer protein capsid. Inside is the viral genome, a circular, double stranded DNA containing about 8000 base pairs in size and encode eight genes as shown in Figure 1 (18,19). There are more than 200 types of HPV that have been identified. Based on the sequence of the major coat protein of the virus, the L1 nucleotide sequence, these human papillomaviruses can be further divided into five phylogenetic groups: alpha- (α), beta- (β), gamma- (γ), mu- (μ), and nu- (ν) papillomaviruses (20). Papillomaviruses (PV) have co-evolved with their various hosts over millions of years resulting in genotype-specific host-restriction. This means that there is no cross-species transmission and the molecular mechanisms and disease associations are not shared between divergent PVs (21,22). Therefore, it is impossible to infect species other than humans with normal human papillomavirus.

Other than the genotype, these HPVs also show diversity in epithelial tropism and pathogenicity. In other words, the most discrete characteristics of HPV groups are their preference of particular anatomical sites with site-specific patterns of gene expression and gene function (23). The alpha-type HPV is the largest phylogenetic group, which can

be further categorized by cutaneous and mucosal tropism. Mucosal type HPVs can be classified into two subtypes based on their association with cancer. High-risk types, such as HPV types 16 and 18 are more closely associated with malignant tumors; while low-risk types, such as HPV 6 and 11, are more associated with benign condyloma (22,23).

The lifecycle between low and high risk type HPV is also different. High-risk type HPVs drive aggressive cell transformation and proliferation after infecting basal cells. Alternatively, low-risk type HPVs divide slowly, remaining in the epithelium basal layer as transit-amplifying cells that differentiate to complete their life cycles (20). HPV infects basal membrane cells through a wound area or abrasion in the epithelium. Because HPV does not encode DNA polymerase in its genome, the lifecycle of the virus requires replication machinery from the host's genome. After entering the host cells and uncoating the capsid, viral DNA is transferred to the cell nucleus and maintained in basal cells at low copy numbers around 50-100 copies (24). In normal stratified epithelial cells, the basal cells would divide, migrate, change shape and finally terminally differentiate into cornified cells on the epithelial surface. Once the basal cells detach from the basement membrane, they will exit the cell cycle, suppress replication and stop dividing. In order to maintain the viral genome, the major oncoprotein E6/E7 degrades p53, disrupting the interaction between Rb and E2F, and hijacks the silenced cell cycle resulting in rapid cell proliferation (25,26). The viral genome will be amplified to thousands of copies in the spinous layer of the epidermis with tremendous amplification and late gene expression in the terminal cornified layer. Late genes L1/L2, which are responsible for the capsid coat, will not be expressed until the viral genome is ready to be released from surface cornified

cells. Although L1 and L2 are immunogenic, the immune surveillance function is poor in the epithelial surface (27). Therefore, this unique lifecycle enables HPV to escape from immune-surveillance.

Limitations of traditional HPV tumor models gave us space for improvement.

With species-restricted infection, strict squamous epithelial tropism, and differentiation-dependent life cycle, the development of an ideal HPV-associated cancer model has had a long history. The most well-established *in vitro* model uses immortalized HPV-infected keratinocytes in organotypic raft culture to study productive lifecycle of HPV, especially several high-risk types (28-31). However, some tumor biology questions, such as process of disease progression or host immune system reaction, cannot be addressed without *in vivo* animal models. Due to the papillomaviruses species-restricted infection manner, HPV can only infect and complete their life cycle in the human body. In addition, the susceptibility of developing precancerous or invasive cancer lesions from an HPV infection is limited to certain epithelial areas, such as the cervical transformation zone, the anal transformation zone, and the oropharynx (20,32). All these characteristics hamper the development of an HPV+ tumor animal model. Although traditional models, which use animal papillomaviruses to infect their natural hosts (summarized in Table 1), are of great value, the characteristics of limited cross-species transmission suggests different molecular mechanisms between divergent PVs (21,33). Therefore, different papillomavirus species models are limited in their accurate representation of the molecular mechanism of gene expression and behavior of infected cells from HPV infection.

For HPV in vivo models, early studies used HPV-infected human tissue fragments, such as cervix or foreskin tissue and performed xenografts in athymic immunocompromised mice to reproduce some of the histologic features of HPV infection (34-41). Although these models showed histologic features of HPV infection and contain HPV antigen and DNA from type 16, the production of virions and the passage of the infection to uninfected tissue were not demonstrated. Later on, W. Bonneze et al. used human foreskin fragments infected with high-risk HPV16 and implanted them into several combined immunodeficient mice (42). Although this model caused lesions identical to intraepithelial neoplasia, the precursor to carcinoma, the tumor microenvironment was different from clinical infection-to-cancer progression with different anti-infection immunity.

Another area of HPV animal models involves the implantation of immortalized tumor cell lines with persistent expression of oncogenes from high risk HPV types. These have been widely used for anti-tumor therapeutic evaluation, especially for the development of HPV vaccines (43-46). The most widely used is the TC-1 cell line, which was originated from C57BL/6 mice lung epithelial cells expressing HPV16-E6, E7 and activated human c-Ha-ras genes (47). Another well-known cell line is C3, which was originated from C57BL/6 embryonic cells transfected with a plasmid containing the complete HPV16 genome (48). However, considering the mechanism of spontaneous tumorigenesis after persistent infection, these tumor challenge models have similar issues to the xenograft transplantation models. They are not able to accurately address the tumor

microenvironment and the mechanisms which enable the tumor to escape immune-surveillance. To improve these limitations, transgenic animal models were developed to express viral gene products constitutively under exogenous promoter control (49-52). For the high-risk α -HPV types, Lambert PF and his colleagues have done a lot of the work using transgenic mice (49,52-56). They used either single transgenic, bi-transgenic or tri-transgenic mice with high-risk HPV16 E6/E7 or combined other oncogenes to evaluate the molecular function of individual genes. They also examined the consequences of HPV16 E6/E7 expression under the control of the basal cell promoter keratin 14 (52) for site-specific expression or time-specific expression using ligand-regulated transgene expression (56). Although those transgenic mice can resemble disease progression from transformed epithelial cells, these transgenic models are limited by tumor generation rate. Furthermore, it may take from 8-12 months to generate malignant cancer in 30-40% mice (57,58). In addition, these transgenic mouse models continuously express HPV oncogenes E6/E7. The immunity against HPV oncogenes are tolerized because the immune system recognizes these oncogenes as self antigens. This is quite different from clinical infection in which the immune system meets the foreign antigens for the first time upon HPV infection. This means that transgenic mice cannot be used to evaluate immunotherapy strategies due to the issue of immune tolerance. In addition, these transgenic mice express HPV throughout their whole body, which cannot recapitulate the tumor microenvironment of the clinically localized disease. All these limitations warrant the development of an improved HPV+ preclinical tumor model.

An ideal HPV infection-cancer animal model would:

1. Resemble a complete viral life cycle
2. Recapitulate anatomical predilections for disease
3. Mimic a clinically relevant tumor microenvironment
4. Form spontaneous tumors with clinically relevant disease progression
5. Be compatible with evaluating immunotherapy

Sleeping Beauty Transposon system helps to generate a promising tumor model

After HPV infection, the viral DNA needs to integrate into the host genome to utilize the host's replication machinery to complete its lifecycle. In order to recapitulate the clinical HPV lifecycle, we hypothesized that local injection of high risk HPV16 E6/E7 DNA can mimic HPV infection. To efficiently introduce the plasmids DNA into mice epithelial cells, we use electroporation. Electroporation is a physical transfection method that uses an electrical pulse to create temporary pores in cell membranes through which substances like nucleic acids can pass into cells. Electroporation has been shown to be a highly efficient tool used to introduce foreign nucleic acids into many cell types, including bacteria and mammalian cells (59).

Although electroporation achieves very stable transfection, the gene expression is typically transient. Because we wanted to generate a long-term HPV infection model resulting in carcinogenesis, we used the Sleeping Beauty (SB) transposable element system delivered as plasmid DNA to achieve chromosomal integration and long-term expression which can mimic viral DNA integration(60). Sleeping Beauty is a synthetic transposable element composed of a transposon DNA substrate and a transposase

enzyme. SB transposase regulates excision and insertion of transposon DNA into a TA dinucleotide of the host genomic DNA in a cut-and-paste manner (61). Previously, Wiesner et al. utilized the SB system to induce brain tumors in mice, de novo using plasmid DNA (62). We modeled this design by using a transposase plasmid and transposon plasmid. The transposon plasmid contained the SB transposase enzyme to initiate chromosome integration and long-term expression of high-risk HPV oncogenes.

After addressing the issue of transfection efficiency and long-term gene expression, the next step was addressing tumor generation rate. Previous transgenic mice models have shown that high risk HPV E6/E7 alone is not enough to efficiently generate malignant tumors; therefore, we were interested in combining E6/E7 with other oncogenes. The RAS oncogene has high tumorigenesis potency with a promising tumor generation rate, as described in a previous publication (62). In addition, the synergistic effect between RAS and E6/E7 genes in cellular transformation has been well documented (63,64). Although cervical cancer is the most clinically relevant HPV malignancy, the cervix is a challenging area to study. As a result, I first tested my hypothesis using the mouse buccal area, which is representative of the subset of HPV-associated oropharyngeal carcinomas. In **Chapter 2**, we utilized HPV16 E6/E7 combined with NRAS^{G12V} oncogene to generate a preclinical buccal tumor model. This part of the dissertation has been submitted for publication. In **Chapter 3**, we utilized keratinocyte-restricted promoter K14 to drive HPV16 E6/E7 in the tumor model. Lastly, in **Chapter 4**, we utilized HPV16 E6/E7 combined with AKT plasmids DNA in a cervico-vaginal tumor model to generate a clinically-relevant carcinoma. (65).

In summary, my thesis work provides a usable, alternative HPV+ spontaneous tumor model with cost and time-efficient properties. In our buccal model we show its capability for immunotherapy as well as regional metastasis, which recapitulates clinical disease progression. In our cervico-vaginal tumor model, the combination of HPV16 E6/E7 and AKT caused clinically relevant carcinomas. I believe both of these models will be excellent candidates to evaluate cancer immunotherapy because they do not possess the issue of immune tolerance as compared to transgenic mice models. In addition, because of the properties of localized spontaneous tumor formation followed by regional lymph node metastasis, these models can be used to study tumor microenvironment, tumor biology and metastasis biology.

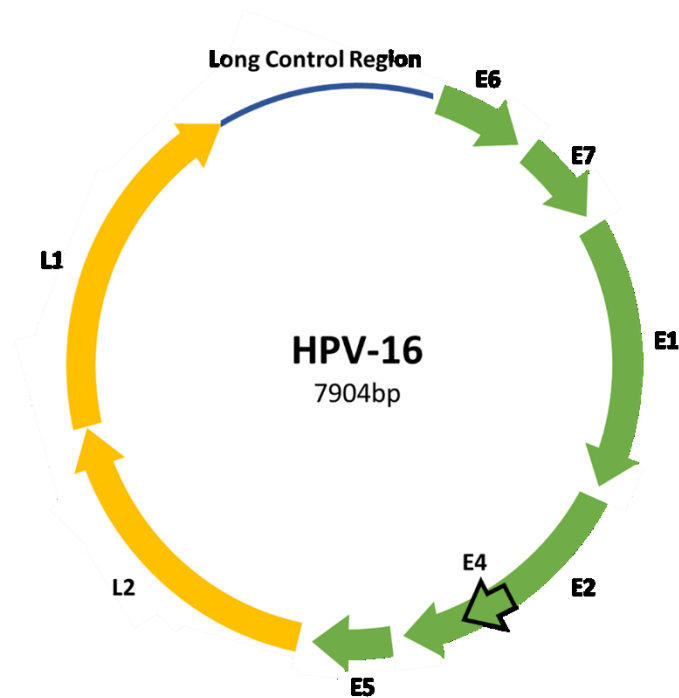


Figure 1. The HPV16 genome. The HPV genome encodes eight genes. Six of these are early genes, E1, E2, E4, E5, E6, E7, which are non-structural proteins. In these non-structure proteins, E6 and E7 are the most well-known onco-proteins, which are associated with degradation of p53 and pRb. E1 is an ATP-dependent helicase and is responsible for viral genome replication. E2 is a coactivator through the recruitment of E1 to viral replication origin and plays a role as E6/E7 transcription factor. E4 is associated with viral transmission and E5 is a small transmembrane protein contributing to evade immune response. The remaining two, the late genes (L1, L2), are structural proteins, in which L1 is the major and L2 is the minor capsid protein. (20)

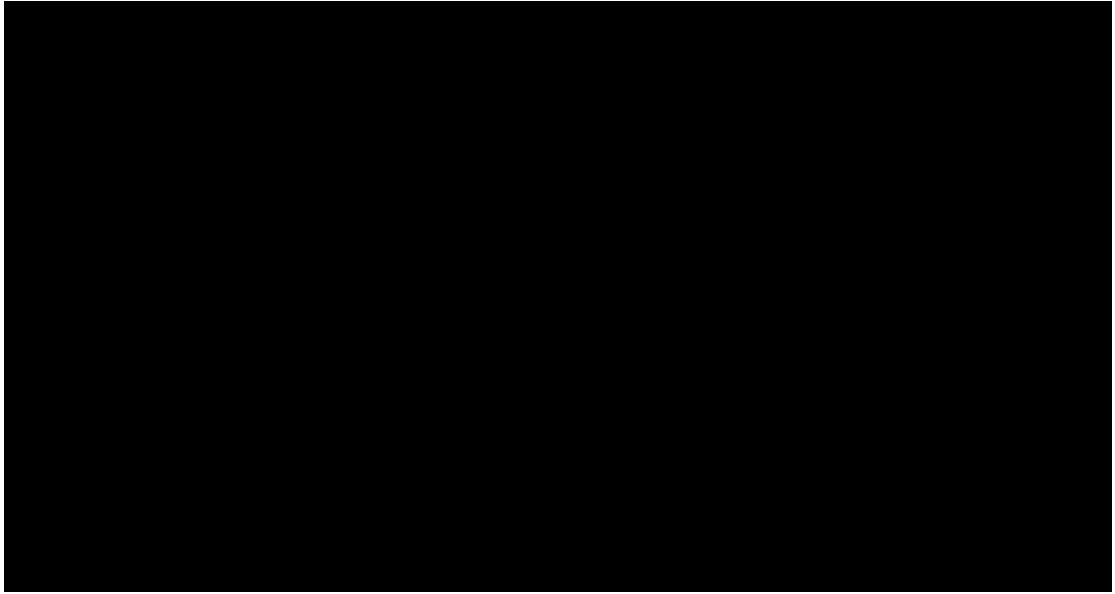


Table 1. Summary of animal papillomaviruses models (66-78)

CHAPTER 2

Generation of a spontaneous HPV+ oral tumor model by submucosal injection of oncogenic DNA plasmids with electroporation

Introduction

As described in Chapter 1, HPVs are responsible for causing a multitude of diseases ranging from benign warts to lethal malignant tumors (79). Persistent infections with high risk HPV type (i.e. HPV type 16 and 18) are associated with precancerous lesions, and sometimes progress into invasive cancer (80,81). In the case of HPV-positive head and neck squamous cell carcinoma (HNSCC), patients do not usually present symptoms until an advanced stage, during which lymph node metastasis is common (82,83). Typically, surgery, radiation therapy, and chemotherapy are used for the treatment of HPV-associated head and neck cancer; however, these therapeutic methods often result in irreversible damage to anatomical structure as well as reduced quality of life (84-86). It has been suggested that anti-tumor immunogenicity and the tumor immune microenvironment is important for tumor prognosis. Many attempts have been made to generate HPV tumor models useful for the evaluation of candidate immunotherapeutic agents against HPV-associated head and neck cancers that have the potential to be better tolerated and more effective than existing conventional therapies (70).

Traditionally preclinical HPV+ oral tumor models were generated by implanting tumor cell lines immortalized by HPV oncogenes into the oral cavity of mice (45,87,88).

One major drawback of these tumor challenge models is their inability to capture major aspects of tumorigenesis caused by HPV infection, including the processes of cellular transformation after viral entry, as well as the disease progression from precancerous lesion to invasive cancer (89). An alternative method used to create a preclinical HPV tumor model involves the generation of immunocompetent transgenic mice that expresses the HPV oncogenes E6 and E7 (49-52,56,90). However, because the conventional transgenic tumor model continuously expresses HPV16 E6 and E7, the mice become immunotolerant to these oncogenes, rendering the model less effective at evaluating immunotherapy (70). Zhong et al has recently published an inducible transgenic HPV+ oral tumor model that may be able to circumvent the immune tolerance issue (91). However, since the HPV16 E6 and E7 becomes universally expressed in the epithelium after induction, the anti-tumor immunogenicity is expected to be different from that of the clinically localized tumor. As a result, there is still room to improve preclinical HPV oral tumor models. The ideal preclinical HPV oral tumor model should possess the following characteristics: 1) forms spontaneous, localized, HPV+ oral tumor with clinically relevant histology, 2) displays an immune microenvironment that closely resembles that of HPV+ oral tumor in patients, 3) the tumor-bearing mice can respond appropriately to immune therapies and generate anti-tumor immunity, 4) tumor formation should follow clinical progression, from precancerous to invasive and metastatic state.

Previously, it has been demonstrated that HPV16 E6/E7 and mutant Ras oncogenes synergistically enhance the rate of tumor formation in vivo (64). In addition, this synergistic, carcinogenic effect is confined in epithelial transition zones where HPV-

associated transformation occurs. In the buccal area this transition zone is located between the outer skin of the lip and the inner buccal mucosa. Resultantly, direct introduction of viral oncogenes HPV16 E6/E7 as well as mutant Ras oncogene to the buccal area may result in efficient tumor formation.

HPV infects basal membrane cells through a wound area in epithelium. Because HPV does not encode DNA polymerase in its genome, integration of the HPV viral genome into the host genome, and the continual expression of E6 and E7 are important for HPV oncogenesis. HPV oncoproteins E6 and E7 can degrade p53, disrupt the interaction between Rb and E2F, and reinitiate the silenced cell cycle, resulting in rapid cell proliferation (25,26).

In order to simulate the clinical HPV viral lifecycle, we hypothesized that local introduction of high risk HPV16 E6/E7 DNA can mimic viral DNA entering the cells after HPV infection. The introduction of plasmids encoding HPV16 oncogenes into epithelial cells can be achieved with the use of electroporation. Electroporation is a physical transfection method that uses an electrical pulse to create temporary pores in cell membranes through which substances like nucleic acids can pass into cells. It has been shown that electroporation is highly efficient in introducing foreign nucleic acids into many cell types, including bacteria and mammalian cells (59). However, although electroporation achieves very stable transfection, the gene expression is typically transient. Therefore, an additional method, Sleeping Beauty (SB) transposon system, is required to reproduce the persistent expression of HPV E6 and E7 oncogenes resulting

from HPV DNA integration. We have discussed the details of this synthetic transposable element systems in **Chapter 1**. We hypothesize that the utilization of Sleeping Beauty transposase system can reproduce the integration process of HPV oncogenes into the host genome, and result in continual expression of E6 and E7 oncoproteins in the transfected cells.

In this study, we developed a novel, spontaneous, HPV+ buccal tumor model using plasmids encoding oncogenes HPV16 E6/E7, mutant Ras, Luciferase as a reporter gene, and SB transposase. The introduction of SB transposases results in the integration of E6, E7, and mutant Ras into the host genome. The integration of oncogenes resulted in stable expression of the oncoproteins, leading to the transformation of the transfected cells and consequently the formation of spontaneous HPV+ buccal tumor, a process that closely resembles the tumorigenesis of HPV-associated oral cancer in human patient. In addition, we used this preclinical model to evaluate the antitumor efficacy of a clinical-grade plasmid vaccine and demonstrated that DNA vaccination in mice bearing the spontaneous HPV+ tumor model resulted in the generation of potent therapeutic responses and the control of the spontaneous oral tumor.

Materials & Methods

Mice and Animal Care

Six to eight-week-old female C57BL/6NCr (strain #556), FVB/NCr (strain #559), BALB/cAnNCr (strain #555) and athymic nude (Athymic NCr-nu/nu, strain #553) mice

were purchased from Charles Rivers Laboratories (Frederick, MD, USA). All mice were maintained at Johns Hopkins University School of Medicine (Baltimore, MD) animal facility under specific pathogen free conditions. All procedures were performed according to protocols approved by the Johns Hopkins Institutional Animal Care and Use Committee and in accordance with recommendations for the proper use and care of laboratory animals.

Plasmid Vectors

To generate pcDNA3-Luc, Luciferase was cloned into XbaI/XhoI sites of pcDNA3 plasmid vector by primers (aaatctagaatggaagacgccccaaaacat and aaactcgagcagcgcatctttccgcct).

To generate pcDNA3-Luc- T2a-E7, T2a-E7 was cloned into Xho I/EcoRI sites of pcDNA3-Luc by primers (aaactcgaggaggcagaggaagtcttctaacaatgcggtgacgtggaggagaatcccgccctatgcatggagatacct and ttgaattctggttctgagaacagatgg).

To generate luciferase E7 and E6 oncogene fusion construct, pcDNA3-Luc- T2a-E7- T2a-E6), T2a-E6 was cloned into EcoRI/BamHI sites of pcDNA3-Luc- T2a-E7 by primers (aaagaattcgaggcagaggaagtcttctaacaatgcggtgacgtggaggagaatcccgccctatgcacaaaagagaact, and ttggatcccagctgggttctctacgtg).

To generate Pkt2-Luc-T2a-E7- T2a-E6, Luc-T2a- E7-T2a- E6 was removed from pcDNA3- Luc-T2a- E7-T2a-E6 by XbaI/BamHI sites and cloned into XbaI/Bgl II sites of the Pkt2/clp-akt vector (62).

To generate Pkt2-Luc- T2a-E7, T2a-E7 was cloned into XhoI and BstXI sites of Pkt2-Luc- T2a-E7- T2a-E6 by primers (aaactcgaggagggcagaggaagtcttct and ttccagctagctggttatggttctgagaacaga).

To generate Pkt2-Luc- T2a-E6, T2a-E6 was cloned into XhoI and BstXI sites of Pkt2-Luc-T2a- E7-T2a- E6 by primers (aaactcgaggagggcagaggaagtcttct and ttccagctagctggttacagctgggttctctacg).

In the DNA constructs, t2a (EGRGSLLTCDGVEENPGP), a self-cleavage peptide from the *T. asigna* virus, was inserted between each gene allowing for the production of each protein individually from a single fusion protein (92). Cleavage of the t2a sequence occurs due to a ribosomal skip mechanism at the point between the final glycine and proline residues (92).

The construction of the pT/Caggs-NRAV12 plasmid has been described previously (62). The plasmid was purchased from Addgene (plasmid #20205).

The construction of the pCMV(CAT)T7-SB100 plasmid has been described previously (93). The plasmid was purchased from Addgene (plasmid #34879).

The construction of the pT2/C-Luc//PGK-SB13 plasmid has been described previously (62). The plasmid was purchased from Addgene (plasmid #20207).

DNA vaccine

The DNA vaccine, pNGVL4a-CRT/E7(detox), has been described previously (94) and expresses a fusion of human calreticulin (CRT) and detoxified HPV16 E7 antigen. CRT is a 46 kDa protein located in the lumen of the cell's endoplasmic reticulum (ER) and has been shown to strengthen MHC class I presentation for the activation of CD8+ T cells. E7(detox) represents a HPV16 E7 gene with mutations at positions 24 and 26, which disrupt the Rb-binding site of E7 and thus abolish the capacity of E7 to transform cells (95). The plasmid backbone, pNGVL-4a, was obtained from the NIH National Gene Vector Laboratory and has been used in several clinical studies (96). Clinical grade pNGVL4a-CRT/E7(detox) plasmid was prepared by the NCI's Rapid Access to Interventional Development (RAID) program.

In vivo tumor formation

For the generation of tumor in immune-deficient mice, athymic nude mice (five per group) were submucosally injected with 1) plasmids encoding Luciferase and HPV16-E6/E7, mutant Ras (NRAS^{G12V}) and SB100, 2) plasmids encoding Luciferase and HPV16-E6, mutant Ras (NRAS^{G12V}), and SB100, 3) plasmids encoding Luciferase and HPV16-E7, mutant Ras(NRAS^{G12V}), and SB100, 4) plasmids encoding Luciferase and HPV16-E6/E7 and SB100, or 5) plasmids encoding mutant Ras (NRAS^{G12V}), SB13, and

Luciferase into the buccal area followed by electroporation. The plasmids were injected with 30G, 3/10ML BD insulin syringe (BD Cat#: 328431). The injection site was on the cheek mucosal area adjacent to muco-cutaneous junction, in which the epithelium transition from the outer skin of upper lip to stratified squamous epithelium lacking follicles. The injection depth is no more than 1mm followed by electroporation (Tweezertrodes™. 72 V, 16 pulses, 20ms period, 200 ms apart).

For the generation of tumor in immune-competent mice, C57BL/6NCr, BALB/C, or FVB/NCr mice (five per group) were submucosally injected with plasmids encoding Luciferase and HPV16-E6/E7, mutant Ras, and SB100 into the buccal area followed by electroporation.

For the generation of tumor in immune-suppressed mice, C57BL/6NCr mice (five per group) received one of the following treatments:

- 1) Intraperitoneal injection of 100µg monoclonal Anti-CD3 antibody (Clone: 17A2, Cat#: BE0002) per day for three consecutive days and on the following day after last anti-CD3 antibody injection followed by submucosal injection of plasmids encoding Luciferase and HPV16-E/6E7, mutant Ras, and SB100 into the buccal area followed by electroporation;
- 2) Intraperitoneal injection of 100µg monoclonal Anti-CD4 (Clone: GK1.5, Cat#: BE0003-1) per day for three consecutive days and on the following day after three anti-CD4 antibody injection followed by submucosal injection of plasmids encoding Luciferase and HPV16-E6/E7, mutant Ras, and SB100 into the buccal area followed by electroporation. The mice continued to receive anti-CD4 antibody injection in weekly

intervals; 3) Intraperitoneal injection of 200 μ g monoclonal Anti-CD8 antibody (Clone: 2.43 Catalog#: BP0061) per day for three consecutive days and on the following day after three anti-CD8 antibody injection followed by submucosal injection of plasmids encoding Luciferase and HPV16-E6/E7, mutant Ras, and SB100 into the buccal area followed by electroporation. The mice continued to receive anti-CD8 antibody injection at 4-day intervals; 4) Submucosal injection of plasmids encoding Luciferase and HPV16-E6/E7, mutant Ras, and SB100 into the buccal area followed by electroporation with no antibody treatment.

The length and width surface dimensions of the tumor were measured with digital calipers. To record the survival of the tumor-bearing mice, either natural death or a buccal tumor diameter greater than 7mm leading requiring euthanasia for humane reasons and was counted as death.

In vivo bioluminescence image

After oncogene plasmids injection, buccal tumor growth was monitored 1-2 times per week by IVIS Spectrum in vivo imaging system series 2000 (PerkinElmer). In summary, mice were anesthetized by intramuscular injection of Ketamine/Xylazine solution (5:1 ratio). After intraperitoneal injection of substrate D-luciferin (3.9mg/mL with total injection volume 200 μ L and 10 min reaction time, GoldBio), bioluminescence imaging for luciferase expression was conducted on a cryogenically cooled IVIS system using Living Image acquisition and analysis software (Xenogen). Images were acquired 10 minutes after D-luciferin administration. The levels of light from the bioluminescent

cells were detected by the IVIS imager, integrated, and digitized. The region of interest from displayed images was quantified as total photon counts using Living Image 2.50 software (Xenogen).

Tumor treatment experiments

C57BL/6NCr mice (five per group) received intraperitoneal injection of 100µg monoclonal Anti-CD3 antibody per day for three consecutive days and on the following day after last anti-CD3 antibody injection followed by submucosal injection of plasmids encoding Luciferase and HPV16-E6/E7, NRAS^{G12V}, and SB100 into the buccal area followed by electroporation. 10 days after plasmids injection, mice were vaccinated with pNGV4a-CRT/E7(detox) or empty pNGVL4a vector only (20µg/dose/mice) via intramuscular injection followed by electroporation. The mice continued to receive the same vaccination in 4-day intervals.

Evaluation of Metastasis Capability

When the tumor size exceeds 7mm in diameter, mice were considered to be unrecoverable from tumor burden, and euthanized according to the protocol. At the time of sacrifice, enlarged tumor side superficial cervical lymph nodes were surgically removed, minced, treated with tissue digestion buffer, filtered, then cultured in RPMI-based antibiotics containing medium in 6-well-plate. After cell proliferation, the whole cell mixture was transferred to T75 tissue culture flask. Once the cell expansion covered more than 70% of the flask surface, the cells were trypsinized, PBS washed, re-suspend in 40µL PBS solution, followed by submucosal buccal injection into immune-deficient

athymic mice. After lymph node cells injection, the mice were followed with in vivo bioluminescence image system.

Histology and Immunohistochemistry staining

When the tumor size exceeds 7mm in diameter, mice were considered to be unrecoverable from tumor burden, and euthanized according to the protocol. The buccal tumors were surgical removed, isolated and placed into 10% Neutral buffered formalin solution for adequate fixation with a minimum 48 hours at room temperature. The tumor samples were then sent to Johns Hopkins University Oncology Tissue Services for subsequent procedures including paraffin embedding, tissue sectioning, hematoxylin and eosin (H&E) staining and immunohistochemical (IHC) staining. The histology slides were reviewed by Dr. T.-C. Wu of the Pathology Department in the Johns Hopkins University School of Medicine.

***In situ* hybridization to detect HPV16 oncogenes**

In situ hybridization was performed using the RNAscope® 2.0 HD Brown Chromogenic Reagent Kit (Advanced Cell Diagnostics, Hayward, CA) using the supplied protocol and a target probe against HPV16 E6/E7 (Advanced Cell Diagnostics #311521). Briefly, fresh cut formalin-fixed, paraffin embedded slides were baked at 60°C overnight. After deparaffinization, slides were air-dried, circled with a hydrophobic barrier pen (Vector labs, ImmEdge pen Cat# H-4000), and then exposed to pretreatment solutions 1, 2, and 3. Target probes were hybridized for 2 hours at 40°C in hybridization chamber, and followed by a series of signal amplification and washing steps. The signals were detected

by chromogenic reactions using DAB chromogen followed by undiluted Gill's hematoxylin (Sigma-Aldrich) counterstaining.

Tetramer staining and Flow cytometry

Peripheral blood was collected into 1.5-ml EDTA coated Eppendorf tubes from ventral artery of mouse tail by single edge blade cutting. After red blood cell lysis with ACK lysing buffer (Quality Biological, Gaithersburg, MD, USA), PBMCs were then stained with fluorescein isothiocyanate (FITC)-conjugated monoclonal rat anti-mouse CD3 (BD Pharmingen, Cat# 555274), allophycocyanin (APC) conjugated monoclonal rat anti-mouse CD8a (Biolegend, Cat# 100712), and phycoerythrin(PE)-conjugated H-2D^b tetramer loaded with HPV16 E7aa49–57 peptide at 4 °C for at least 30min. After washing with FACS washing buffer, the cells were stained with 7-AAD before flow cytometry analysis to exclude dead cells. Then cytokine responses were acquired immediately using a BD FACSCalibur flow cytometer. Flow cytometry results were analyzed with Flowjo V.10 software.

Ex vivo luciferase bioluminescence assay

Athymic nude mice were received submucosal injection of plasmids DNA in buccal area followed with electroporation. The plasmids included LucE6E7, NRAS^{G12V} and SB100. The mice were sacrificed at the time when tumor diameter grew to reach 15 mm. The tumor and the cervical tumor-draining lymph nodes were harvested for luciferase assay. The spleen and naïve mice were used as negative control. The tissue was homogenized by Mini-Beadbeater-1 with 1mm and 0.1mm glass beads (Bio Spec

Products Inc) in 50000. The mice were sacrificed at the time when tumor diameter grew to reach 15 mm. The tumor and the superficGloMax®-Multi Detection System according to the manufacturer's instruction (Promega Corporation). Relative light units (RLU) was adjusted to each gram of tissue.

Statistical analysis

The statistical analysis was performed with the GraphPad Prism V.6 software (La Jolla, CA, USA). Data were expressed as means \pm standard deviations (SD). Kaplan-Meier survival plots were constructed to estimate either tumor-free rate or survival percentage. The log-rank test was used to compare survival times between treatment groups. Comparisons between individual data points was analyzed by two-tailed Student's t test. A p-value of less than 0.05 was considered statistically significant.

Results

Optimizing plasmids combination to generate HPV16 spontaneous buccal tumor in immunocompromised mice.

To generate spontaneous oral tumor that continuously expresses HPV16 E6 and E7, different combinations of plasmids listed in **Fig. 1** were submucosally injected into the buccal area followed by electroporation in athymic nude mice, which have an abnormal thymus and defective T cell functions. The enzyme luciferase encoded in the plasmids results in the generation of bioluminescence from viable, transfected cells that can be measured quantitatively using an IVIS imager. After plasmid injection, in vivo

tumor growth was monitored using bioluminescence imaging. As shown in **Fig. 2A and 2B**, combination of plasmids encoding Luciferase and HPV16-E6/E7 and NRAS^{G12} oncogenes resulted in the fastest tumor formation and growth rate as suggested by the luminescence intensity. Based on this result, the combination of E6, E7, and NRAS^{G12} oncogenes is most efficient at causing oral tumor formation in mice.

CD3 depletion is necessary for the formation of HPV16 spontaneous buccal tumor in immunocompetent mice.

After demonstrating the ability to effectively generate spontaneous oral tumor in immunodeficient mice by transfecting plasmids encoding HPV16 E6/E7 viral oncogenes, NRAS^{G12} oncogenes, and SB100 sleeping beauty transposase, we sought to apply the same strategy for the generation of spontaneous oral HPV tumor in immune competent mice. Plasmids encoding luciferase, HPV16-E6/E7, NRAS^{G12}, and SB100 were submucosally injected into the buccal area of C57BL/6NCr, BALB/C, or FVB/NCr mice (five per group). As shown in **Fig. 3**, the bioluminescence intensity, which represents transfected luciferase gene expression, decreased steadily after transfection to background level, indicating the immune clearance of transfected cells by immune competent mice, regardless of their immune background. We thus hypothesize that an immune suppressed environment is necessary for spontaneous formation of tumor following plasmids transfection. To test this hypothesis, we treated C57BL/6NCr mice (five per group) with or without different immunosuppressive agents and plasmid transfections using treatment schedules depicted in **Fig. 4A**. The immunosuppressants

included anti-CD3 antibody, anti-CD4 antibody, or anti-CD8 antibody. Administration of anti-CD3, anti-CD4, or anti-CD8 antibodies results in the depletion of total or partial T cell population. As shown in **Fig. 4B**, mice that received anti-CD3 antibody (total T cell depletion) experienced a rapid increase in luminescence signaling after plasmid transfection, suggesting the expansion of plasmid-transfected cells. In contrast, mice that received anti-CD4 or anti-CD8 antibody (partial, CD4⁺ or CD8⁺ T cell depletion, respectively) generated similar luminescence signaling to the controlled mice that did not receive antibody treatment after plasmids transfection.

In addition to the observed increase in luminescence intensity, visible tumors were observed in CD3 depleted mice around 3 weeks after oncogenes transfection. To examine the relationship between T cell depletion and the formation of tumor, total T cell population in CD3-depleted, plasmids transfected mice was measured. As shown in **Fig. 5A**, the amount of systemic CD3⁺ T cells in mice drops sharply following anti-CD3 antibody injection, and remains low until around 9 days after plasmid transfection. During the window of low CD3⁺ T cell population, the luminescence intensity in mice started to increase, and continued to increase when the T cell population started to recover. During spontaneous tumor formation, the recovered T cells provided a relatively immunocompetent environment and an intervention therapeutic window. Of note, the tumor volume of the spontaneous tumors formed after plasmids transfection correlates strongly with its luminescence intensity (**Fig. 5B**), indicating that luminescence intensity is a good estimation of tumor growth. Together, these results suggest that initial total T cell depletion, as compared to partial depletion, is required for the formation of

spontaneous oral HPV tumor in immune competent mice, and that luminescence readout is an effective measurement for monitoring the growth of tumors.

Characteristics of HPV16 spontaneous oral tumor model

To characterize the spontaneous buccal tumor formed after the transfection of oncogenes-encoded plasmids, we treated C57BL/6NCr mice with anti-CD3 antibody daily for 3 days, followed by the transfection of plasmids encoding HPV16-E6, HPV16-E7, NRAS^{G12}, SB100, and luciferase at the buccal area. When the resulted spontaneous tumor reaches 7mm in diameter, the mice were sacrificed and the buccal tumors were surgically isolated, fixed with formalin and embedded in paraffin. The tissue sections of the tumors were prepared and stained for various tumor markers. The spontaneous tumors arose from buccal mucosa area had gross features appearing as a solid, papillary mass with bleeding ulcers as the tumor grew larger (**Fig. 6A**). In microscopic features, H&E staining showed that the tumors were composed of spindle shaped tumor cells with highly mitotic activity in the majority (black arrow in **Fig. 6B**). IHC staining revealed high expression of Ki-67, a cell proliferation biomarker, as well as positive N-Ras and HPV-biomarker p16 expression (**Fig. 6B**). In addition, the RNA scope with HPV16 probe also showed strong HPV-16 staining in the tumor (**Fig. 7**). These results demonstrate that the spontaneous tumors generated through our method possess several relevant features and markers as the HPV16+ buccal tumors originated from persistent HPV16 infection.

Intramuscular injection of therapeutic HPV DNA vaccine in spontaneous HPV16 oral tumor bearing mice generates potent antigen-specific antitumor immune

response.

After we successfully demonstrated the ability to repeatedly generate the HPV16+ spontaneous buccal tumors in C57BL/6NCr mice, we sought to verify whether this model could be used to assess the efficacy of immune therapy. C57BL/6NCr mice (five per group) received intraperitoneal injection of 100µg monoclonal Anti-CD3 antibody per day for three consecutive days. The day after the last anti-CD3 antibody administration, the mice received submucosal injection of plasmids encoding luciferase, HPV16-E6, HPV16-E7, NRAS^{G12}, and SB100 into the buccal area followed by electroporation. 10 days after plasmid injection, mice were vaccinated with a therapeutic HPV DNA vaccine, pNGV4a-CRT/E7(detox), or empty pNGVL4a vector only (20ug/40uL) via intramuscular injection followed by electroporation. The mice received the same vaccination a total of 4 times at 4-day intervals (**Fig. 8A**). As shown in **Fig. 8B**, mice vaccinated with pNGVL4a-CRT/E7(detox) had significantly better survival rates when compared to mice vaccinated with empty pNGVL4a control. Approximately 80% of the mice that received pNGV4a-CRT/E7(detox) DNA vaccination survived more than eight weeks after plasmid transfection, whereas all mice that received empty pNGVL4a vector vaccination died in less than four weeks after plasmids transfection. Furthermore, the ability of the vaccinated mice to control the spontaneous tumor generated by plasmid injection correspond to the amount of E7-specific CD8+ T cells generated in the tumor bearing mice (**Fig. 8C**). The luminescence intensity and the tumor volume of mice were also measured and as shown in **Fig. 9**, mice vaccinated with pNGVL4a-CRT/E7(detox) showed a lower luminescence signal compared to the mice that received treatment of

empty pNGVL4a vector. Furthermore, the luminescence signals in CRT/E7(detox) vaccinated mice gradually decrease overtime back to background level, which translates into the reduction in tumor volume. These results indicate that therapeutic vaccination can lead to the generation of a potent antigen-specific immune response against the spontaneous HPV buccal tumor, resulting in effective tumor control and prolonged survival of tumor bearing mice.

Continued growth of spontaneous HPV16 oral tumor results in metastasis to tumor draining lymph nodes.

When C57BL/6NCr mice bearing HPV16 spontaneous oral tumor were euthanized due to tumor burden, enlarged, superficial neck tumor draining lymph nodes (TDLN) were observed with detectable luciferase activity as compared to non-tumor draining lymph nodes (NTDLN) (**Fig. 10A-B**). We hypothesize that these neck lymph nodes contain transfected plasmids and transformed cells that metastasized from the buccal area. To test our hypothesis, the enlarged lymph nodes were surgically removed, minced, digested and cultured in RPMI-based medium. After cell proliferation, the cell mixture was collected and implanted into the buccal area of immunodeficient athymic nude mice. The re-implanted lymph node cells showed positive luciferase activity, and the formation of buccal tumor in implanted nude mice was observed (**Fig. 10C**). The histological analysis of the tumors formed from the implanted lymph node cells revealed characteristics similar to that of HPV16 spontaneous buccal tumor originated from plasmid transfection. Furthermore, the tumors generated by lymph node cell implantation were positive for HPV marker p16 as well as N-RAS (**Fig. 11**). These findings suggest

that the spontaneous HPV16 tumor cells can migrate to different locations inside tumor-bearing mice, replicating the metastatic process of late stage HPV-associated cancer.

Discussion

In this study, we developed a new, pre-clinical, spontaneous HPV buccal tumor model through transfection of plasmids encoding oncogenes HPV16-E6, HPV16-E7, NRAS^{G12}, as well as sleeping beauty transposase and luciferase reporter genes. Plasmid transfection results in the formation of spontaneous tumor in immunodeficient athymic nude mice as well as immune competent C57BL/6NCr mice subjected to early immune suppression. We demonstrated that these spontaneous tumors express relevant HPV16 biomarkers p16 and detectable HPV16 RNA, can metastasize and migrate to distant locations such as tumor draining lymph nodes, and can be controlled through immune therapeutic treatments.

The novel spontaneous HPV buccal tumor model developed in the current study may be able to address several weaknesses of the existing HPV buccal tumor models. Prior HPV+ HNSCC tumor models mainly utilize the transplantation of tumor cells into immunodeficient mice to generate HPV expressing tumors. While transplantation of tumor cells results in consistent tumor formation, this method fails to replicate the process of tumorigenesis, HPV genome integration following HPV infection, and does not simulate the tumor microenvironment of a spontaneous tumor originated from HPV infection (45,87,88). In conventional HPV transgenic mice, HPV E6 and E7 oncogenes

are constitutively expressed, which may result in immune tolerance and impact tumor development (70). In addition, the establishment of a transgenic mouse model requires multiple rounds of selection to ensure successful genetic modification, a time-consuming process that may last for several months with many uncertainties. Furthermore, the tumor formation process for traditional HPV transgenic mouse models may take several months to over one year (49-52,90). The recently improved transgenic HPV oral model published by Zhong et al utilizes Cre-LoxP recombinase system to generate inducible expression of E6 and E7, which provides conditional and tissue-specific transgene expression (91). This modified transgenic model addresses some issues of earlier models, making it more clinically relevant compared to conventional transgenic models. However, the modified transgenic model requires the integration of three transgenes, which further complicates the selection process. (97). Our spontaneous HPV tumor model utilizes the sleeping beauty transposon system, which is well established and highly potent at enhancing DNA transfection, integration, and long-term transgene expression (60,62,98,99). Our method results in the formation of spontaneous tumor in both athymic nude mice and wild type mice within a few weeks following plasmids transfection (**Figures 1-4**), allowing for time efficient and time-flexible experimental designs compared to the transgenic models mentioned previously. Furthermore, the reliable gene integration resulted in a tumor formation rate of greater than 80%. The high tumor formation rate upon plasmid transfection can potentially reduce the waste of mice while ensuring the generation of a sufficient amount of tumor bearing mice to be used for subsequent evaluations including carcinogenesis and therapeutic intervention. Therefore, our model provided a cost, time, and labor efficient method to generate spontaneous HPV oral tumor that mimics localized

viral gene integration and cellular transformation that occurs during natural HPV disease progression.

In addition to being efficient in cost, labor, and time, this model incorporated the expression of luciferase by the transfected cells that can be monitored through bioluminescence imaging. We have previously utilized the luciferase reporter system in a preclinical HPV transplantation model (100), and the incorporation of luciferase bioluminescence reporter into the spontaneous HPV oral model provides a method for real-time, sequential, longitudinal and dynamic tracking of tumor growth (**Figure 5**). This imaging tool is useful especially for intra-oral tumor, which is relatively difficult to assess by caliper before it grows big enough to be measured from the outside. Also, because luciferase gene is linked to HPV16 E6/E7 oncogenes, the luciferase activity is correlated with the expression of HPV oncoproteins. The intensity of the luminescence signal can serve as an index for the presence of viral gene and oncoproteins, which will be very useful in evaluating pre-clinical tumorigenesis biology.

As mentioned before, most of the traditional transgenic mouse models continuously express E6 and E7, which may result in immune tolerance making them a non-ideal system for evaluating immunotherapy (101-103). While the inducible HPV transgenic models allow for conditional expression of transgenes and thus address the issue of immune tolerance, the expression of HPV oncogenes after induction took place throughout whole body epithelium area rather than confined to the buccal area, which can result in immunogenicity and the generation of an immune response that is much

different from the clinical, localized condition. Our spontaneous HPV tumor model permits local introduction of transgenes and confines the cellular transformation to the buccal region, which should be more clinically relevant in reflecting the biological response to immunotherapy. Using therapeutic HPV DNA vaccine pNGVL4a-CRT/E7(detox), we showed that this model can be used to evaluate the efficacy of immunotherapy (**Fig. 8**). It should also be noted that while the current study utilized immune therapy as the modeled therapeutic method, the spontaneous HPV+ buccal tumor model may also be used to evaluate other forms of treatment, including chemotherapy and radiotherapy.

In our spontaneous tumor model, we demonstrated that initial T cell depletion in immune competent C57BL/6NCr mice is necessary for the tumor formation to occur (**Figure 4**). This likely reflects the natural immunogenicity of HPV oncoproteins E6 and E7 as the vast majority of HPV infections that occur in humans are readily cleared by the immune system (80,81). In a clinical setting, it has been observed that patients experiencing immune suppression, such as human immunodeficiency virus (HIV) infection, have a greatly elevated risk for persistent HPV infection and cervical cancer, supporting the importance of the immune system in mediating HPV-associated disease progression (104-110). Importantly, we demonstrated that despite the decrease in total T cell population caused by early CD3 depletion, vaccination with a therapeutic HPV DNA vaccine, pNGVL4a-CRT/E7(detox), can still effectively enhance the HPV16 E7-specific CD8+ T cell responses in the spontaneous tumor bearing mice, leading to potent tumor control and prolonged mouse survival (**Figure 8-9**). These findings suggest that a potent

therapeutic HPV vaccine can potentially trigger effective HPV-specific immune responses even in immune suppressed patients. Moreover, we have previously demonstrated in a preclinical study that HPV DNA vaccination is capable of controlling HPV-associated tumor in the absence of CD4⁺ T cells (111), and resulted in the clearance of HPV infection.

In terms of disease progression, our model, with the incorporation of NRAS^{G12} oncogene, was able to generate tumor in three weeks, which is faster than normal HPV tumor growth. However, four weeks after oncogene injection, when the mice were sacrificed, enlarged cervical neck lymph nodes in tumor side were observed. These lymph node cells had positive luciferase activity and when implanted into the buccal area of immunodeficient athymic nude mice, resulted in the formation of gross tumor (**Fig. 10**). Our data suggest the metastatic capability of our tumor model from buccal area to regional lymph nodes. This exemplifies clinically relevant malignant tumor behavior and can potentially be utilized in future studies to analyze tumor migration.

Despite all of the potential benefits that our preclinical tumor model may introduce, we recognize that our model still has room for further improvements. In particular, our current spontaneous HPV tumor model involves the transfection and integration of HPV16 E6, HPV16 E7, and NRAS^{G12} oncogenes into mice. While it has been well documented that this combination is highly effective in triggering carcinogenesis (64), clinically reported HPV⁺ oral cancers are not typically associated with RAS mutation (112). In comparison, mutations in PI3K associated pathway is

observed in over 50% of HPV+ head and neck squamous cell carcinoma (112). Thus, the incorporation of mutant genes from the PI3K-AKT signaling pathway instead of NRAS^{G12} may further enhance the clinical relevance of this spontaneous HPV+ oral tumor model.

While the incidence of HPV-associated oropharyngeal cancer has been on the rise in developed countries, such as in North America and some in Europe (113,114), a significant portion of oropharyngeal cancer cases worldwide are still attributed to causes independent of HPV infection such as tobacco smoking (115). Unlike HPV+ oral cancers that are associated with HPV E6 and E7 oncogenes expression and mutation in PI3K signaling pathway, HPV- oral cancers are mainly characterized by mutations in TP53 (112). Previous studies utilized the administration of carcinogen 4-nitroquinoline 1-oxide (4-NQO) in mice to generate HPV- oral cancer (116-120); however, the induction of carcinogenesis by administration of 4-NQO alone is very slow, requiring up to 36 to 40 weeks before the tumor becomes visible. We believe our method to generate a spontaneous HPV+ oral tumor model may also be applied for the generation of a spontaneous HPV- oral tumor model. By integrating mutant TP53 genes into cells located at the buccal area of mice via sleeping beauty transposase system and exposing the mice to carcinogen 4-NQO, we believe we can generate clinically relevant spontaneous HPV- tumor model that forms tumors at a much faster rate, allowing for rapid evaluation of therapeutic options against HPV- oral tumors.

In conclusion, our model provides a fast, efficient, and simple option to induce

spontaneous formation of HPV+ tumor, which can be used to assess therapeutic treatment strategies. This model can potentially be used to identify effective therapeutic intervention, analyze tumor migration, and conduct tumor biology and tumor microenvironment research.

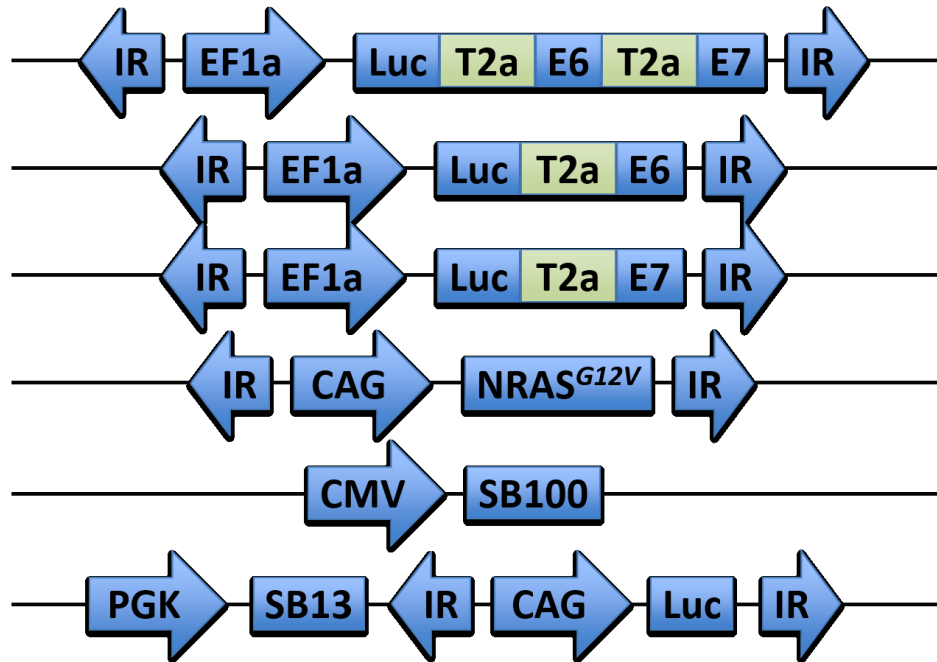
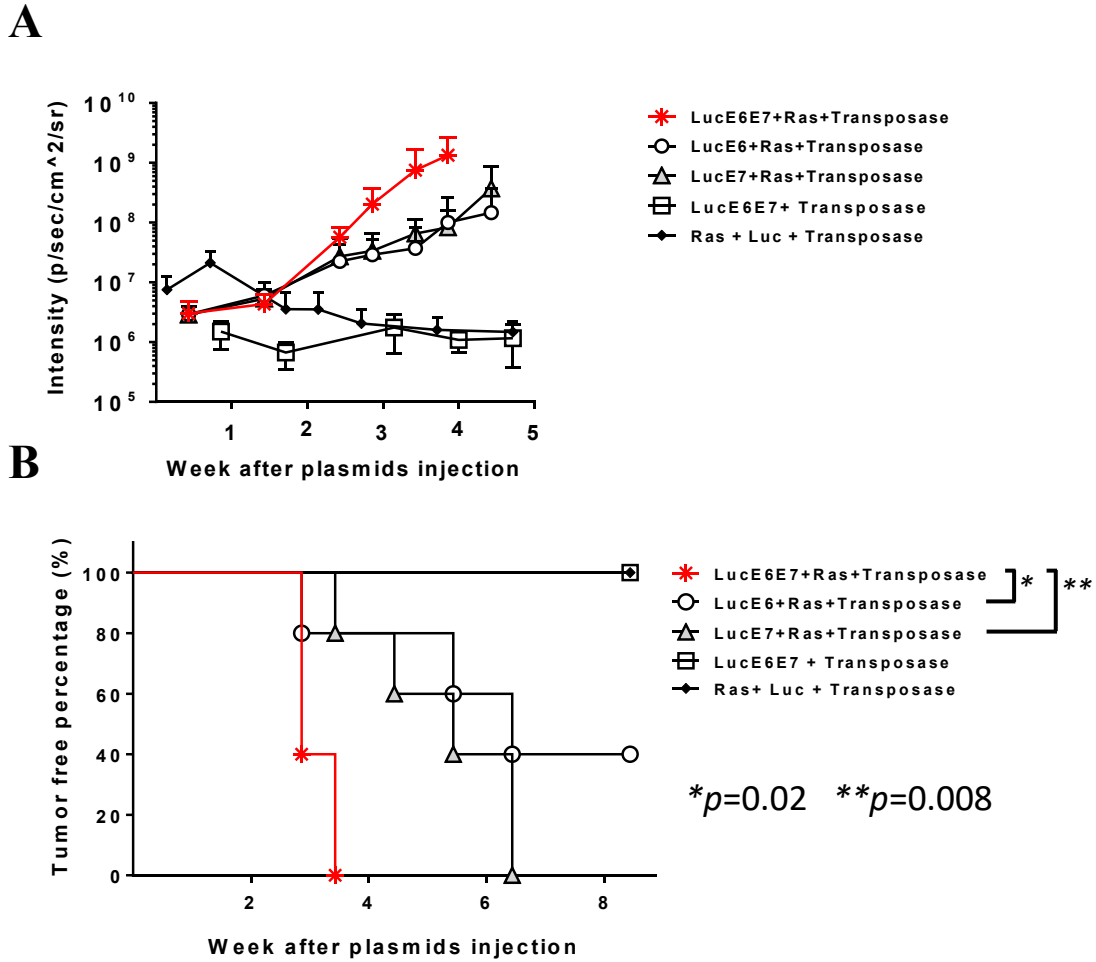


Figure 1. Schematic of plasmids used to induce oral tumors by oncogene transfection. HPV16 E6/E7 was fused with luciferase gene as a reporter gene under EF1a promoter; NRAS^{G12V} under CAG promoter; and transposase SB100 under CMV promoter. Both HPV16 E6/E7 and NRAS^{G12V} were flanked by the inverted repeats (IR) sequence which can be recognized and cut by transposase.



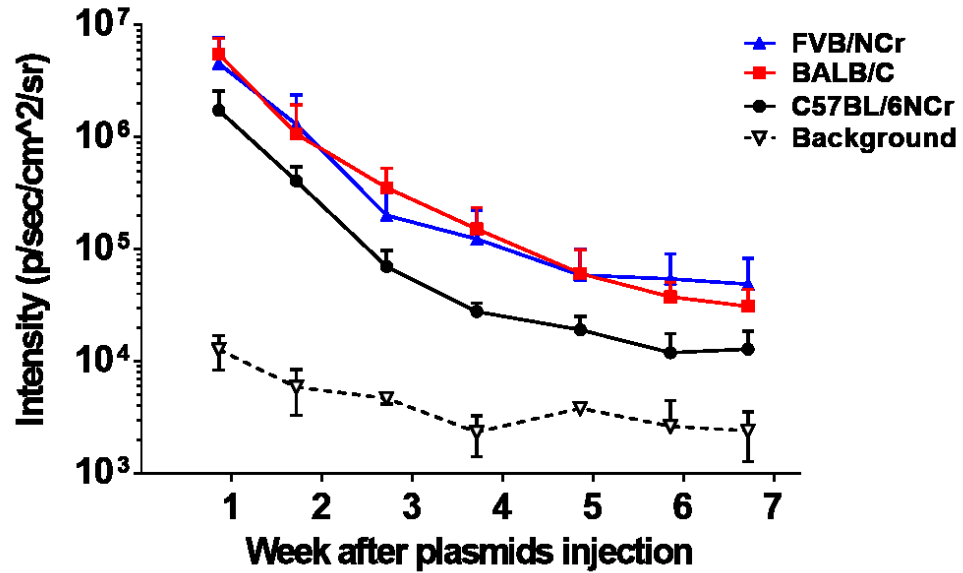


Figure 3. Immune competent mice suppressed tumor formation. C57BL/6NCr, BALB/C or FVB/NCr mice (5 mice in each group) received submucosal plasmids injection plus electroporation with plasmids containing HPV16 E6/E7, NRAS^{G12V} and SB100 transposase each with 10ug in weight and 30uL in total volume. The bioluminescence intensity was recorded by IVIS Spectrum.

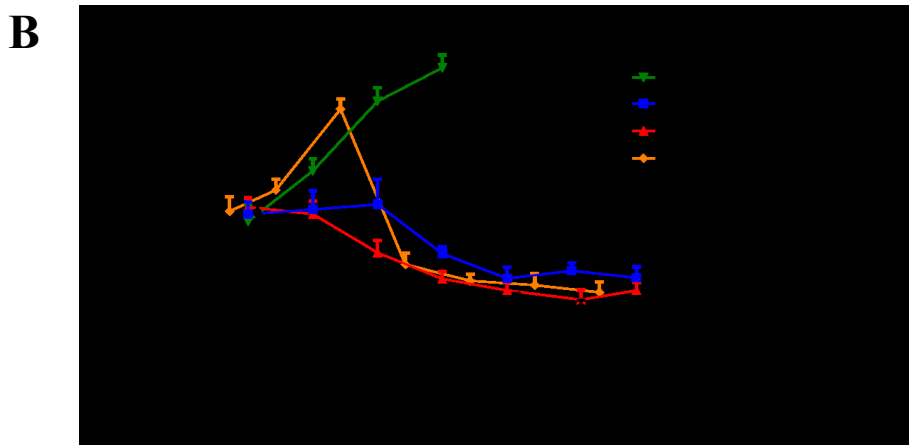
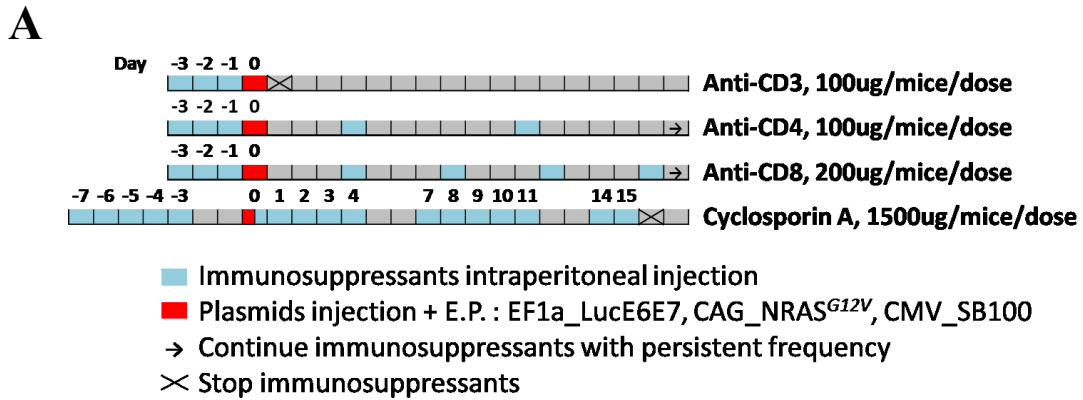


Figure 4. Generation of buccal tumor from immuno-competent mice.

(A) Schematic diagram of treatment protocol. In CD3-depleted group, C57BL/6NCr mice (n=5) received Anti-CD3 antibody 100ug intraperitoneal injection, 3 consecutive doses before injection of plasmids. In CD4-depleted group, C57BL/6NCr mice (n=5) received Anti-CD4 antibody 100ug intraperitoneal injection, 3 doses before and 1 dose every week after plasmids injection. In CD8-depleted group, C57BL/6NCr mice (n=5) received Anti-CD8 antibody 200ug intraperitoneal injection, 3 doses before and 2 doses every week after plasmids injection. In cyclosporine group, C57BL/6NCr mice (n=5) received cyclosporine 1500ug/mice (~75mg/kg) subcutaneous injection, 5 consecutive doses before and continuously every week after plasmids injection. (B) Bioluminescence kinetics of buccal tumor in different groups. (* Stop cyclosporine treatment.)

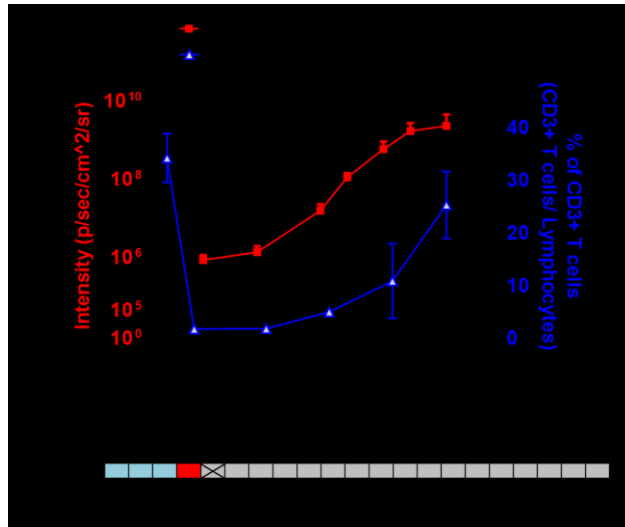
A**B**

Figure 5. CD3 triple depletion HPV16 oral tumor model. C57BL/6NCr mice (n=5 per group) received CD3 depletion with 100ug Anti-CD3 antibody intraperitoneal injection for 3 consecutive days followed with submucosal plasmids injection and electroporation in buccal area. The plasmids contained HPV16 E6/E7, NRAS^{G12}, and SB100 each with 10ug in weight and total 30uL in volume. (A) Bioluminescence kinetics of buccal tumor. Black star indicated visualized overt tumor. (B) Peripheral blood from mice tail artery was taken for flow cytometry to check CD3+ T cells percentage over time. (C) The bioluminescence intensity showed positive correlation with tumor volume.

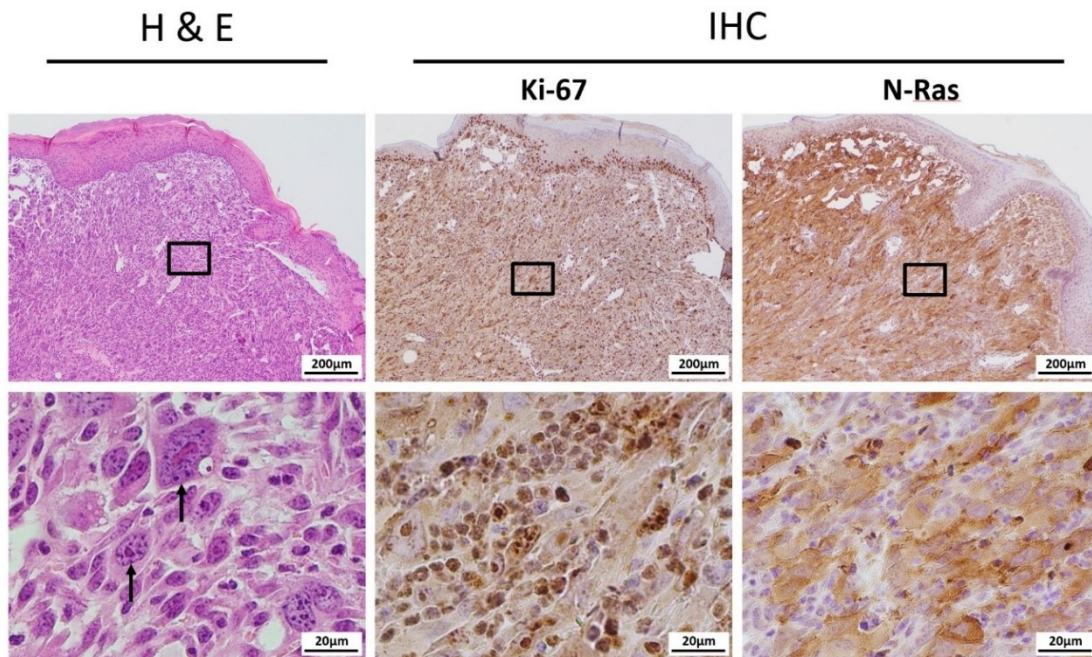
A**B**

Figure 6. Characterization of tumors arising from CD3 triple depletion HPV16 oral tumor model. (A) Representative pictures of gross buccal tumor arising from oncogene co-transfection in C57BL/6 mice. The plasmids contained HPV16 E6/E7, NRAS^{G12V}, and SB100. (B) Representative histology sections with H&E stain and special IHC staining with Ki-67 and N-Ras.

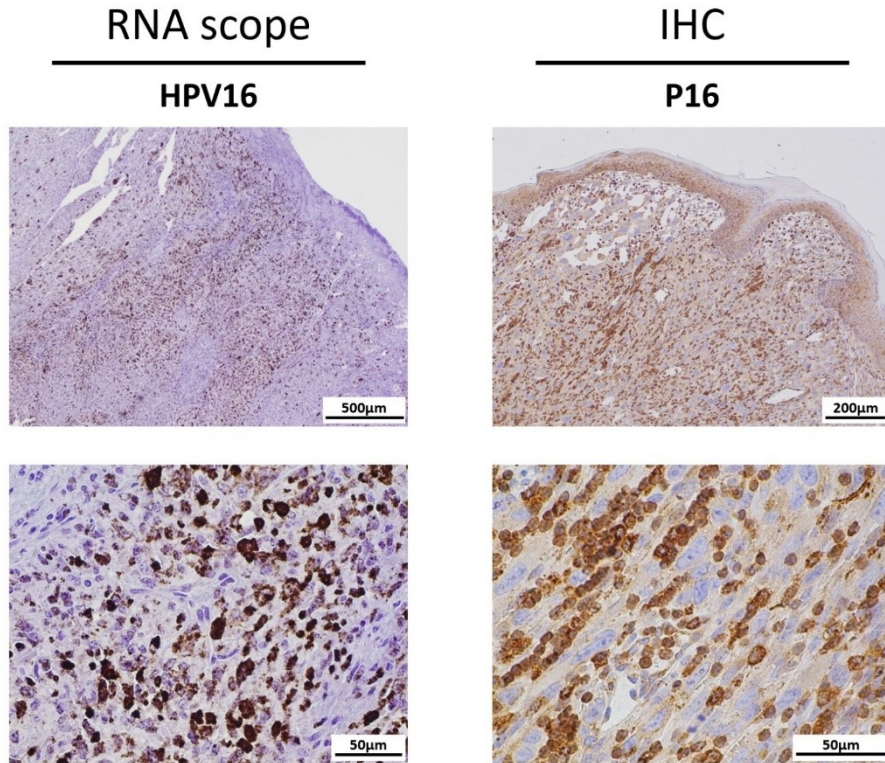
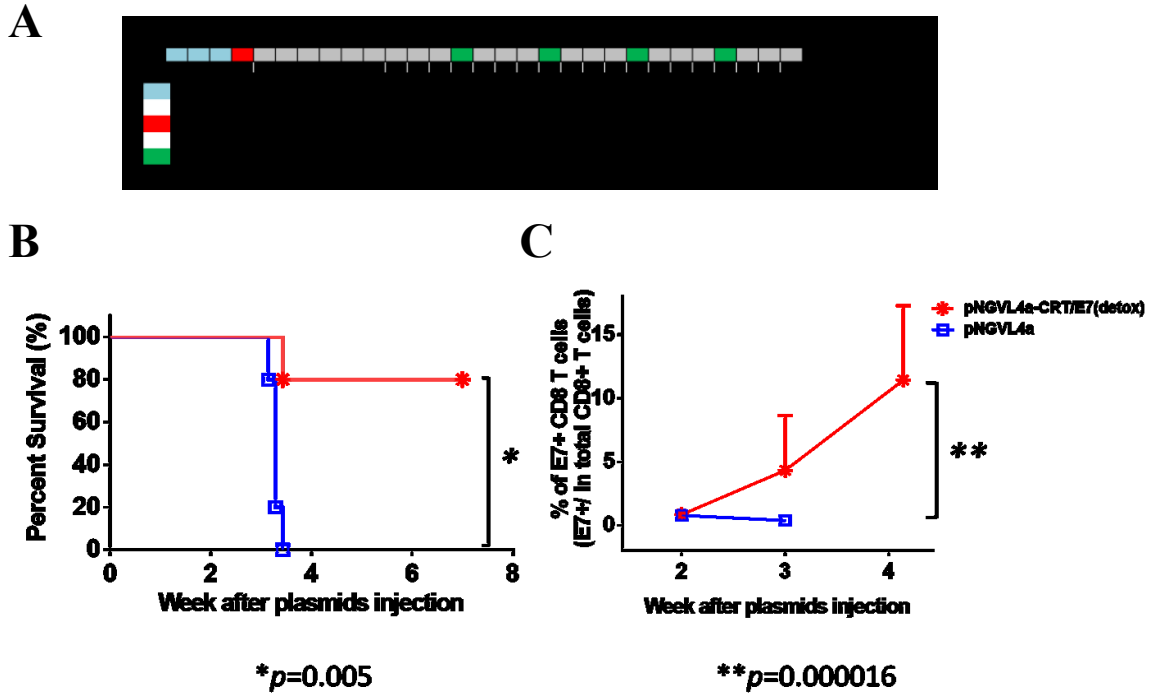


Figure 7. Evidence of HPV expressing tumor of CD3 depletion buccal tumor model.

C57BL/6NCr mice received 3 consecutive days of CD3 depletion followed by buccal plasmids injection and electroporation. The plasmids included HPV16 E6/E7, NRAS^{G12V}, and SB100. Representative section of RNAscope targeting HPV16 RNA and IHC staining with HPV-associated biomarker p16 were shown.



tumor model. (A) Schematic diagram of treatment regimens and the time course. C57BL/6 mice (5 per group) received pretreatment of CD3 depletion followed with submucosal injection and electroporation in buccal area with plasmids containing HPV16 E6/E7, NRAS^{G12V}, and SB100 transposase. After plasmids injection, the mice of treatment group received DNA vaccination with pNGVL4a-CRT/E7 while the control group received pNGVL4a since day 10 with 4-day interval. (B) Kaplan-Meier survival analysis of mice in CD3 triple depleted buccal tumor model. (C) Peripheral blood from mouse tail artery was taken for flow cytometry. E7 specific CD8+ T cells percentage was checked over time since day 14 after plasmids injection with one-week interval.

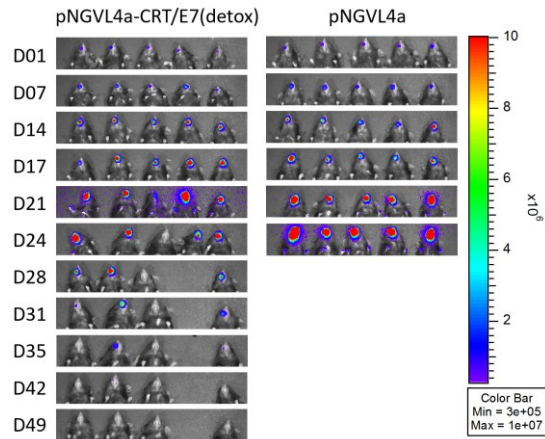
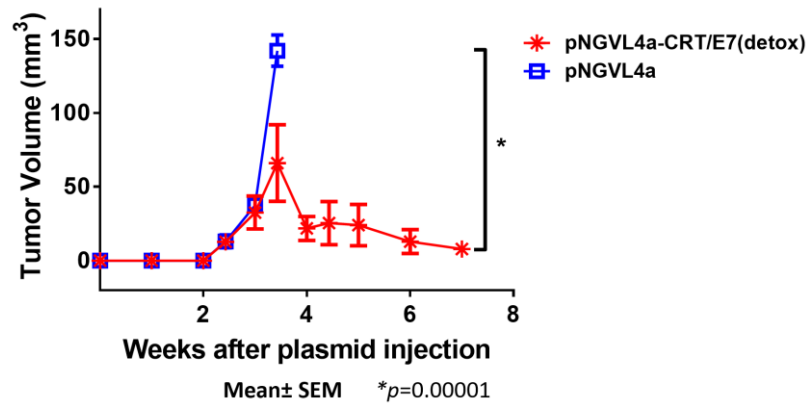
A**B**

Figure 9. Evaluation of DNA vaccination effect in CD3 triple depletion spontaneous tumor model. C57BL/6NCr mice (5 per group) received pretreatment of CD3 depletion for 3 consecutive days followed with submucosal injection and electroporation in buccal area with plasmids containing HPV16 E6/E7, NRAS^{G12V}, and SB100 transposase. After plasmids injection, the mice of treatment group received DNA vaccination with pNGVL4a-CRT/E7 while the control group received pNGVL4a since day 10 with 4-day interval. (A) Real-time bioluminescence image of tumor-bearing mice. (B) Line graph depicting the change in tumor volume of spontaneous tumor bearing mice after plasmids transfection.

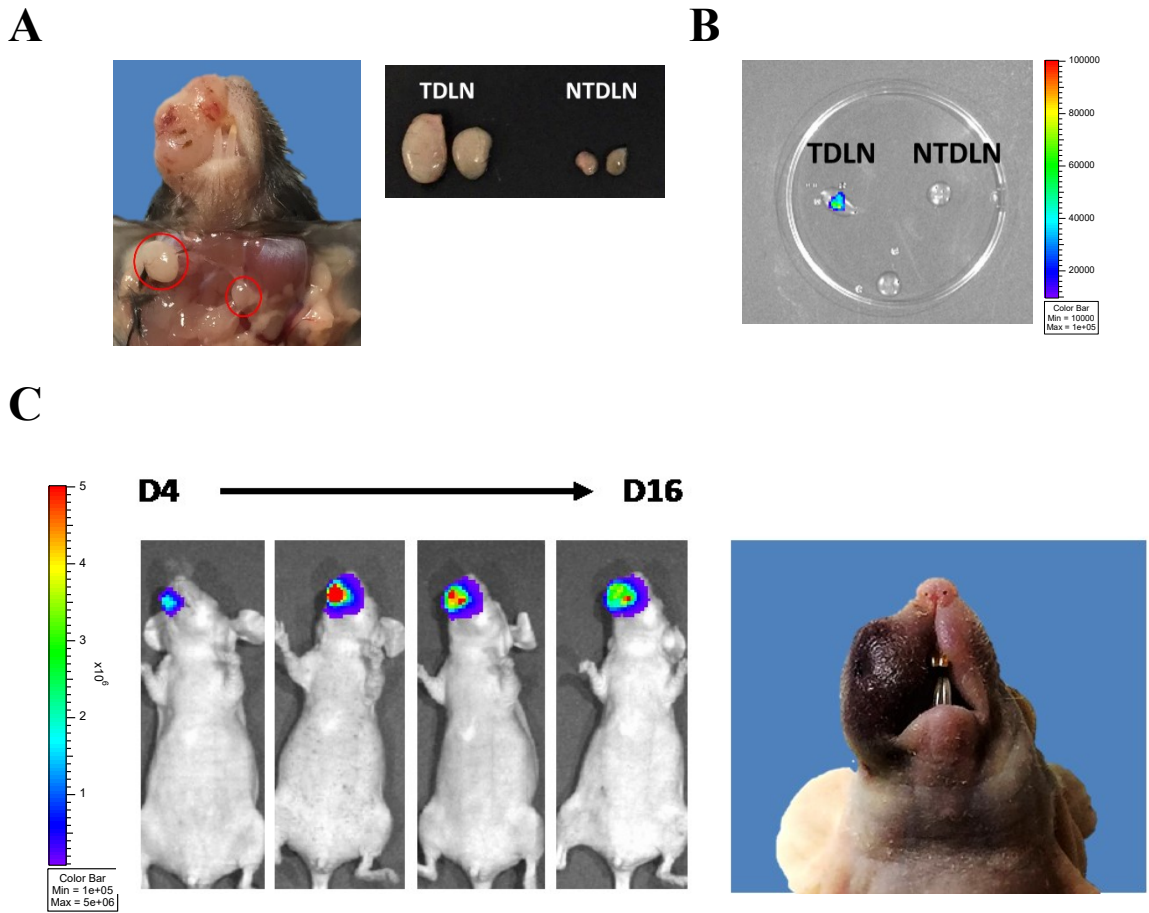


Figure 10. Evidence of metastasis capability of spontaneous tumor model.

Representative mice were presented. C57BL/6NCr mice received Anti-CD3 antibody for 3 consecutive days followed with buccal plasmids injection with HPV16 E6/E7, NRAS^{G12V} and SB100 to deplete T cells. (A) Representative image showing the tumor draining lymph node (TDLN) and non-tumor draining lymph node (NTDLN) of plasmid transfected mice at the time of euthanasia. (B) Enlarged tumor draining lymph nodes showed detectable luciferase activity compared with non-tumor lymph nodes. (C) Re-implantation of proliferated lymph nodes cells showed positive luciferase activity as well as tumor formation.

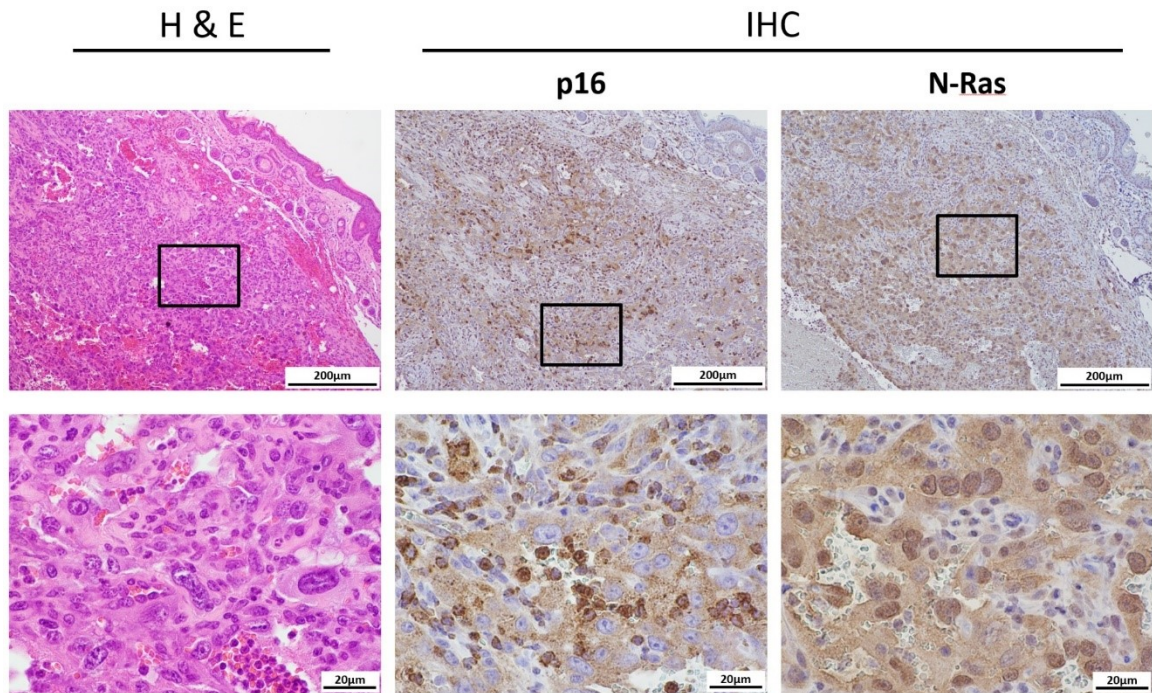


Figure 11. Metastatic lymph nodes induce tumor with original tumor characteristics.

The enlarged tumor side superficial cervical lymph nodes were surgically removed, minced, treated with tissue digestion buffer, filtered, then cultured in RPMI-based antibiotics containing medium. After cell expansion, the cells were trypsinized, PBS washed, re-suspend in 40uL PBS solution, followed by submucosal buccal injection into immune-deficient athymic mice. Representative histology showed reproducing tumor characteristics after re-implantation of lymph nodes cells.

CHAPTER 3

Attempt to generate clinically relevant carcinoma with keratinocyte-restricted K14 promoter

Introduction

In **Chapter 2**, we presented a HPV16 expressing pre-clinical buccal tumor model that forms tumor at a consistent rate, develops antitumor immunity in response to immunotherapy, and possesses metastatic capability. However, there are still some limitations to this model. One such limitation is the histological features of the resulting tumor. Our buccal tumor model showed microscopic features more similar to those of soft tissue sarcoma. While HPV has tropism for epithelial tissue (121,122), the susceptibility of developing precancerous or invasive cancer lesions from HPV infection is limited to some special epithelial areas, such as the cervical transformation zone, the anal transformation zone and the oropharynx (20,32). The transformation zone is where two different cell types meet, such as the squamocolumnar junction where squamous cells on the exocervix meet with glandular cells on the endocervix.

In order to understand the tumor biology of head and neck squamous cell carcinoma (HNSCC), several transgenic mouse models combined HPV oncogene E6/E7 with oncogenes, such as KRAS, knockout p53 and UVB irradiation or chemical carcinogens such as 4-Nitroquinolone 1-oxide (4-NQO), to induce cancers (117,123,124). Furthermore, to successfully generate HPV-positive carcinoma, many models used

keratinocyte-restricted K14 promoter in their transgenic mice to drive the expression of either E6/E7 or other oncogenes. For example, Strati et. al combined 4-NQO in the drinking water of K14-E6/K14-E7 bi-transgenic mice to generate carcinoma on the tongue (89). Zhong et al used triple transgenic mice containing the HPV-Luc, K14-CreERTam, and LSL-Kras transgenes, with tamoxifen treatment resulted in the induction of HPV+ oral carcinoma development (91).

Based off of the success of previous studies in generating preclinical HPV+ carcinoma models through the utilization of Keratinocytes-restricted promoter K14, in this chapter, we attempt to generate carcinoma by using either K14-driven HPV16 E6/E7 or K14-driven transposase SB100.

Materials & Methods

Mice and Animal Care

Six to eight-week-old female athymic nude (Athymic NCr-nu/nu, strain #553) mice were purchased from Charles Rivers Laboratories (Frederick, MD, USA). All mice were maintained at Johns Hopkins University School of Medicine (Baltimore, MD) animal facility under specific pathogen free conditions. All procedures were performed according to protocols approved by the Johns Hopkins Institutional Animal Care and Use Committee and in accordance with recommendations for the proper use and care of laboratory animals.

Plasmid Vectors

To generate pcDNA3-Luc, luciferase was cloned into XbaI/XhoI sites of pcDNA3 by primers (aaatctagaatggaagacgccaaaacat and aaactcgagcagcgcatctttccgcct). To generate pcDNA3-Luc-T2a-E7, T2a-E7 was cloned into Xho I/EcoRI sites of pcDNA3-Luc by primers (aaactcaggaggcagaggaagtcttctaacaatgcggtgacgtggaggagaatcccggccctatgcatggagatacact and tttgaattctggttctgagaacagatgg). To generate luciferase E7 and E6 oncogene fusion construct, pcDNA3-Luc- T2a-E7- T2a-E6), T2a-E6 was cloned into EcoRI/BamHI sites of pcDNA3-Luc- T2a-E7 by primers (aaagaattcaggggcagaggaagcttcaacaatgcggtgacgtggaggagaatcccggccctatgcacaaaagagaact, and tttgatcccagctgggttctctacgtg). To generate Pkt2-Luc-T2a-E7- T2a-E6, Luc-T2a- E7-T2a- E6 was removed from pcDNA3- Luc-T2a- E7-T2a-E6 by XbaI/BamHI sites and cloned into XbaI/Bgl II sites of the Pkt2/clp-akt vector (62). To generate K14-Luc-T2a-E7-T2a-E6, K14 promoter was cloned into AgeI and XbaI sites of pkt2-Luc-T2a-E7-T2a-E6 by primers (AAAaccggtGCTAGGGTTCTGGTGTGGTGCG and AAAtctagaGAGGAGGGAGG-TGAGCGAGCGA). To generate K14 SB100, K14 promoter was cloned into DraI and XbaI sites of pCMV(CAT)T7-SB100 by primers (gggtcactacgtgGCTAGGGTTCTGG-TGTTGGTGCG and AAActcgagGAGGAGGGAGGTGAGCGAGCGA).

In vivo buccal tumor formation

For the generation of tumor in immune-deficient mice, athymic nude mice (five per group) were submucosally injected with (1) plasmids encoding Luciferase and HPV16 E6/E7 under K14 promoter, mutant Ras (pT/Caggs-NRAS^{G12V}, addgene #20205) and SB100 (pCMV(CAT)T7-SB100, addgene #34879) or (2) plasmids encoding Luciferase and HPV16 E6/E7, mutant Ras and SB100 under K14 promoter, or (3)

plasmids encoding Luciferase and HPV16 E6/E7 under K14 promoter, SB100 under K14 promoter and NRAS^{G12} into buccal area followed by electroporation. Each plasmid was 10ug in weight and 30uL in total injection volume.

In vivo vaginal tumor formation

After dilatation with vaginal swab, athymic nude mice (five per group) were submucosally injected in lower third of vaginal mucosa with plasmids combination as described in the previous paragraph. Each plasmid was 10ug in weight and 30uL in total injection volume.

The surface dimensions of the tumor were measured with digital calipers. To record the survival of the tumor-bearing mice, either natural death or tumor diameter greater than 7mm was counted as death.

In vivo bioluminescence image

This procedure is described in **Chapter 1**.

Histology and Immunohistochemistry staining

For buccal tumors, when the tumor size exceeded 7mm in diameter, mice were considered to have an unsustainable tumor burden, and euthanized according to protocol. For vaginal tumors, when the tumor size exceeds 10mm in diameter, mice were considered to have excessive tumor burden, and euthanized according to protocol. The tumors were surgically removed, isolated and placed into 10% Neutral buffered formalin

solution for adequate fixation with a minimum 48 hours at room temperature. The tumor samples were then sent to Johns Hopkins University Oncology Tissue Services for subsequent procedures including paraffin embedding, tissue sectioning, hematoxylin and eosin (H&E) staining and immunohistochemical (IHC) staining. The histology slides were reviewed by Dr. T.-C. Wu.

Statistical analysis

The statistical analysis was performed with the GraphPad Prism V.6 software (La Jolla, CA, USA). Data were expressed as means \pm standard deviations (SD).

Results

HPV16 E6/E7 under K14 promoter generate buccal tumor with a slow growth rate.

Based on the promising tumor generation rate of our CD3 depletion buccal tumor model shown in **Chapter 2**, I changed the components of the original plasmid combination by modifying the promoters of the plasmid. First, I replaced the plasmid encoding EF1a-driven HPV16 E6/E7 and luciferase (EF1a_LucE6E7) with plasmid encoding K14-driven HPV16 E6/E7 and luciferase (K14_LucE6E7) (**Fig. 1**). Plasmids encoding K14_LucE6E7, NRAS^{G12V}, and transposase SB100 were submucosally injected in the buccal area followed by electroporation of athymic nude mice, which have abnormal thymus with T cell function deficiency. The enzyme luciferase encoded in the plasmids can catalyze chemical reactions of molecular oxygen with the substrate luciferin. This reaction generates visible light from viable, transfected cells that can be

measured quantitatively. After injection of plasmids, in vivo tumor growth was monitored by in vivo bioluminescence image with IVIS spectrum. Compared with original EF1a_LucE6E7, bioluminescence kinetics of buccal tumor from K14_LucE6E7 increased slowly (**Fig. 2A**) with significantly lower tumor generation rate (**Fig. 2B**). In addition, we observed a wide variation for the tumor growth rate. Under K14 promoter, only two out of five (40%) mice generate gross buccal tumor (**Fig. 3**).

HPV16 E6/E7 under K14 promoter in buccal tumor model cannot generate clinically relevant carcinoma

With K14_LucE6E7 plasmid, spontaneous tumors arising from mucosa area have gross features resembling the exophytic type oral cancer, appearing as a solid, papillary mass that caused bleeding ulcer when it grew larger (**Fig. 4A**). The gross features were similar to the tumor from EF1a_LucE6E7 plasmid. Representative sections of histological examination were shown in **Fig. 4B-C**. In microscopic features, the tumors showed spindle shaped tumor cells with highly mitotic activity. The cytokeratin epithelium marker showed relatively negative staining inside the tumor mass. Compared with **Fig. 6B** in **Chapter 2**, the tumor arising from K14_LucE6E7 showed relatively less expression of a cell proliferation biomarker Ki-67, which was compatible with its relatively slow tumor growth (**Fig. 4B**). The special IHC staining revealed positive HPV-biomarker p16 expression (**Fig. 4C**).

Characteristics of buccal tumor arising from K14-driven transposase SB100

In a separate experiment, I used K14-driven transposase SB100 to replace original

CMV-driven SB100 (Fig. 1). Plasmids EF1a_LucE6E7, NRAS^{G12V}, and K14_SB100 were submucosally injected into buccal mucosa of athymic nude mice followed by electroporation. As shown in **Figure 5**, replacing CMV-driven SB100 with a K14 promoter had no significant difference in tumor kinetics and tumor generation rate. For the histological characteristics, buccal tumors formed from K14_SB100 showed spindle shaped tumor cells, the majority of which lacked classical carcinoma features (**Fig. 6B**). These sarcoma-like microscopic features were similar to the buccal tumors arising from the original plasmids combination without K14 promoters as shown in **Chapter 2, Figure 6**.

Combining K14-driven HPV16 E6/E7 and K14-driven transposase showed no difference in tumor generation.

Subsequently, I tried to do buccal submucosal injection with plasmids encoding K14_LucE6E7, K14_SB100, and original NRAS^{G12V}. In addition to delivering the plasmids via injection with electroporation, I also performed a separate experiment to deliver the plasmids via gene gun. However, compared with the original plasmids combination, combining K14_LucE6E7 and K14_SB100 resulted in significantly slower tumor kinetics, while the kinetics from gene gun delivery was even slower than that of plasmid injection with electroporation. With this plasmids combination, neither of the DNA delivery methods could generate buccal tumor efficiently (**Fig. 7**).

K14-driven HPV16 E6/E7 generate clinically relevant carcinoma in cervico-vaginal tumor model

While our attempt to generate a preclinical model of HPV+ buccal carcinoma using K14-driven genes was not successful, we also attempted to apply K14_LucE6E7 with NRAS^{G12V}, and transposase SB100 in vaginal mucosa to generate preclinical model of HPV+ cervical carcinoma. Athymic nude mice (n=5) received submucosal injection of plasmids DNA followed by electroporation in the cervico-vaginal track. After injection of plasmids, in vivo tumor growth was monitored by in vivo bioluminescence imaging with IVIS spectrum. We observed the bioluminescence kinetics of vaginal tumor from K14_LucE6E7 increased much slower than tumors formed from the original EF1a_LucE6E7 encoding plasmid (**Fig. 8**). Similar to our observation from previous experiments, there were individual variations in tumor size and growth rate. Of the 5 transfected mice, only three (60%) successfully developed tumor. The first tumor formation was observed in the 4th week after plasmids transfection while other two tumors were not observed until the end of second month (**Fig. 9**). When the tumor grew to exceed 10mm in one diameter, the mouse was sacrificed.

In macroscopic appearance, we noted in the vaginal tumor that a major portion of the tumor consisted of fluid, with a minor portion consisting of solid mass (**Fig. 10A**). After surgical removal, the tumor was placed in 10% Neutral buffered formalin for subsequent histology examination. In terms of the microscopic features, the vaginal tumor showed malignant, small, round-to-oval nuclei, and finely granular chromatin with abundant mitotic characters (**Fig. 10B**). The special IHC staining showed positive proliferating marker Ki-67 as well as carcinoma biomarker cytokeratin. (**Fig. 10B**) The tumor also showed positive HPV biomarker p16 in IHC staining (**Fig. 10C**).

K14-driven HPV16 cervical tumor showed poor correlation between tumor size and luciferase activity.

For cervical tumors formed from K14_LucE6E7, we noted inconsistent correlation between tumor growth and bioluminescence intensity, with some of the resulted tumor mass displaying little bioluminescence intensity (**Fig. 11**). This inconsistency was also reflected in the difference of tumor histology. For tumors with similar tumor size, the tumor with higher bioluminescence intensity, which correlated with HPV16 E6/E7 gene expression, displayed microscopic features consistent with the characteristics of a carcinoma, while the tumor with low bioluminescence intensity mainly consisted of cystic structure inside the tumor (**Fig. 11**).

Discussion

In the second part of my thesis project, we noted the resultant tumor kinetics with keratinocyte-restricted promoter K14 differed from the original plasmids combination we used in CD3 depletion buccal model. Not only did the tumors display slower growth speed, there were also huge individual variations in the tumor generation rate. Additionally, K14 promoter cannot guarantee the formation of carcinoma. I suspected that this condition was due to technical limitations.

K14 is a keratinocyte-restricted promoter, and keratinocytes are located in the most superficial layer of epithelium above basal layer. The keratin layer is a very thin layer of the mucosal structure and is very difficult to introduce DNA by manual injection.

The submucosal injection is typically performed below basal layer and lamina propria. The lack of an efficient method to target and deliver the plasmids to the keratinocytes in submucosal area resulted in inactive K14 promoter. In the combination with K14_LucE6E7, insufficient HPV16 E6/E7 expression caused the majority of the transfected cells to consist of only NRAS^{G12V} and SB100 expression. The single oncogene expression resulted in weaker tumorigenesis. For the cells that were transfected with NRAS^{G12V} or SB100 alone, the tumor formation was even weaker. In addition, these cells should have no luciferase activity due to inactive K14. However, occasional diffusion of the K14-driven plasmids to epithelial keratinocytes caused HPV16 E6/E7 expression. This occasional expression was able to synergize NRAS^{G12V} and induce cell transformation. These epithelial cell transformations resulted in tumors with carcinoma histology characteristics. However, the expression of K14_LucE6E7 was unpredictable with great uncertainty. This may explain the different tumor growth rates, rare carcinoma formation, and inconsistent bioluminescence activity we observed in models with K14_LucE6E7.

For the plasmids combination with K14_SB100, the expression of transposase is also very rare because of the inability to target keratinocytes in submucosal area. However, the two major oncogenes, HPV16 E6/E7 and NRAS^{G12V} can be expressed in most cells. The injected plasmids may have random chromosomal integration and transient gene expression without the help of the sleeping beauty transposon system. However, the synergistic tumorigenesis effect of HPV16 E6/E7 and NRAS^{G12V} is highly potent and thus maintained similar tumor generation rate as original plasmids

combination.

To overcome technical limitations and introduce oncogenic plasmids into HPV-targeted epithelial cells, DNA introduction via gene gun was attempted. However, the latency of gene expression and tumor formation was worse, and none of the mice generated gross tumor (Fig. 7). In future experiments, we would like to try plasmids combination of K14-driven RAS after determining an efficient way to introduce DNA to the keratin layer.

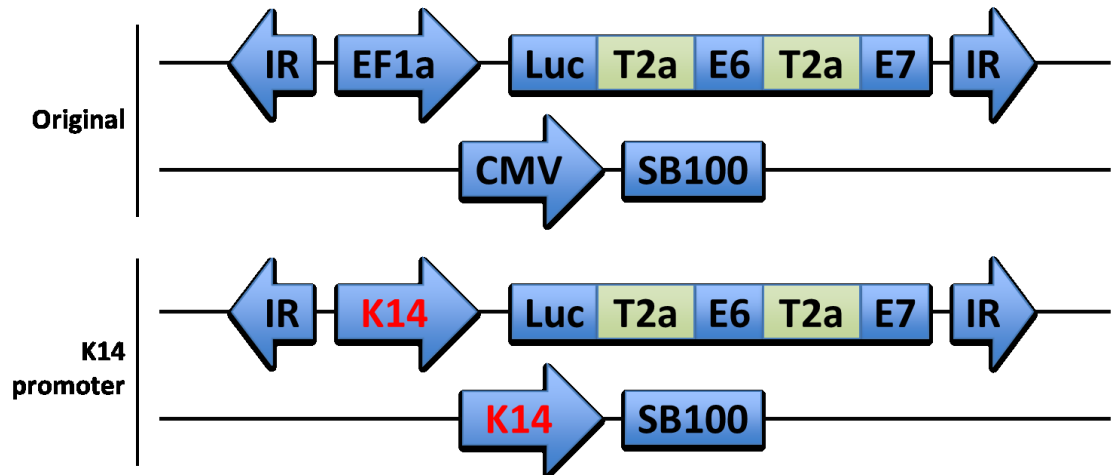


Figure 1. Schematic of plasmids with K14 promoter. Original plasmids in CD3 depletion buccal tumor model were shown in upper panel. For K14-driven plasmids, HPV16 E6/E7 was fused with luciferase gene as a reporter under keratinocytes-restricted promoter K14. Transposase SB100 is also cloned under K14 promoter. NRAS^{G12} is still under CAG promoter. Both HPV16 E6/E7 and NRAS^{G12V} were flanked by the inverted repeats (IR) sequence that can be recognized and cut by transposase protein SB100.

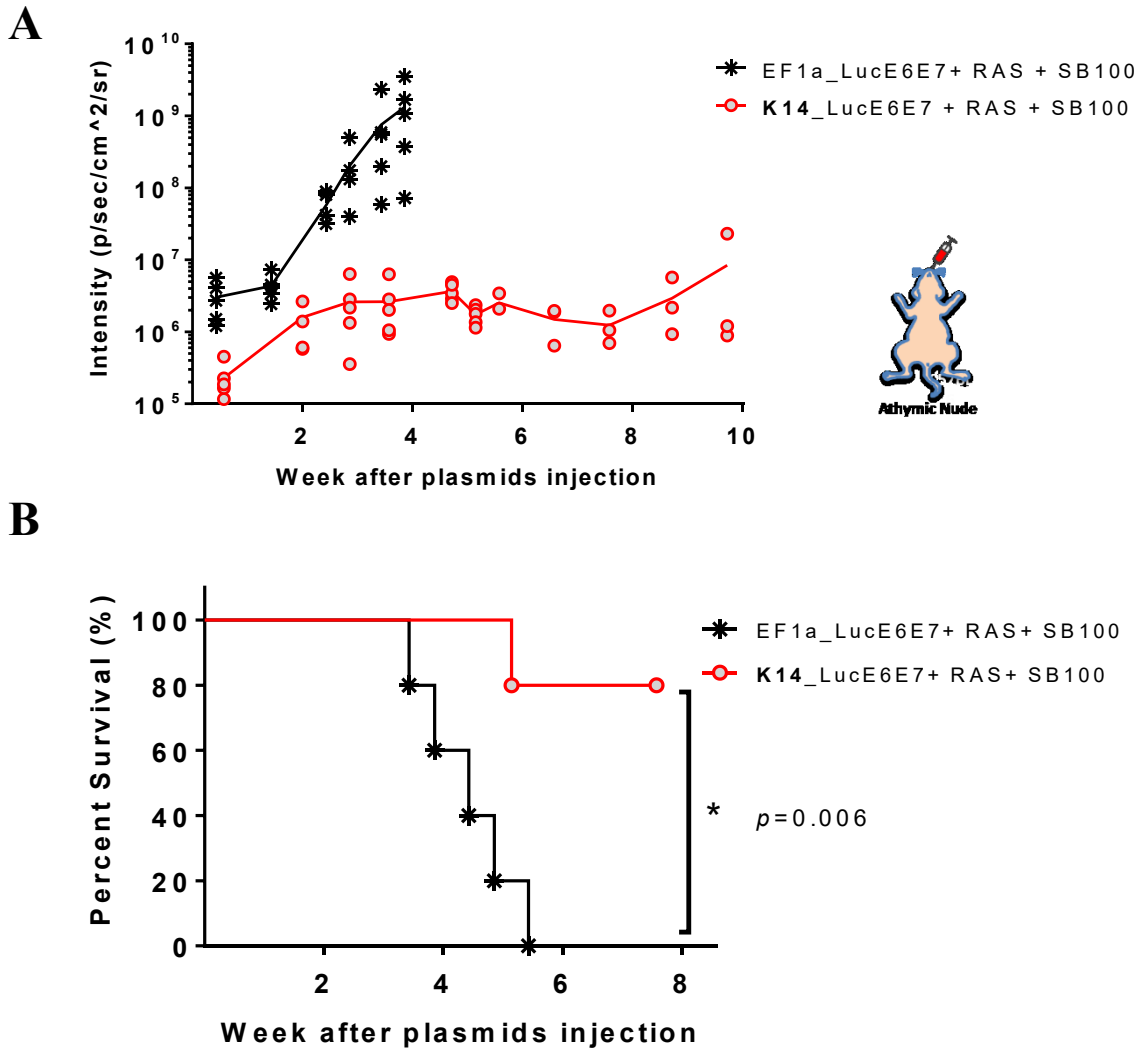


Figure 2. Buccal tumors arising from K14-driven HPV16 E6/E7. Athymic nude mice (n=5 in each group) received submucosal injection of plasmids DNA followed by electroporation in buccal area. One group received plasmids including EF1a_LucE6E7, NRAS^{G12V} and SB100. The other group received plasmids including K14_LucE6E7, NRAS^{G12V} and SB100. All plasmids were given with 10ug in weight and 30uL in total injection volume. (A) Bioluminescence kinetics were recorded by IVIS spectrum system. (B) Kaplan–Meier Survival curve. Defination of death: tumor logest diameter > 7 mm.

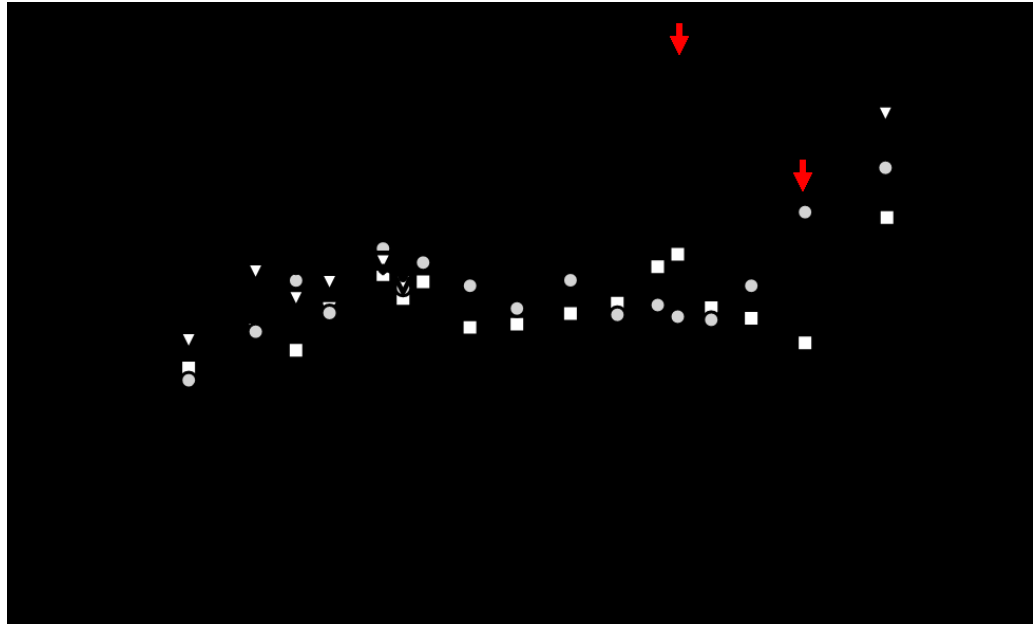


Figure 3. Bioluminescence kinetics of each buccal tumors arising from HPV16 E6/E7 under K14 promoter. Athymic nude mice (n=5) received submucosal injection of plasmids DNA followed by electroporation in buccal area. These plasmids contained K14_LucE6E7, NRAS^{G12V}, and SB100 each with 10ug in weight and 30uL in total volume. Bioluminescence kinetics of buccal tumor in each mouse were recorded by IVIS Spectrum. Red arrows indicate gross tumor formation.

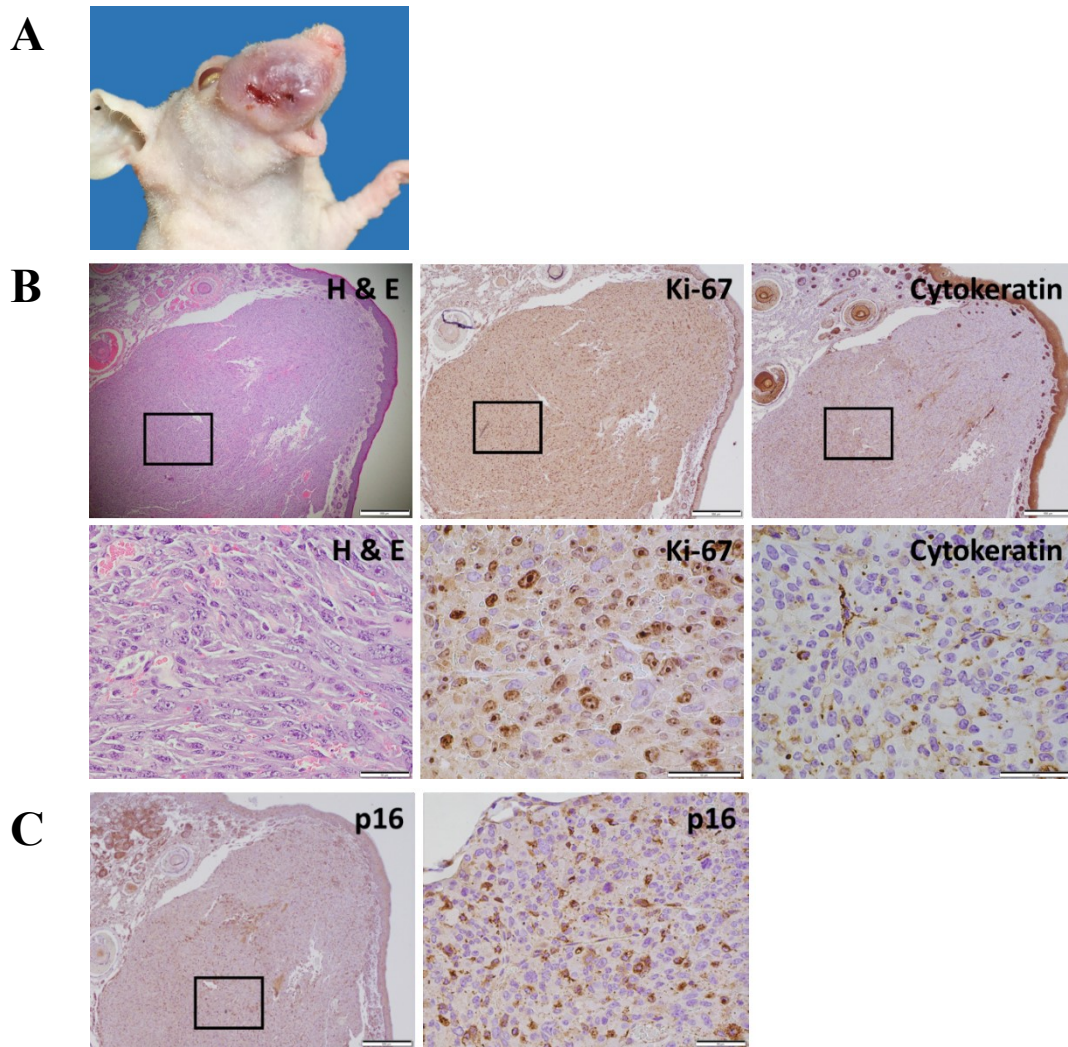


Figure 4. Characterization of buccal tumors arising from HPV16 E6/E7 under K14 promoter. Athymic nude mice (n=5) received submucosal injection of plasmids DNA followed by electroporation in buccal area. These plasmids contained K14_LucE6E7, NRAS^{G12V}, and SB100 each with 10ug in weight and 30uL in total volume. (A) On day77 after plasmids injection, at the time of sacrifice, gross buccal tumor picture was taken. (B) Representative histology sections with H&E stain and special IHC staining with Ki-67 and cytokeratin. (C) Evidence of HPV(+) tumor: IHC staining with HPV associated biomarker p16.

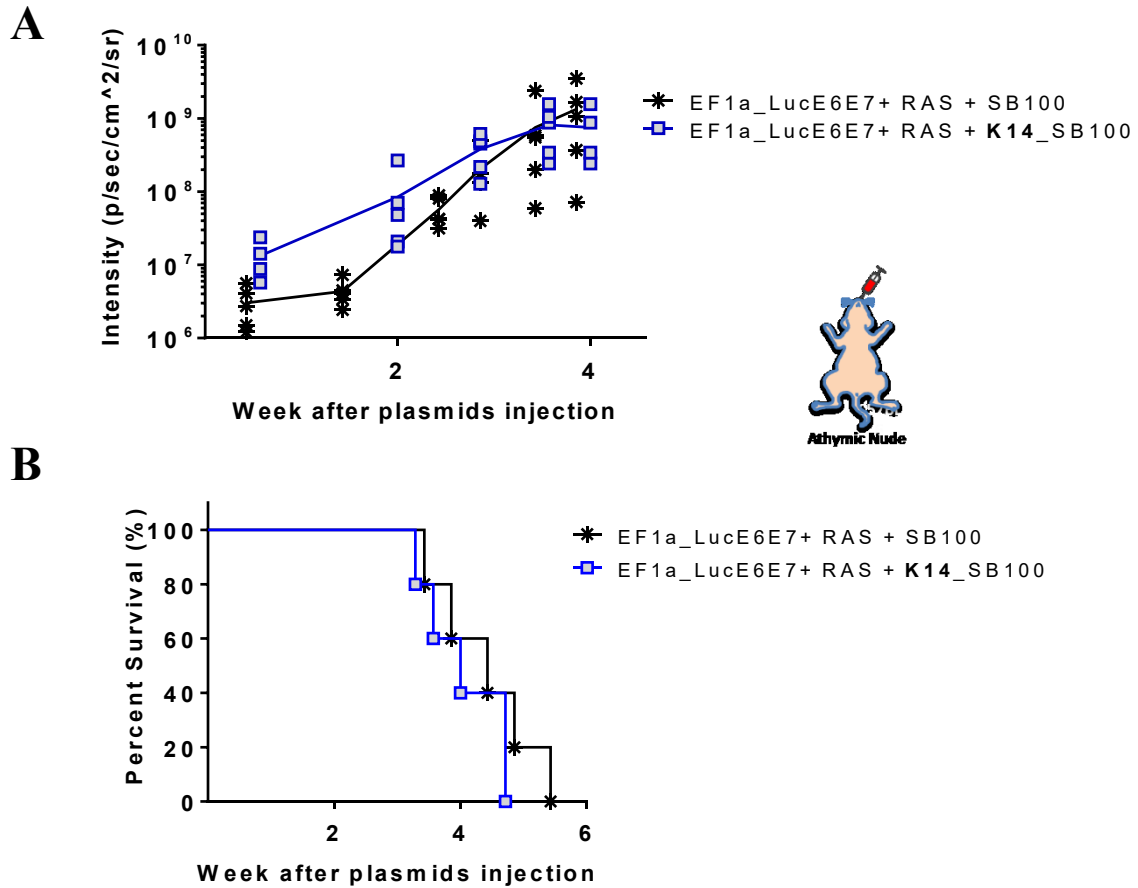


Figure 5. Buccal tumors arising from K14-driven transposase SB100. Athymic nude mice (n=5 in each group) received submucosal injection of plasmids DNA followed by electroporation in buccal area. One group received plasmids including EF1a_LucE6E7, NRAS^{G12V} and SB100. The other group received plasmids including EF1a_LucE6E7, NRAS^{G12V} and K14_SB100. All plasmids were given with 10ug in weight and 30uL in total injection volume. (A) Bioluminescence kinetics were recorded by IVIS spectrum system. (B) Kaplan–Meier Survival curve. Definition of death: tumor diameter >7 mm.

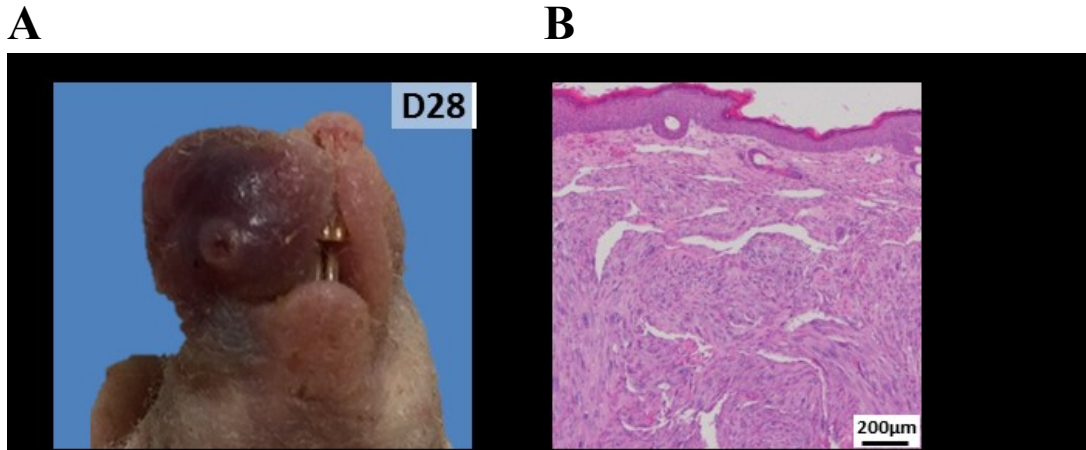


Figure 6. Characterization of buccal tumors arising from SB100 under K14 promoter. Athymic nude mice (n=5) received submucosal injection of plasmids DNA followed by electroporation in buccal area. These plasmids contained EF1a_LucE6E7, NRAS^{G12V}, and K14_SB100 each with 10ug in weight and 30uL in total volume. (A) Macroscopic features of buccal tumors on day28 after plasmids injection. (B) Microscopic histological features under H&E staining.

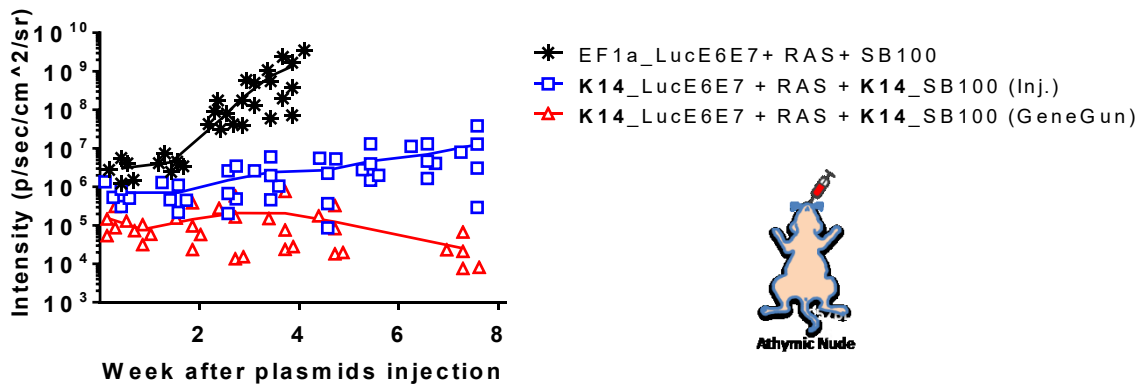


Figure 7. Combing K14-driven HPV16 E6/E7 and K14-driven SB100 with different plasmids delivery route. Athymic nude mice (n=5 in each group) received submucosal injection of plasmids DNA followed by electroporation in buccal area. The plasmids combination were indicated in the figure with each individual plasmid 10ug in weight and 30uL in total injection volume. Bioluminescence kinetics were recorded by IVIS spectrum system.

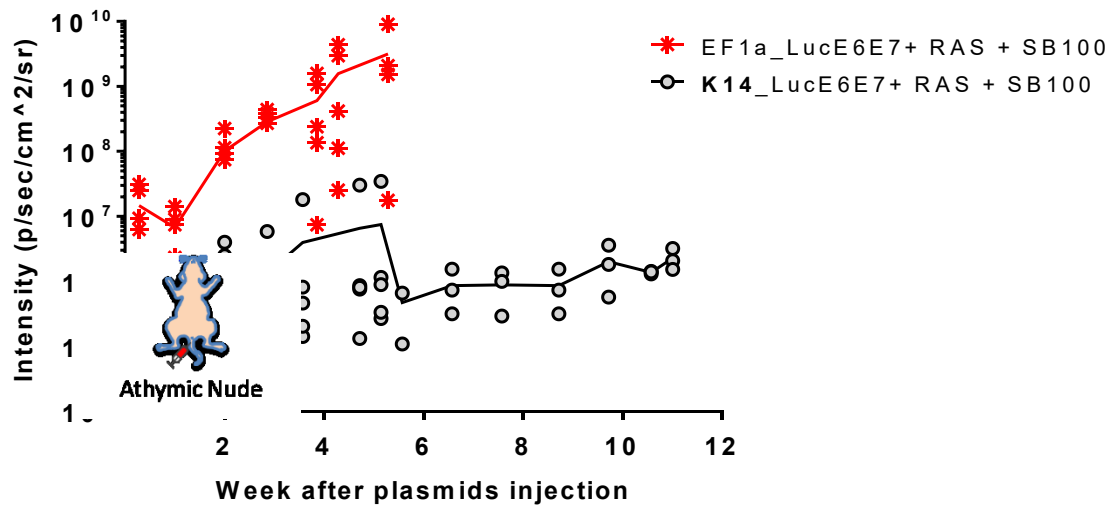


Figure 8. Bioluminescence kinetics of vaginal tumors from different promoters.

Athymic nude mice (n=5 in each group) received submucosal injection of plasmids DNA followed by electroporation in vaginal area. One group received plasmids including EF1a_LucE6E7, NRAS^{G12V} and SB100. The other group received plasmids including K14_LucE6E7, NRAS^{G12V} and SB100. The plasmids combination were prepared with 10 ug of each indicated plasmids in 30uL total injection volume. Bioluminescence kinetics was recorded by IVIS spectrum system.

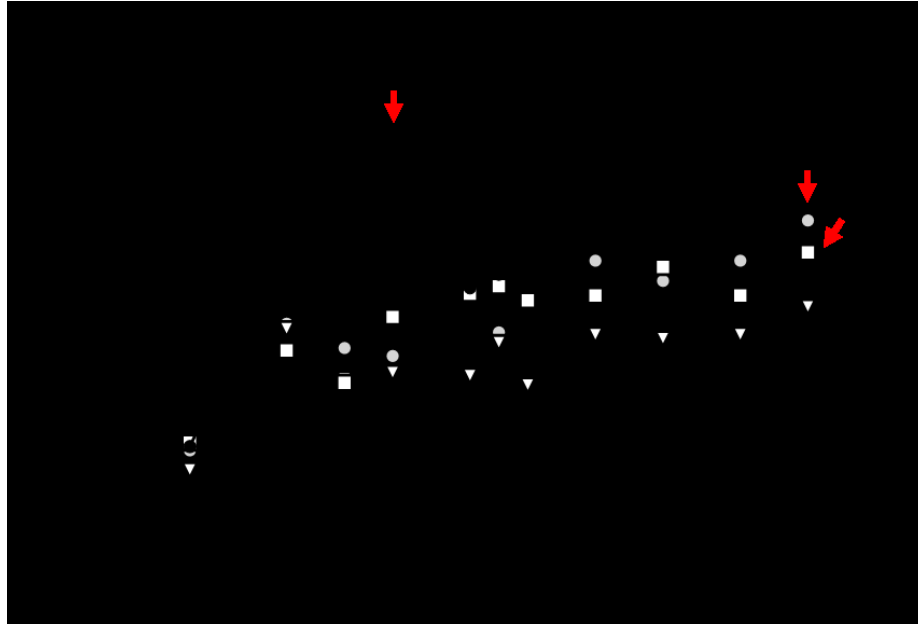


Figure 9. Bioluminescence kinetics of individual vaginal tumor arising from K14-driven HPV16 E6/E7. Athymic nude mice (n=5) received submucosal injection of plasmids DNA followed by electroporation in vaginal area. These plasmids contained K14_LucE6E7, NRAS^{G12V}, and SB100 with each plasmid 10ug in weight and 30uL in total volume. Bioluminescence kinetics of vaginal tumor in each mouse were recorded by IVIS Spectrum. Red arrows indicate gross tumor formation.

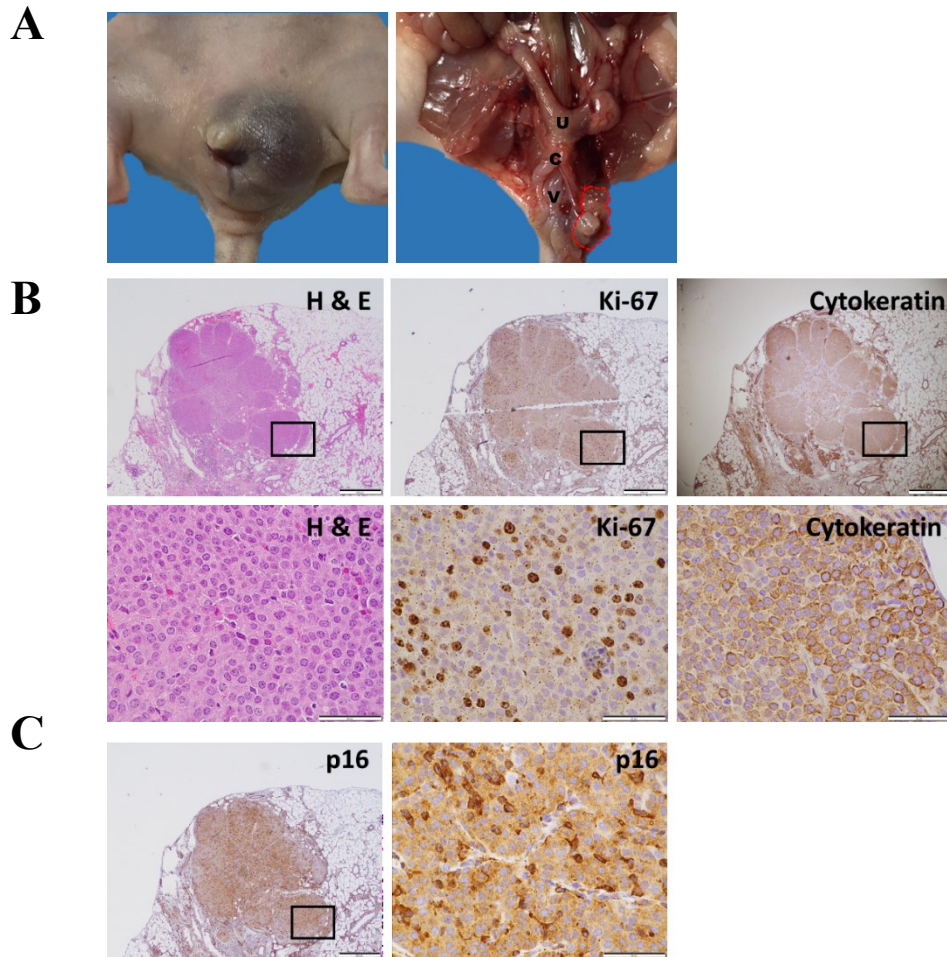


Figure 10. Characterization of vaginal tumors arising from K14-driven HPV16 E6/E7. Athymic nude mice (n=5) received submucosal injection of plasmids DNA followed by electroporation in the vagina. These plasmids contained K14_LucE6E7, NRAS^{G12V}, and SB100 with each plasmid 10ug in weight and 30uL in total volume. (A) Left side is the gross vaginal tumor picture. Right picture: vaginal tumor contained major cystic part and minor solid part (red dash circle). U: uterus, C: cervix, V: vagina. (B) Representative histology sections with H&E stain and special IHC staining with Ki-67 and cytokeratin. (C) Evidence of HPV(+) tumor: IHC staining with HPV associated biomarker p16.

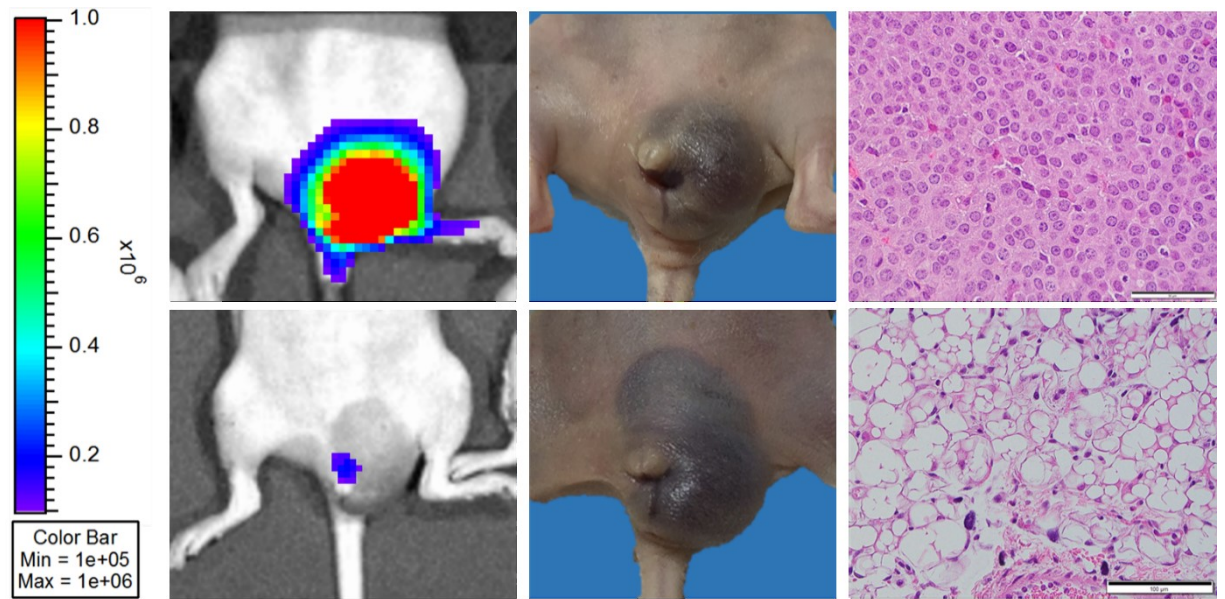


Figure 11. Inconsistent correlation between bioluminescence intensity and tumor

growth. Athymic nude mice (n=5) received submucosal injection of plasmids DNA

followed by electroporation in vagina. These plasmids contained K14_LucE6E7,

NRAS^{G12V}, and SB100 with each plasmid 10ug in weight and 30uL in total volume. Two

vaginal tumors with similar gross size have uncorrelated bioluminescence intensity. Right

column: representative histology sections of H&E stains from these two vaginal tumors.

CHAPTER 4

Combining HPV16 E6/E7 and AKT could induce clinically relevant carcinoma in cervico-vaginal tumor model

Introduction

It is well known that HPV infection alone is not enough to generate cancer. In addition to the tumorigenic properties of the HPV oncoproteins E6/E7, the consequence of HPV DNA integration into the host genome is considered to be a driver of the neoplastic process. The DNA integration causes enhanced expression of viral oncoproteins, alteration of critical cellular genes, and changes in global promoter methylation and transcription (65). Furthermore, all of these consequences, may lead to loss of function of tumor suppressor genes, enhanced oncogene expression, loss of function of DNA repair genes, or other vital cellular functions. Many studies have generated a comprehensive overview of the genomic landscape of human papillomavirus (HPV)-associated cancers using next-generation sequencing techniques, including whole genome/exome sequencing, RNA-Seq, miRNA-Seq and methylation analyses (125-129). These studies showed multiple concurrent somatic mutations in HPV-associated cancers, which may be associated with HPV integration or other independent events after infection. In addition to the HPV DNA integration consequences, the most common additional genomic alteration is associated with the phosphatidylinositol-3-kinase (PI3K)/AKT pathway.

The PI3K/AKT pathway is considered to be an important regulator of many growth factors and regulators. Specifically, the activation of growth factor receptor protein tyrosine kinase can recruit and activate PI3K. PI3K is a lipid kinase which can phosphorylate phosphatidylinositol-3,4-bisphosphate, PI(3,4)P₂, to generate second messenger PI(3,4,5)P₃. PIP₃ can recruit a subset of signaling proteins to the membrane, including PDK1 and AKT. AKT has multiple downstream targets, such as mTOR, which is associated with cell growth, and MDM2 or Bad, which are associated with cell cycle control and apoptosis (130). Therefore, activation of AKT causes a disturbance in cell growth control and cell survival, which contributes to a competitive growth advantage, metastatic competence and therapeutic resistance (131). Many previous publications have documented hyperactivation of AKT kinases in human solid tumors and hematological malignancies such as breast cancer, prostate cancer, colorectal cancer and leukemia (132-137). Additionally, cancer controlled by chemotherapy or radiation depends primarily on the induction of apoptosis. Aberration of PI3K/AKT pathway will hamper apoptosis and is an important mechanism in therapeutic resistance in tumor cells (138). Furthermore, previous publications have shown inhibition of PI3K/AKT signaling pathway can reduce cancer invasion and metastasis (139,140).

PI3K/AKT pathway is thought to be involved in 22-56% of HPV-positive head and neck squamous cell carcinoma and approximately 14% of HPV-positive cervical carcinoma (1). This means that one in every two HNSCC patients has an abnormal PIK3/AKT pathway. Because of its high incidence in HPV-associated carcinoma, we are interested in combining AKT and HPV16 E6/E7 to generate a spontaneous tumor model

that resembles carcinoma characteristics.

Materials & Methods

Mice and Animal Care

Six to eight-week-old female athymic nude (Athymic NCr-nu/nu, strain #553) mice were purchased from Charles Rivers Laboratories (Frederick, MD, USA). All mice were maintained at Johns Hopkins University School of Medicine (Baltimore, MD) animal facility under specific pathogen free conditions. All procedures were performed according to protocols approved by the Johns Hopkins Institutional Animal Care and Use Committee and in accordance with recommendations for the proper use and care of laboratory animals.

Plasmid Vectors

The EF1a_LucE6E7 was generated as described in Chapter 2. The construction of the pCMV(CAT)T7-SB100 plasmid was described previously (93) and purchased from addgene (plasmid #34879). The construction of PKT2/CLP-AKT plasmid encoding human AKT cDNA was described in a previous publication (62) and purchased from Addgene (plasmid #20281). Both EF1a_LucE6E7 and PKT2/CLP-AKT are transposon backbones, in which the transposon DNA is flanked between two inverted sequences and can be recognized and cut by transposase.

In vivo buccal tumor formation

Immuno-deficient athymic nude mice (five per group) received submucosal

injection with plasmids EF1a_LucE6E7 which encodes Luciferase and HPV16 E6/E7, PKT2/CLP-AKT, as well as transposase SB100 into buccal area followed by electroporation. Each plasmid was 10ug in weight and 30uL in total injection volume. After plasmids injection, the transfected gene expression and tumor growth were monitored using in vivo bioluminescence imaging.

The surface dimensions (length and width) of the tumor were measured with digital calipers. To record the survival of the tumor-bearing mice, either natural death or tumor diameter greater than 7mm leading to irreversible tumor burden were counted as death.

In vivo vaginal tumor formation

After dilatation with vaginal swab, athymic nude mice (five per group) received submucosal injection with plasmids EF1a_LucE6E7, PKT2/CLP-AKT, and transposase SB100 into lower third of vaginal mucosa. Each plasmid was 10ug in weight and 30uL in total injection volume.

The length and width surface dimensions of the tumor were measured with digital calipers. To record the survival of the tumor-bearing mice, either natural death or tumor diameter greater than 15mm leading to irreversible tumor growth was counted as death.

In vivo bioluminescence image

This procedure is similar to the procedure as described in **Chapter 2**.

Histology and Immunohistochemistry staining

For buccal tumor, when the tumor size exceeds 7mm in diameter, mice were considered to be unrecoverable from tumor burden, and euthanized according to the protocol. For vaginal tumor, when the tumor size exceeds 15mm in diameter, mice were considered to be unrecoverable from tumor burden, and euthanized according to the protocol. The tumors were surgically removed, isolated and placed into 10% Neutral buffered formalin solution for adequate fixation with a minimum 48 hours at room temperature. The tumor samples were then sent to Johns Hopkins University Oncology Tissue Services for subsequent procedures including paraffin embedding, tissue sectioning, hematoxylin and eosin (H&E) staining and immunohistochemistry (IHC) staining. The histology slides were reviewed by Dr. T.-C. Wu.

Statistical analysis

The statistical analysis was performed with the GraphPad Prism V.6 software (La Jolla, CA, USA). Data were expressed as means \pm standard deviation (SD).

Results

In buccal tumor model, combining HPV16 E6/E7 and AKT oncogenes slowed tumor formation rate.

Athymic nude mice (five per group) received submucosal injection of the plasmids, EF1a_LucE6E7, AKT, and transposase SB100 in buccal area. After plasmids injection, tumor growth was monitored by in vivo bioluminescence imaging. Compared

with tumors from original plasmids combination using EF1a_LucE6E7, NRAS^{G12V}, and SB100, replacing NRAS^{G12V} with AKT caused slower tumor formation as well as lower bioluminescence intensity (**Fig. 1A**). The AKT combination also showed significantly better survival rate (**Fig. 1B**). The overt tumors caused by HPV16 E6/E7 and AKT were generated by the end of 8th week after plasmids injection. In spite of slower tumor growth, the tumor generation rate was still 80% (**Fig. 2A-B**). The macroscopic features of these buccal tumors were flat, dark-red in color, small in size (<6 mm in longest diameter), and hematoma-like in appearance (**Fig. 2C**). The microscopic characteristics showed non-neoplastic tissue with hemorrhage, fibrin exudation, and hyalinization, which was confirmed in the hematoma suspension (**Fig. 2D**)

In vaginal tumor model, combining HPV16 E6/E7 and AKT generated clinically relevant carcinoma.

After vaginal dilation with vaginal swab, athymic nude mice (five in each group) received submucosal injection of plasmids followed by electroporation in the lower third vaginal area. After injection of plasmids, gene expression and tumor growth were monitored using in vivo bioluminescence imaging. The tumor formation rate from EF1a_LucE6E7 and AKT is slower than original EF1a_LucE6E7 and NRAS^{G12V} combination but faster than K14_LucE6E7 and NRAS^{G12V} combination (**Fig. 3**). In contrast with the buccal tumor model, AKT had a more significant synergic effect of carcinogenesis with HPV16 E6/E7 in vaginal mucosa. (Refer to **Figure 2**) All mice (5 out of 5) developed overt vaginal tumors by the end of the seventh week after plasmids injection (**Fig. 4A-B**). These vaginal tumors were solid mass, fixed, oval shape, with

smooth contours (**Fig. 4C**). The microscopic features revealed classic malignant cell characteristics, including large, abundant eosinophilic cytoplasm and a large, often vesicular, nucleus (**Fig. 5A**). These tumors also showed classic carcinoma characteristics with multiple tumor cell islands, variable keratinization with keratin pearls as well as invasion features (**Fig. 5A**). The special immunohistochemistry staining provided evidence of positive cytokeratin staining, which is a carcinoma biomarker (**Fig. 5B**). Other special IHC staining revealed positive proliferation marker ki-67 as well as HPV-associated biomarker p16 (**Fig. 5C**)

Discussion

In this chapter, we noted synergic effects of HPV-16 E6/E7 and AKT oncogenes on tumorigenesis in vaginal mucosa but not in buccal mucosa. Additionally, the tumor biology and histology of vaginal mucosa and buccal mucosa are different as well. With submucosal injection of plasmids containing EF1a_LucE6E7, AKT, and SB100, the vaginal tumors had clinically relevant carcinoma features and consistent gross tumor developing by the end of 7th week after plasmids injection. However, the buccal tumors revealed major hematoma microscopic characteristics with inconsistent tumor growth rate. All of the plasmid preparations, injection doses, and electroporation parameter settings were the same at these two injection sites and all performed by myself. Therefore, individual technical variation could be excluded as the reason for these tumor differences. Comparing the histology structures between mouse vaginal and oral mucosa, both of them have stratified epithelium composed of multiple layers of cells which show a non-keratinized pattern of differentiation. Underlying epithelium layers are the basal

membrane, lamina propria of connective tissue, submucosa, muscular layer, and the innermost adventia. The mouse oral cavity (including the labial, buccal, palatine and gingival mucosa) is lined by variably orthokeratinized squamous epithelium. The thickness of keratin layer varies with diet and frequency of ingestion. Fasted or anorexic mice will have increased keratin thickness and occasionally adherent bacterial colonies, especially in the distal esophagus and nonglandular stomach (141).

The mouse vaginal mucosa is composed of stratified squamous epithelium and is folded into longitudinal elevations with no glands. The morphology of the vaginal epithelium changes during the different stages of the estrus cycle, for example, the vaginal mucosa may move toward para-keratinization during the midpoint of the menstrual cycle (141). And it has been proven that sex hormones, especially estrogen, are the carcinogenesis co-factor in the HPV transgenic mouse model, contributing to the onset, persistence, and malignant progression of tumor (49). Although the mice are randomly selected without being screened for the stage of their estrus cycle, the significant difference in carcinogenesis potential between buccal and vaginal mucosa led us to believe that this may be caused by hormone influence. This can be explained from previous HPV transgenic mouse models which proved that estrogen was a carcinogenic cofactor with HPV oncogenes and chronic administration of hormone estradiol increased tumor generation (142,143).

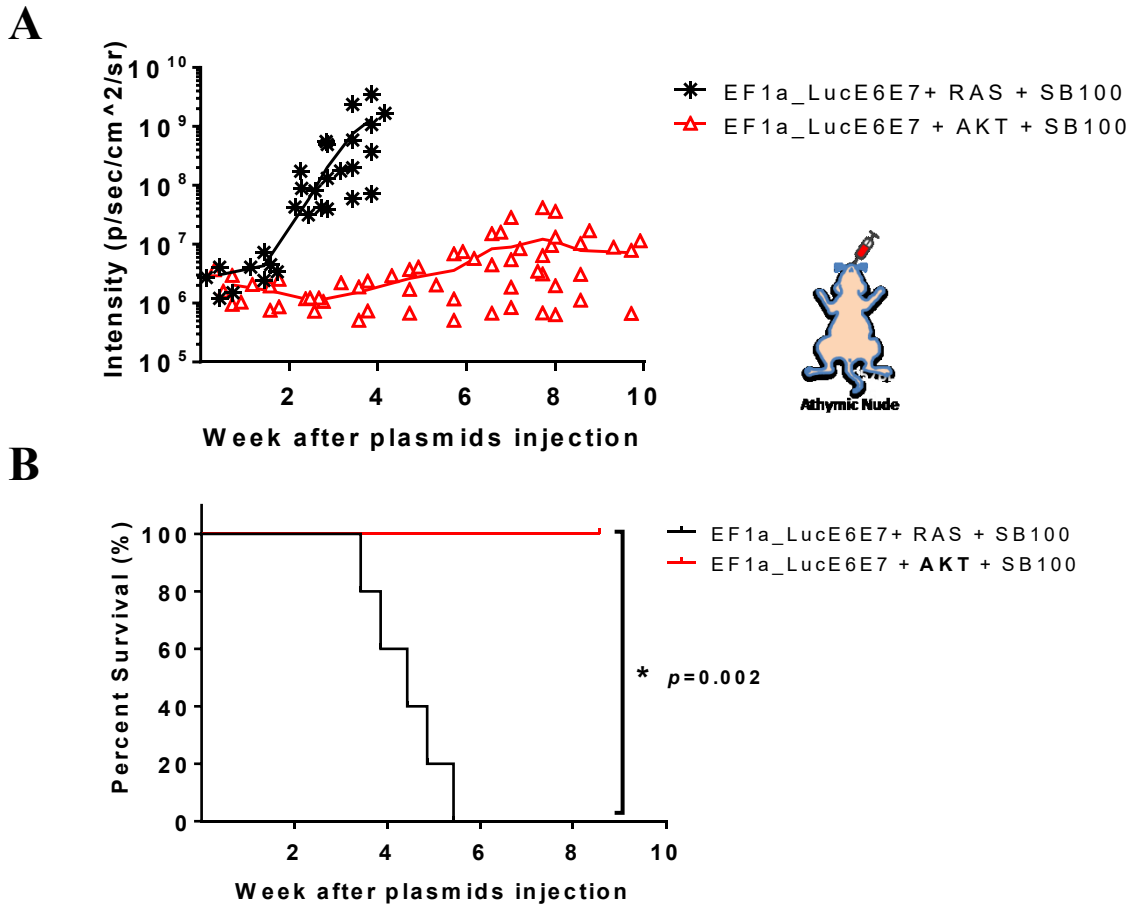


Figure 1. Bioluminescence kinetics of buccal tumors in immunodeficient mice.

Athymic nude mice (n=5 in each group) received submucosal injection of plasmids DNA followed by electroporation in buccal area. One group received plasmids including EF1a_LucE6E7, NRAS^{G12} and SB100. The other group received plasmids including EF1a_LucE6E7, AKT and SB100. All injected plasmids were 10ug in weight and 30uL in total injection volume. Bioluminescence kinetics were recorded by IVIS spectrum system.

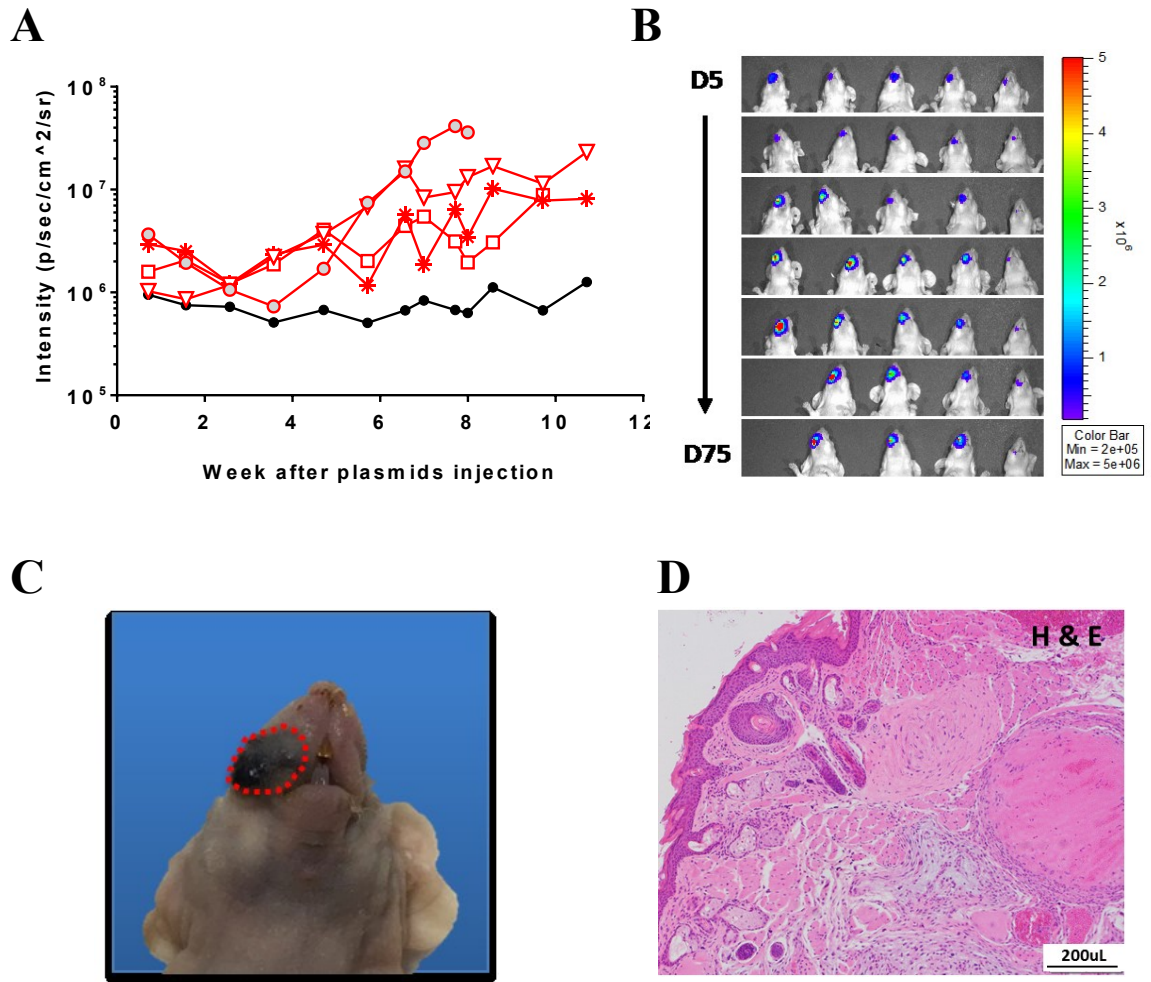


Figure 2. Buccal tumors arising from HPV16 E6/E7 and AKT oncogenes. Athymic nude mice (n=5) received submucosal injection of plasmid DNA followed by electroporation in buccal area. These plasmids contained EF1a_LucE6E7, AKT, and SB100, each 10ug in weight and 30uL in total volume. (A) Bioluminescence kinetics of buccal tumor in each mouse was recorded by IVIS Spectrum. Red color indicates mice with gross tumor formation in the end of experiment. (B) Bioluminescence image (C) Gross picture of the buccal tumor. (D) Microscopic features of the buccal tumor.

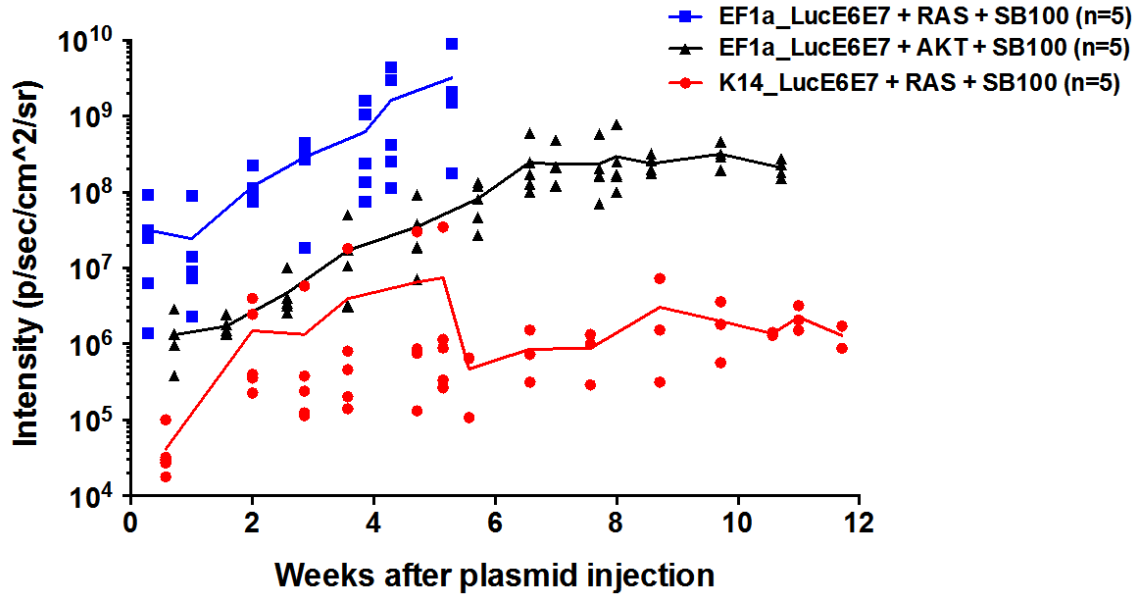


Figure 3. Bioluminescence kinetics of vaginal tumors arising from different plasmid combinations in immunodeficient mice. Athymic nude mice (n=5 in each group) received submucosal injection of plasmid DNA followed by electroporation in lower third of vaginal mucosa. One group received plasmids including EF1a_LucE6E7, NRAS^{G12V} and SB100. One group received plasmids including EF1a_LucE6E7, AKT and SB100. One group received plasmids including K14_LucE6E7, NRAS^{G12V} and SB100. All plasmids were 10ug in weight and 30uL in total injection volume. Bioluminescence kinetics were recorded using IVIS spectrum system.

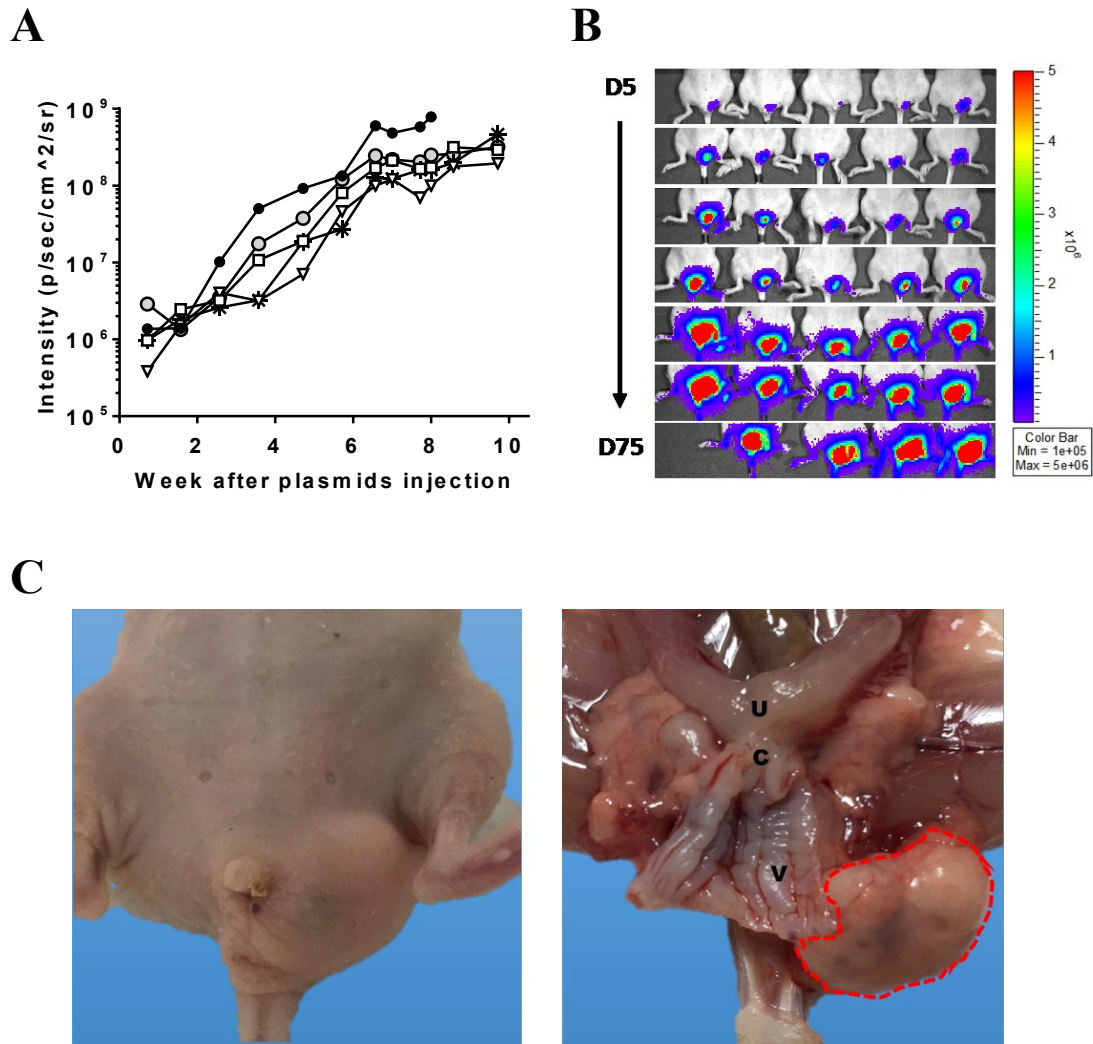
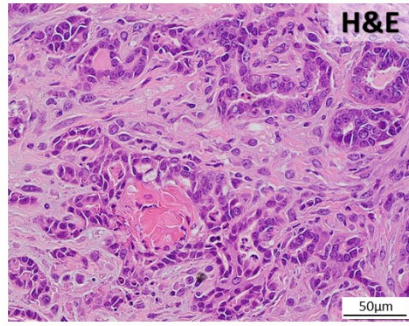
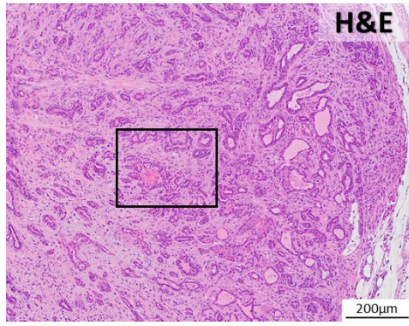
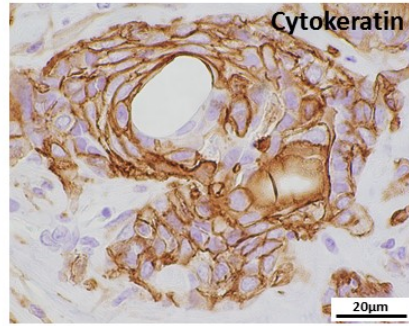
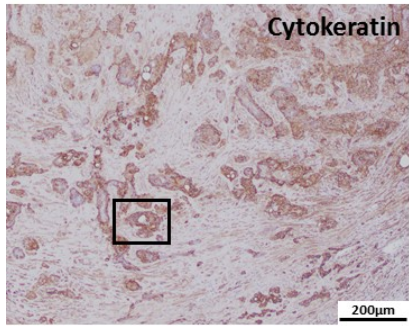


Figure 4. Vaginal tumors arising from HPV16 E6/E7 and AKT oncogenes. Athymic nude mice (n=5) received submucosal injection of plasmids DNA followed by electroporation in lower third of vaginal mucosa. These plasmids contained EF1a_LucE6E7, AKT, and SB100, each 10ug in weight and 30uL in total volume. (A) Bioluminescence kinetics of vaginal tumor in each mouse was recorded by IVIS Spectrum. Red color indicates mice with gross tumor formation at the end of experiment. (B) Bioluminescence image (C) Macroscopic features of the vaginal tumor.

A



B



C

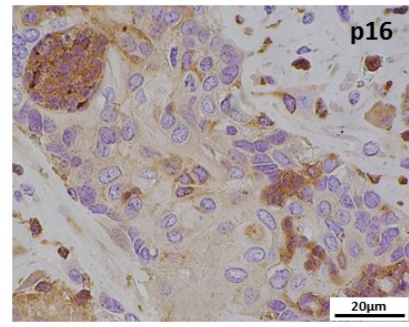
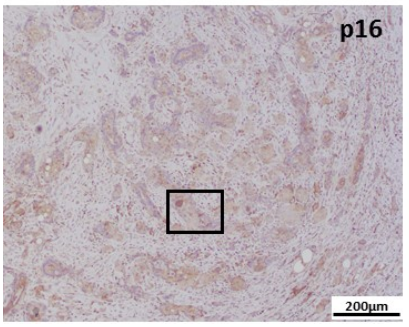
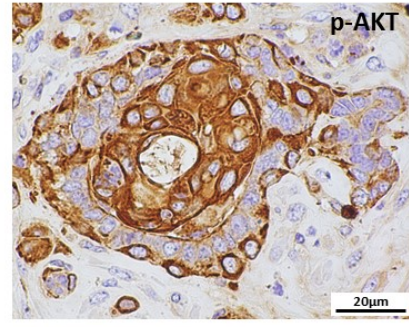
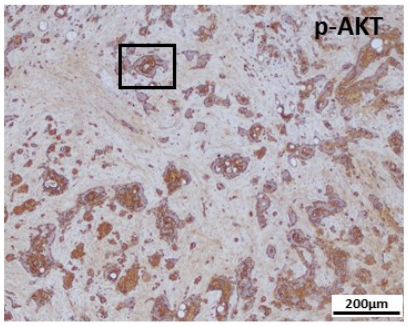
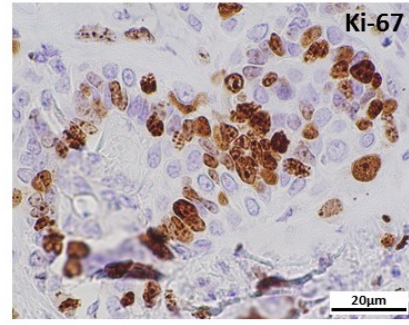
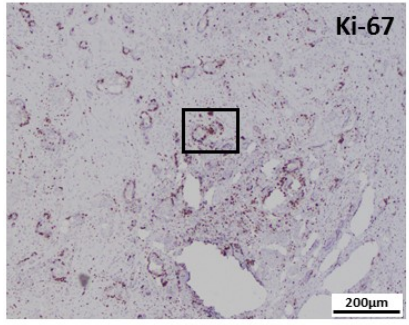


Figure 5. Characterization of vaginal tumors arising from HPV16 E6/E7 and AKT oncogenes. Athymic nude mice (n=5) received submucosal injection of plasmids DNA followed by electroporation in lower third of vaginal mucosa. These plasmids contained EF1a_LucE6E7, AKT, and SB100 with each 10ug in weight and 30uL in total volume. (A) Representative histology sections with H&E stain (B) Special IHC staining with cytokeratin epithelium marker. (C) Special IHC staining with Ki-67, p-Akt and HPV associated biomarker p16.

CHAPTER 5

Summary

Despite the availability of preventative HPV vaccines, HPV-associated cancer is still a common global health issue. For patients with an existing HPV infection, there is an urgent need for therapeutic strategies to control infection and prevent further carcinogenesis. Persistent high-risk HPV infection is considered a major risk factor for the development of precancerous disease and cancer. Currently, there are no efficient therapeutic treatment methods for existing HPV-infection and HPV-associated malignancies. The only treatment option is to monitor the infection regularly. That is the reason why I'm interested in developing an HPV-expression pre-clinical tumor model. Unfortunately, existing HPV models have limitations, for example, xenograft tumor transplantation models cannot depict tumor microenvironment after HPV infection, or the transgenic mouse models have immune tolerance issues. The drawbacks of traditional HPV cancer models inspired me to generate an improved model. With continuous HPV expression, which can mimic HPV infection, our ideal model should be able to address tumor microenvironment, evaluate therapeutic strategies especially for immunotherapy, and depict precancerous to cancerous disease progression from cell transformation by HPV infection.

In **Chapter 2**, I developed a useful pre-clinical HPV spontaneous buccal tumor model. By submucosal injection of plasmids, EF1a_LucE6E7, NRAS^{G12V}, and CMV_SB100, into mice buccal area, the plasmids co-transfection resulted in spontaneous

tumor formation in immune-deficient athymic nude mice while tumor suppression was observed in immune-competent background. However, with CD3⁺ T cells depletion during the early stage of cell transformation, the formation of spontaneous oral tumor could be achieved even when T cells gradually recovered. With the help of luciferase reporter gene, the tumors can be tracked sequentially, longitudinally and dynamically because of the correlation between tumor size and bioluminescence intensity. These tumors express HPV16 biomarker p16 as well as detectable HPV16 RNA. Furthermore, these tumors can metastasize to draining lymph nodes which is correlated with clinical disease progression and can be controlled through immune therapeutic treatments which is useful for future research of immunotherapy.

This CD3 depletion HPV buccal tumor model developed from a straightforward method by injecting oncogenic plasmids directly in mucosal area. Traditional transgenic mouse models result in insufficient tumor formation and are limited by time and labor consuming. The model proposed in **Chapter 2** is cheaper, faster and has more efficient tumor generation (>80%). These benefits make it a useful tool to evaluate HPV infection consequence and therapeutic intervention.

However, we also encountered some limitations in this model. One such limitation was the overexpression of HPV16 E6/E7 by artificial promoter and artificial genome integration with multi-copy expression, both of which are much different from natural viral gene expression. Another limitation is the microscopic histological characteristics of this spontaneous buccal tumors which are different from clinically

relevant HPV-associated oropharyngeal carcinoma. Therefore, in **Chapter 3** and **Chapter 4**, I've tried different plasmids to make spontaneous tumors with microscopic features better resemble the clinical HPV+ carcinoma.

Based on experiences from previous transgenic mouse models, keratinocyte-restricted promoter K14 can help to generate clinically relevant carcinoma. In **Chapter 3**, I used promoter K14 to drive either HPV16 E6/E7 or transposase SB100. I injected the plasmids combination in both buccal mucosa and the lower third vaginal mucosa area. However, I found that, plasmids combinations containing K14-driven HPV16 E6/E7 have much lower tumor generation efficiency (40-60%) in buccal area as well as in vaginal area. Although we had observed vaginal tumor with carcinomatous histology, the incidence was very rare, only one out of forty (2.5%) had carcinoma characteristics. With K14-driven SB100, I found the tumor kinetics, overt tumor formation rate, and the microscopic histology is similar to the plasmids combination containing original commercialized CMV_SB100 (pCMV(CAT)T7-SB100), EF1a_LucHPV16 E6E7, and NRAS^{G12V} plasmids.

In **Chapter 3**, we suspected that the technical limitations in our model caused unavailability of plenty keratinocytes around the injection site and resulted in insufficient gene expression. To resolve this issue, we used gene gun delivery of the oncogenic plasmids in buccal mucosa as well as in the external perineal area. However, the gene gun cannot generate efficient DNA delivery or persistent gene expression in mucosa. We also used pseudovirions delivery which turned out very poor infectivity with insufficient

transgene expression. After trying different plasmids delivery methods, we still cannot get satisfied tumor formation with carcinoma characteristics under K14 promoter both in buccal and vaginal area. Therefore, this push us to combine HPV16 E6/E7 with another oncogene in **Chapter 4**.

In **Chapter 4**, I replaced NRAS^{G12V} with PKT2/CLP-AKT, which contains human AKT cDNA to induce a clinically relevant carcinoma. With the help of next-generation sequencing techniques, many studies have generated a comprehensive overview of the genomic landscape of human papillomavirus (HPV)-associated cancers (125-129). There are many consequences after HPV DNA integration. The most important events for carcinogenesis are caused by oncoprotein E6 and E7. E6 oncoprotein is thought to promote cell proliferation by stimulating degradation of the tumor suppressor p53 (144). Oncoprotein E7 can bind 'pocket domain' sequences of Rb, disrupt the interaction between Rb and E2F, resulting in the release of E2F factors in their transcriptionally active forms and stimulating replication and cell-division (25,145,146). In addition, previous publications indicated the most common additional genomic alterations, phosphatidylinositol-3-kinase (PI3K)/AKT pathway, is estimated to be involved in 22-56% of HPV-positive head and neck squamous cells carcinoma and in approximately 14% HPV-positive cervical carcinoma (1).

In **Chapter 4**, I injected mice submucosally with plasmids, EF1a_LucE6E7, PKT2/CLP-AKT, and CMV_SB100, in both buccal area as well as lower third vagina area in immune-compromised athymic nude mice. I noted that this combination had

carcinogenic potential functionally, predominantly in the vagina area but not in the buccal area. All mice that received vaginal mucosa injection developed clinically relevant carcinoma by the end of 7th week after plasmids injection. Considering the anatomy difference, the mucosal structure in vagina is similar to buccal mucosa. The only difference is that vaginal mucosa has periodical changes with the menstrual and hormone cycle. Therefore, I suspect the difference in carcinogenesis synergic effect is due to the insensitivity of hormone change in mouse buccal mucosa.

Compared to the traditional transgenic mouse model, this HPV-associated cervico-vaginal spontaneous cancer model depends on manual injection of plasmids into vaginal mucosa, provides a cheaper, faster and more efficient tumor model.

As summarized in Table 2, my thesis provides a useful HPV+ spontaneous buccal tumor model, which is suitable for evaluating immunotherapy strategies and metastasis biology. In the future, this buccal model could be used to do molecular analysis associated with tumor metastasis. It would also be very useful to test different immunotherapeutic strategies in eliminating HPV infection, preventing tumor formation and controlling disease progression. For HPV+ spontaneous vaginal model, we generated a clinically relevant carcinoma cervico-vaginal spontaneous model. However, it warrants further investigation regarding full disease progression and tumor microenvironment evaluation. After applying this strategy in immune-competent mice, this cervico-vaginal model is also very useful in studying tumor biology and testing multiple immunotherapeutic strategies.

HPV+ preclinical tumor models							
Plasmids Injection + electroporation							
	Major HPV oncogenes		Synergic oncogenes		Sleeping beauty transposase		Result
	EF1a_LucE6E7	K14_LucE6E7	NRAS ^{G12V}	PKT2/CLP-AKT	CMV_SB100	K14_SB100	
Buccal mucosa	●		●		●		- Promising tumor formation - Reginal metastatic capability - Eligible to test immunotherapy - Histological limitations
		●	●		●		- Inconsistent tumor formation - No clinically relevant carcinoma
	●		●			●	- Promising tumor formation - No clinically relevant carcinoma
		●	●			●	- Inconsistent tumor formation - No clinical relevant carcinoma
	●			●	●		- Inconsistent tumor formation - No clinically relevant carcinoma
Vaginal mucosa	●		●		●		- Promising tumor formation - No clinically relevant carcinoma
		●	●			●	- Inconsistent tumor formation - Inconsistent microscopic features
	●		●		●		- Promising tumor formation - No clinically relevant carcinoma
		●	●			●	- Inconsistent tumor formation - No clinical relevant carcinoma
	●			●	●		- Promising tumor formation - Clinically relevant carcinoma

Table 2. HPV+ preclinical tumor models. This table summarizes different plasmid combinations tested in my thesis. The red color results indicate the models we prefer for future researches.

References

1. de Martel C, Ferlay J, Franceschi S, Vignat J, Bray F, Forman D, et al. Global burden of cancers attributable to infections in 2008: a review and synthetic analysis. *The Lancet Oncology* 2012;13(6):607-15.
2. Forman D, de Martel C, Lacey CJ, Soerjomataram I, Lortet-Tieulent J, Bruni L, et al. Global burden of human papillomavirus and related diseases. *Vaccine* 2012;30 Suppl 5:F12-23.
3. Parkin DM, Bray F. Chapter 2: The burden of HPV-related cancers. *Vaccine* 2006;24 Suppl 3:S3/11-25.
4. Trimble CL. HPV Infection-Associated Cancers: Next-Generation Technology for Diagnosis and Treatment. *Cancer immunology research* 2014;2(10):937-42.
5. Derkay CS. Task force on recurrent respiratory papillomas. A preliminary report. *Archives of otolaryngology--head & neck surgery* 1995;121(12):1386-91.
6. Hu D, Goldie S. The economic burden of noncervical human papillomavirus disease in the United States. *American journal of obstetrics and gynecology* 2008;198(5):500 e1-7.
7. Chesson HW, Ekwueme DU, Saraiya M, Watson M, Lowy DR, Markowitz LE. Estimates of the annual direct medical costs of the prevention and treatment of disease associated with human papillomavirus in the United States. *Vaccine* 2012;30(42):6016-9.
8. Gillison ML, Chaturvedi AK, Lowy DR. HPV prophylactic vaccines and the potential prevention of noncervical cancers in both men and women. *Cancer*

2008;113(10 Suppl):3036-46.

9. Winer RL, Hughes JP, Feng Q, O'Reilly S, Kiviat NB, Holmes KK, et al. Condom use and the risk of genital human papillomavirus infection in young women. *The New England journal of medicine* 2006;354(25):2645-54.
10. Chaturvedi AK, Engels EA, Pfeiffer RM, Hernandez BY, Xiao W, Kim E, et al. Human papillomavirus and rising oropharyngeal cancer incidence in the United States. *Journal of clinical oncology : official journal of the American Society of Clinical Oncology* 2011;29(32):4294-301.
11. Molano M, Van den Brule A, Plummer M, Weiderpass E, Posso H, Arslan A, et al. Determinants of clearance of human papillomavirus infections in Colombian women with normal cytology: a population-based, 5-year follow-up study. *American journal of epidemiology* 2003;158(5):486-94.
12. Franco EL, Villa LL, Sobrinho JP, Prado JM, Rousseau MC, Desy M, et al. Epidemiology of acquisition and clearance of cervical human papillomavirus infection in women from a high-risk area for cervical cancer. *The Journal of infectious diseases* 1999;180(5):1415-23.
13. Moscicki AB. Impact of HPV infection in adolescent populations. *The Journal of adolescent health : official publication of the Society for Adolescent Medicine* 2005;37(6 Suppl):S3-9.
14. Ho GY, Burk RD, Klein S, Kadish AS, Chang CJ, Palan P, et al. Persistent genital human papillomavirus infection as a risk factor for persistent cervical dysplasia. *Journal of the National Cancer Institute* 1995;87(18):1365-71.
15. Schiffman M, Kjaer SK. Chapter 2: Natural history of anogenital human

- papillomavirus infection and neoplasia. *Journal of the National Cancer Institute Monographs* 2003(31):14-9.
16. Hildesheim A, Schiffman MH, Gravitt PE, Glass AG, Greer CE, Zhang T, et al. Persistence of type-specific human papillomavirus infection among cytologically normal women. *The Journal of infectious diseases* 1994;169(2):235-40.
 17. Schlecht NF, Platt RW, Duarte-Franco E, Costa MC, Sobrinho JP, Prado JC, et al. Human papillomavirus infection and time to progression and regression of cervical intraepithelial neoplasia. *Journal of the National Cancer Institute* 2003;95(17):1336-43.
 18. Kajitani N, Satsuka A, Kawate A, Sakai H. Productive Lifecycle of Human Papillomaviruses that Depends Upon Squamous Epithelial Differentiation. *Frontiers in microbiology* 2012;3:152.
 19. Smith B, Chen Z, Reimers L, van Doorslaer K, Schiffman M, Desalle R, et al. Sequence imputation of HPV16 genomes for genetic association studies. *PloS one* 2011;6(6):e21375.
 20. Egawa N, Egawa K, Griffin H, Doorbar J. Human Papillomaviruses; Epithelial Tropisms, and the Development of Neoplasia. *Viruses* 2015;7(7):3863-90.
 21. Van Doorslaer K, Bernard HU, Chen Z, de Villiers EM, zur Hausen H, Burk RD. Papillomaviruses: evolution, Linnaean taxonomy and current nomenclature. *Trends in microbiology* 2011;19(2):49-50; author reply 50-1.
 22. Gottschling M, Goker M, Stamatakis A, Bininda-Emonds OR, Nindl I, Bravo IG. Quantifying the phylodynamic forces driving papillomavirus evolution. *Molecular biology and evolution* 2011;28(7):2101-13.

23. Kehmeier E, Ruhl H, Volland B, Stoppler MC, Androphy E, Stoppler H. Cellular steady-state levels of "high risk" but not "low risk" human papillomavirus (HPV) E6 proteins are increased by inhibition of proteasome-dependent degradation independent of their p53- and E6AP-binding capabilities. *Virology* 2002;299(1):72-87.
24. Moody CA, Laimins LA. Human papillomaviruses activate the ATM DNA damage pathway for viral genome amplification upon differentiation. *PLoS pathogens* 2009;5(10):e1000605.
25. Chellappan S, Kraus VB, Kroger B, Munger K, Howley PM, Phelps WC, et al. Adenovirus E1A, simian virus 40 tumor antigen, and human papillomavirus E7 protein share the capacity to disrupt the interaction between transcription factor E2F and the retinoblastoma gene product. *Proceedings of the National Academy of Sciences of the United States of America* 1992;89(10):4549-53.
26. Yim EK, Park JS. The role of HPV E6 and E7 oncoproteins in HPV-associated cervical carcinogenesis. *Cancer research and treatment : official journal of Korean Cancer Association* 2005;37(6):319-24.
27. Bodily J, Laimins LA. Persistence of human papillomavirus infection: keys to malignant progression. *Trends in microbiology* 2011;19(1):33-9.
28. Wang HK, Duffy AA, Broker TR, Chow LT. Robust production and passaging of infectious HPV in squamous epithelium of primary human keratinocytes. *Genes & development* 2009;23(2):181-94.
29. Meyers C, Laimins LA. In vitro systems for the study and propagation of human papillomaviruses. *Current topics in microbiology and immunology* 1994;186:199-

215.

30. Flores ER, Allen-Hoffmann BL, Lee D, Sattler CA, Lambert PF. Establishment of the human papillomavirus type 16 (HPV-16) life cycle in an immortalized human foreskin keratinocyte cell line. *Virology* 1999;262(2):344-54.
31. Fang L, Meyers C, Budgeon LR, Howett MK. Induction of productive human papillomavirus type 11 life cycle in epithelial cells grown in organotypic raft cultures. *Virology* 2006;347(1):28-35.
32. Ernani V, Saba NF. Oral Cavity Cancer: Risk Factors, Pathology, and Management. *Oncology* 2015;89(4):187-95.
33. Shah SD, Doorbar J, Goldstein RA. Analysis of host-parasite incongruence in papillomavirus evolution using importance sampling. *Molecular biology and evolution* 2010;27(6):1301-14.
34. Kreider JW, Howett MK, Wolfe SA, Bartlett GL, Zaino RJ, Sedlacek T, et al. Morphological transformation in vivo of human uterine cervix with papillomavirus from condylomata acuminata. *Nature* 1985;317(6038):639-41.
35. Dollard SC, Chow LT, Kreider JW, Broker TR, Lill NL, Howett MK. Characterization of an HPV type 11 isolate propagated in human foreskin implants in nude mice. *Virology* 1989;171(1):294-7.
36. Kreider JW, Howett MK, Stoler MH, Zaino RJ, Welsh P. Susceptibility of various human tissues to transformation in vivo with human papillomavirus type 11. *International journal of cancer* 1987;39(4):459-65.
37. Kreider JW, Howett MK, Lill NL, Bartlett GL, Zaino RJ, Sedlacek TV, et al. In vivo transformation of human skin with human papillomavirus type 11 from

- condylomata acuminata. *Journal of virology* 1986;59(2):369-76.
38. Kreider JW, Howett MK, Leure-Dupree AE, Zaino RJ, Weber JA. Laboratory production in vivo of infectious human papillomavirus type 11. *Journal of virology* 1987;61(2):590-3.
 39. Kreider JW, Patrick SD, Cladel NM, Welsh PA. Experimental infection with human papillomavirus type 1 of human hand and foot skin. *Virology* 1990;177(1):415-7.
 40. Sterling J, Stanley M, Gatward G, Minson T. Production of human papillomavirus type 16 virions in a keratinocyte cell line. *Journal of virology* 1990;64(12):6305-7.
 41. Brandsma JL, Brownstein DG, Xiao W, Longley BJ. Papilloma formation in human foreskin xenografts after inoculation of human papillomavirus type 16 DNA. *Journal of virology* 1995;69(4):2716-21.
 42. Bonnef W, DaRin C, Borkhuis C, de Mesy Jensen K, Reichman RC, Rose RC. Isolation and propagation of human papillomavirus type 16 in human xenografts implanted in the severe combined immunodeficiency mouse. *Journal of virology* 1998;72(6):5256-61.
 43. Huang B, Mao CP, Peng S, He L, Hung CF, Wu TC. Intradermal administration of DNA vaccines combining a strategy to bypass antigen processing with a strategy to prolong dendritic cell survival enhances DNA vaccine potency. *Vaccine* 2007;25(45):7824-31.
 44. Li YL, Ma ZL, Zhao Y, Zhang J. Immunization with mutant HPV16 E7 protein inhibits the growth of TC-1 cells in tumor-bearing mice. *Oncology letters*

- 2015;9(4):1851-56.
45. Paolini F, Massa S, Manni I, Franconi R, Venuti A. Immunotherapy in new pre-clinical models of HPV-associated oral cancers. *Human vaccines & immunotherapeutics* 2013;9(3):534-43.
 46. Tseng CW, Monie A, Wu CY, Huang B, Wang MC, Hung CF, et al. Treatment with proteasome inhibitor bortezomib enhances antigen-specific CD8⁺ T-cell-mediated antitumor immunity induced by DNA vaccination. *J Mol Med (Berl)* 2008;86(8):899-908.
 47. Lin KY, Guarnieri FG, Staveley-O'Carroll KF, Levitsky HI, August JT, Pardoll DM, et al. Treatment of established tumors with a novel vaccine that enhances major histocompatibility class II presentation of tumor antigen. *Cancer research* 1996;56(1):21-6.
 48. Feltkamp MC, Smits HL, Vierboom MP, Minnaar RP, de Jongh BM, Drijfhout JW, et al. Vaccination with cytotoxic T lymphocyte epitope-containing peptide protects against a tumor induced by human papillomavirus type 16-transformed cells. *European journal of immunology* 1993;23(9):2242-9.
 49. Brake T, Lambert PF. Estrogen contributes to the onset, persistence, and malignant progression of cervical cancer in a human papillomavirus-transgenic mouse model. *Proceedings of the National Academy of Sciences of the United States of America* 2005;102(7):2490-5.
 50. Riley RR, Duensing S, Brake T, Munger K, Lambert PF, Arbeit JM. Dissection of human papillomavirus E6 and E7 function in transgenic mouse models of cervical carcinogenesis. *Cancer research* 2003;63(16):4862-71.

51. Schaeffer AJ, Nguyen M, Liem A, Lee D, Montagna C, Lambert PF, et al. E6 and E7 oncoproteins induce distinct patterns of chromosomal aneuploidy in skin tumors from transgenic mice. *Cancer research* 2004;64(2):538-46.
52. Song S, Pitot HC, Lambert PF. The human papillomavirus type 16 E6 gene alone is sufficient to induce carcinomas in transgenic animals. *Journal of virology* 1999;73(7):5887-93.
53. Lambert PF, Pan H, Pitot HC, Liem A, Jackson M, Griep AE. Epidermal cancer associated with expression of human papillomavirus type 16 E6 and E7 oncogenes in the skin of transgenic mice. *Proceedings of the National Academy of Sciences of the United States of America* 1993;90(12):5583-7.
54. Hilditch-Maguire PA, Lieppe DM, West D, Lambert PF, Frazer IH. T cell-mediated and non-specific inflammatory mechanisms contribute to the skin pathology of HPV 16 E6E7 transgenic mice. *Intervirology* 1999;42(1):43-50.
55. Frazer IH, Lieppe DM, Dunn LA, Liem A, Tindle RW, Fernando GJ, et al. Immunological responses in human papillomavirus 16 E6/E7-transgenic mice to E7 protein correlate with the presence of skin disease. *Cancer research* 1995;55(12):2635-9.
56. Jabbar SF, Abrams L, Glick A, Lambert PF. Persistence of high-grade cervical dysplasia and cervical cancer requires the continuous expression of the human papillomavirus type 16 E7 oncogene. *Cancer research* 2009;69(10):4407-14.
57. Arbeit JM, Munger K, Howley PM, Hanahan D. Progressive squamous epithelial neoplasia in K14-human papillomavirus type 16 transgenic mice. *Journal of virology* 1994;68(7):4358-68.

58. Elson DA, Riley RR, Lacey A, Thordarson G, Talamantes FJ, Arbeit JM. Sensitivity of the cervical transformation zone to estrogen-induced squamous carcinogenesis. *Cancer research* 2000;60(5):1267-75.
59. Potter H. Transfection by electroporation. *Current protocols in molecular biology* / edited by Frederick M Ausubel [et al] 2003;Chapter 9:Unit 9 3.
60. Ohlfest JR, Demorest ZL, Motooka Y, Vengco I, Oh S, Chen E, et al. Combinatorial antiangiogenic gene therapy by nonviral gene transfer using the sleeping beauty transposon causes tumor regression and improves survival in mice bearing intracranial human glioblastoma. *Molecular therapy : the journal of the American Society of Gene Therapy* 2005;12(5):778-88.
61. Ivics Z, Izsvak Z. Transposons for gene therapy! *Current gene therapy* 2006;6(5):593-607.
62. Wiesner SM, Decker SA, Larson JD, Ericson K, Forster C, Gallardo JL, et al. De novo induction of genetically engineered brain tumors in mice using plasmid DNA. *Cancer research* 2009;69(2):431-9.
63. DiPaolo JA, Woodworth CD, Popescu NC, Notario V, Doniger J. Induction of human cervical squamous cell carcinoma by sequential transfection with human papillomavirus 16 DNA and viral Harvey ras. *Oncogene* 1989;4(4):395-9.
64. Schreiber K, Cannon RE, Karrison T, Beck-Engeser G, Huo D, Tennant RW, et al. Strong synergy between mutant ras and HPV16 E6/E7 in the development of primary tumors. *Oncogene* 2004;23(22):3972-9.
65. Rusan M, Li YY, Hammerman PS. Genomic landscape of human papillomavirus-associated cancers. *Clinical cancer research : an official journal of the American*

- Association for Cancer Research 2015;21(9):2009-19.
66. Amella CA, Lofgren LA, Ronn AM, Nouri M, Shikowitz MJ, Steinberg BM. Latent infection induced with cottontail rabbit papillomavirus. A model for human papillomavirus latency. *The American journal of pathology* 1994;144(6):1167-71.
 67. Borgogna C, Landini MM, Lanfredini S, Doorbar J, Bouwes Bavinck JN, Quint KD, et al. Characterization of skin lesions induced by skin-tropic alpha- and beta-papillomaviruses in a patient with epidermodysplasia verruciformis. *The British journal of dermatology* 2014;171(6):1550-4.
 68. Borgogna C, Lanfredini S, Peretti A, De Andrea M, Zavattaro E, Colombo E, et al. Improved detection reveals active beta-papillomavirus infection in skin lesions from kidney transplant recipients. *Modern pathology : an official journal of the United States and Canadian Academy of Pathology, Inc* 2014;27(8):1101-15.
 69. Christensen ND. Cottontail rabbit papillomavirus (CRPV) model system to test antiviral and immunotherapeutic strategies. *Antiviral chemistry & chemotherapy* 2005;16(6):355-62.
 70. Doorbar J. Model systems of human papillomavirus-associated disease. *The Journal of pathology* 2016;238(2):166-79.
 71. Iwasaki T, Maeda H, Kameyama Y, Moriyama M, Kanai S, Kurata T. Presence of a novel hamster oral papillomavirus in dysplastic lesions of hamster lingual mucosa induced by application of dimethylbenzanthracene and excisional wounding: molecular cloning and complete nucleotide sequence. *The Journal of general virology* 1997;78 (Pt 5):1087-93.
 72. Maeda H, Kubo K, Sugita Y, Miyamoto Y, Komatsu S, Takeuchi S, et al. DNA

- vaccine against hamster oral papillomavirus-associated oral cancer. *The Journal of international medical research* 2005;33(6):647-53.
73. Moore RA, Nicholls PK, Santos EB, Gough GW, Stanley MA. Absence of canine oral papillomavirus DNA following prophylactic L1 particle-mediated immunotherapeutic delivery vaccination. *The Journal of general virology* 2002;83(Pt 9):2299-301.
74. Nafz J, Kohler A, Ohnesorge M, Nindl I, Stockfleth E, Rosl F. Persistence of *Mastomys natalensis* papillomavirus in multiple organs identifies novel targets for infection. *The Journal of general virology* 2007;88(Pt 10):2670-8.
75. Quint KD, Genders RE, de Koning MN, Borgogna C, Gariglio M, Bouwes Bavinck JN, et al. Human Beta-papillomavirus infection and keratinocyte carcinomas. *The Journal of pathology* 2015;235(2):342-54.
76. Vinzon SE, Braspenning-Wesch I, Muller M, Geissler EK, Nindl I, Grone HJ, et al. Protective vaccination against papillomavirus-induced skin tumors under immunocompetent and immunosuppressive conditions: a preclinical study using a natural outbred animal model. *PLoS pathogens* 2014;10(2):e1003924.
77. Wilgenburg BJ, Budgeon LR, Lang CM, Griffith JW, Christensen ND. Characterization of immune responses during regression of rabbit oral papillomavirus infections. *Comparative medicine* 2005;55(5):431-9.
78. Lange CE, Favrot C. Canine papillomaviruses. *The Veterinary clinics of North America Small animal practice* 2011;41(6):1183-95.
79. Ljubojevic S, Skerlev M. HPV-associated diseases. *Clinics in dermatology* 2014;32(2):227-34.

80. Ghittoni R, Accardi R, Chiocca S, Tommasino M. Role of human papillomaviruses in carcinogenesis. *Ecancermedicalsecience* 2015;9:526.
81. Ostor AG. Natural history of cervical intraepithelial neoplasia: a critical review. *International journal of gynecological pathology : official journal of the International Society of Gynecological Pathologists* 1993;12(2):186-92.
82. Mehanna H, Beech T, Nicholson T, El-Hariry I, McConkey C, Paleri V, et al. Prevalence of human papillomavirus in oropharyngeal and nonoropharyngeal head and neck cancer--systematic review and meta-analysis of trends by time and region. *Head & neck* 2013;35(5):747-55.
83. Garbuglia AR. Human papillomavirus in head and neck cancer. *Cancers* 2014;6(3):1705-26.
84. Monk BJ, Sill MW, McMeekin DS, Cohn DE, Ramondetta LM, Boardman CH, et al. Phase III trial of four cisplatin-containing doublet combinations in stage IVB, recurrent, or persistent cervical carcinoma: a Gynecologic Oncology Group study. *Journal of clinical oncology : official journal of the American Society of Clinical Oncology* 2009;27(28):4649-55.
85. Lutz ST, Chow EL, Hartsell WF, Konski AA. A review of hypofractionated palliative radiotherapy. *Cancer* 2007;109(8):1462-70.
86. Tewari KS, Sill MW, Long HJ, 3rd, Penson RT, Huang H, Ramondetta LM, et al. Improved survival with bevacizumab in advanced cervical cancer. *The New England journal of medicine* 2014;370(8):734-43.
87. Williams R, Lee DW, Elzey BD, Anderson ME, Hostager BS, Lee JH. Preclinical models of HPV+ and HPV- HNSCC in mice: an immune clearance of HPV+

- HNSCC. *Head & neck* 2009;31(7):911-8.
88. Kimple RJ, Harari PM, Torres AD, Yang RZ, Soriano BJ, Yu M, et al. Development and characterization of HPV-positive and HPV-negative head and neck squamous cell carcinoma tumorgrafts. *Clinical cancer research : an official journal of the American Association for Cancer Research* 2013;19(4):855-64.
 89. Strati K, Pitot HC, Lambert PF. Identification of biomarkers that distinguish human papillomavirus (HPV)-positive versus HPV-negative head and neck cancers in a mouse model. *Proceedings of the National Academy of Sciences of the United States of America* 2006;103(38):14152-7.
 90. Herber R, Liem A, Pitot H, Lambert PF. Squamous epithelial hyperplasia and carcinoma in mice transgenic for the human papillomavirus type 16 E7 oncogene. *Journal of virology* 1996;70(3):1873-81.
 91. Zhong R, Pytynia M, Pelizzari C, Spiotto M. Bioluminescent imaging of HPV-positive oral tumor growth and its response to image-guided radiotherapy. *Cancer research* 2014;74(7):2073-81.
 92. Szymczak AL, Workman CJ, Wang Y, Vignali KM, Dilioglou S, Vanin EF, et al. Correction of multi-gene deficiency in vivo using a single 'self-cleaving' 2A peptide-based retroviral vector. *Nature biotechnology* 2004;22(5):589-94.
 93. Mates L, Chuah MK, Belay E, Jerchow B, Manoj N, Acosta-Sanchez A, et al. Molecular evolution of a novel hyperactive Sleeping Beauty transposase enables robust stable gene transfer in vertebrates. *Nature genetics* 2009;41(6):753-61.
 94. Kim JW, Hung CF, Juang J, He L, Kim TW, Armstrong DK, et al. Comparison of HPV DNA vaccines employing intracellular targeting strategies. *Gene therapy*

- 2004;11(12):1011-8.
95. Munger K, Werness BA, Dyson N, Phelps WC, Harlow E, Howley PM. Complex formation of human papillomavirus E7 proteins with the retinoblastoma tumor suppressor gene product. *The EMBO journal* 1989;8(13):4099-105.
 96. Jurk M, Vollmer J. Therapeutic applications of synthetic CpG oligodeoxynucleotides as TLR9 agonists for immune modulation. *BioDrugs : clinical immunotherapeutics, biopharmaceuticals and gene therapy* 2007;21(6):387-401.
 97. Thyagarajan B, Guimaraes MJ, Groth AC, Calos MP. Mammalian genomes contain active recombinase recognition sites. *Gene* 2000;244(1-2):47-54.
 98. Ivics Z, Hackett PB, Plasterk RH, Izsvak Z. Molecular reconstruction of Sleeping Beauty, a Tc1-like transposon from fish, and its transposition in human cells. *Cell* 1997;91(4):501-10.
 99. Carlson CM, Frandsen JL, Kirchhof N, McIvor RS, Largaespada DA. Somatic integration of an oncogene-harboring Sleeping Beauty transposon models liver tumor development in the mouse. *Proceedings of the National Academy of Sciences of the United States of America* 2005;102(47):17059-64.
 100. Kim D, Hung CF, Wu TC. Monitoring the trafficking of adoptively transferred antigen- specific CD8-positive T cells in vivo, using noninvasive luminescence imaging. *Hum Gene Ther* 2007;18(7):575-88.
 101. Dunn LA, Evander M, Tindle RW, Bulloch AL, de Kluyver RL, Fernando GJ, et al. Presentation of the HPV16E7 protein by skin grafts is insufficient to allow graft rejection in an E7-primed animal. *Virology* 1997;235(1):94-103.

102. Azoury-Ziadeh R, Herd K, Fernando GJ, Lambert P, Frazer IH, Tindle RW. Low level expression of human papillomavirus type 16 (HPV16) E6 in squamous epithelium does not elicit E6 specific B- or T-helper immunological responses, or influence the outcome of immunisation with E6 protein. *Virus Res* 2001;73(2):189-99.
103. Frazer IH, De Kluyver R, Leggatt GR, Guo HY, Dunn L, White O, et al. Tolerance or immunity to a tumor antigen expressed in somatic cells can be determined by systemic proinflammatory signals at the time of first antigen exposure. *J Immunol* 2001;167(11):6180-7.
104. Strickler HD, Burk RD, Fazzari M, Anastos K, Minkoff H, Massad LS, et al. Natural history and possible reactivation of human papillomavirus in human immunodeficiency virus-positive women. *J Natl Cancer Inst* 2005;97(8):577-86.
105. Engels EA, Pfeiffer RM, Goedert JJ, Virgo P, McNeel TS, Scoppa SM, et al. Trends in cancer risk among people with AIDS in the United States 1980-2002. *AIDS* 2006;20(12):1645-54.
106. Angeletti PC, Zhang L, Wood C. The viral etiology of AIDS-associated malignancies. *Adv Pharmacol* 2008;56:509-57.
107. Engels EA, Biggar RJ, Hall HI, Cross H, Crutchfield A, Finch JL, et al. Cancer risk in people infected with human immunodeficiency virus in the United States. *Int J Cancer* 2008;123(1):187-94.
108. Dempsey AF. Human papillomavirus: the usefulness of risk factors in determining who should get vaccinated. *Rev Obstet Gynecol* 2008;1(3):122-8.
109. Chaturvedi AK, Madeleine MM, Biggar RJ, Engels EA. Risk of human

- papillomavirus-associated cancers among persons with AIDS. *J Natl Cancer Inst* 2009;101(16):1120-30.
110. Gross ND, Hanna EY. The Role of Surgery in the Management of Recurrent Oropharyngeal Cancer. *Recent Results Cancer Res* 2017;206:197-205.
111. Peng S, Song L, Knoff J, Wang JW, Chang YN, Hannaman D, et al. Control of HPV-associated tumors by innovative therapeutic HPV DNA vaccine in the absence of CD4+ T cells. *Cell & bioscience* 2014;4(1):11.
112. Cancer Genome Atlas N. Comprehensive genomic characterization of head and neck squamous cell carcinomas. *Nature* 2015;517(7536):576-82.
113. Ang KK, Harris J, Wheeler R, Weber R, Rosenthal DI, Nguyen-Tan PF, et al. Human papillomavirus and survival of patients with oropharyngeal cancer. *The New England journal of medicine* 2010;363(1):24-35.
114. Stein AP, Saha S, Kraninger JL, Swick AD, Yu M, Lambert PF, et al. Prevalence of Human Papillomavirus in Oropharyngeal Cancer: A Systematic Review. *Cancer J* 2015;21(3):138-46.
115. Gillison ML, D'Souza G, Westra W, Sugar E, Xiao W, Begum S, et al. Distinct risk factor profiles for human papillomavirus type 16-positive and human papillomavirus type 16-negative head and neck cancers. *J Natl Cancer Inst* 2008;100(6):407-20.
116. Tang XH, Knudsen B, Bemis D, Tickoo S, Gudas LJ. Oral cavity and esophageal carcinogenesis modeled in carcinogen-treated mice. *Clin Cancer Res* 2004;10(1 Pt 1):301-13.
117. Kanojia D, Vaidya MM. 4-nitroquinoline-1-oxide induced experimental oral

- carcinogenesis. *Oral oncology* 2006;42(7):655-67.
118. Schoop RA, Noteborn MH, Baatenburg de Jong RJ. A mouse model for oral squamous cell carcinoma. *J Mol Histol* 2009;40(3):177-81.
 119. Li J, Liang F, Yu D, Qing H, Yang Y. Development of a 4-nitroquinoline-1-oxide model of lymph node metastasis in oral squamous cell carcinoma. *Oral Oncol* 2013;49(4):299-305.
 120. de Visscher SA, Witjes MJ, van der Vegt B, de Bruijn HS, van der Ploeg-van den Heuvel A, Amelink A, et al. Localization of liposomal mTHPC formulations within normal epithelium, dysplastic tissue, and carcinoma of oral epithelium in the 4NQO-carcinogenesis rat model. *Lasers Surg Med* 2013;45(10):668-78.
 121. Esquenazi D, Bussoloti Filho I, Carvalho Mda G, Barros FS. The frequency of human papillomavirus findings in normal oral mucosa of healthy people by PCR. *Brazilian journal of otorhinolaryngology* 2010;76(1):78-84.
 122. Syrjanen S, Lodi G, von Bultzingslowen I, Aliko A, Arduino P, Campisi G, et al. Human papillomaviruses in oral carcinoma and oral potentially malignant disorders: a systematic review. *Oral diseases* 2011;17 Suppl 1:58-72.
 123. Buitrago-Perez A, Hachimi M, Duenas M, Lloveras B, Santos A, Holguin A, et al. A humanized mouse model of HPV-associated pathology driven by E7 expression. *PloS one* 2012;7(7):e41743.
 124. Shin MK, Pitot HC, Lambert PF. Pocket proteins suppress head and neck cancer. *Cancer research* 2012;72(5):1280-9.
 125. Comprehensive genomic characterization of head and neck squamous cell carcinomas. *Nature* 2015;517(7536):576-82.

126. Seiwert TY, Zuo Z, Keck MK, Khattri A, Pedamallu CS, Stricker T, et al. Integrative and comparative genomic analysis of HPV-positive and HPV-negative head and neck squamous cell carcinomas. *Clinical cancer research : an official journal of the American Association for Cancer Research* 2015;21(3):632-41.
127. Parfenov M, Pedamallu CS, Gehlenborg N, Freeman SS, Danilova L, Bristow CA, et al. Characterization of HPV and host genome interactions in primary head and neck cancers. *Proceedings of the National Academy of Sciences of the United States of America* 2014;111(43):15544-9.
128. Akagi K, Li J, Broutian TR, Padilla-Nash H, Xiao W, Jiang B, et al. Genome-wide analysis of HPV integration in human cancers reveals recurrent, focal genomic instability. *Genome research* 2014;24(2):185-99.
129. Ojesina AI, Lichtenstein L, Freeman SS, Pedamallu CS, Imaz-Rosshandler I, Pugh TJ, et al. Landscape of genomic alterations in cervical carcinomas. *Nature* 2014;506(7488):371-5.
130. Fresno Vara JA, Casado E, de Castro J, Cejas P, Belda-Iniesta C, Gonzalez-Baron M. PI3K/Akt signalling pathway and cancer. *Cancer treatment reviews* 2004;30(2):193-204.
131. Hennessy BT, Smith DL, Ram PT, Lu Y, Mills GB. Exploiting the PI3K/AKT pathway for cancer drug discovery. *Nature reviews Drug discovery* 2005;4(12):988-1004.
132. Bellacosa A, Kumar CC, Di Cristofano A, Testa JR. Activation of AKT kinases in cancer: implications for therapeutic targeting. *Advances in cancer research* 2005;94:29-86.

133. Chang F, Lee JT, Navolanic PM, Steelman LS, Shelton JG, Blalock WL, et al. Involvement of PI3K/Akt pathway in cell cycle progression, apoptosis, and neoplastic transformation: a target for cancer chemotherapy. *Leukemia* 2003;17(3):590-603.
134. Bitting RL, Armstrong AJ. Targeting the PI3K/Akt/mTOR pathway in castration-resistant prostate cancer. *Endocrine-related cancer* 2013;20(3):R83-99.
135. Ma CX, Crowder RJ, Ellis MJ. Importance of PI3-kinase pathway in response/resistance to aromatase inhibitors. *Steroids* 2011;76(8):750-2.
136. Comprehensive molecular portraits of human breast tumours. *Nature* 2012;490(7418):61-70.
137. Danielsen SA, Eide PW, Nesbakken A, Guren T, Leithe E, Lothe RA. Portrait of the PI3K/AKT pathway in colorectal cancer. *Biochimica et biophysica acta* 2015;1855(1):104-21.
138. West KA, Castillo SS, Dennis PA. Activation of the PI3K/Akt pathway and chemotherapeutic resistance. *Drug resistance updates : reviews and commentaries in antimicrobial and anticancer chemotherapy* 2002;5(6):234-48.
139. Shukla S, Maclennan GT, Hartman DJ, Fu P, Resnick MI, Gupta S. Activation of PI3K-Akt signaling pathway promotes prostate cancer cell invasion. *International journal of cancer* 2007;121(7):1424-32.
140. Schmidt-Kittler O, Zhu J, Yang J, Liu G, Hendricks W, Lengauer C, et al. PI3Kalpha inhibitors that inhibit metastasis. *Oncotarget* 2010;1(5):339-48.
141. Treuting PM, Dintzis SM, Montine KS. Chapter 7. Oral Cavity and Teeth, Chapter 17. Female Reproductive system. *Comparative Anatomy and Histology:*

A Mouse and Human Atlas 2011:101.

142. Arbeit JM, Howley PM, Hanahan D. Chronic estrogen-induced cervical and vaginal squamous carcinogenesis in human papillomavirus type 16 transgenic mice. *Proceedings of the National Academy of Sciences of the United States of America* 1996;93(7):2930-5.
143. Chung SH, Wiedmeyer K, Shai A, Korach KS, Lambert PF. Requirement for estrogen receptor alpha in a mouse model for human papillomavirus-associated cervical cancer. *Cancer research* 2008;68(23):9928-34.
144. Crook T, Tidy JA, Vousden KH. Degradation of p53 can be targeted by HPV E6 sequences distinct from those required for p53 binding and trans-activation. *Cell* 1991;67(3):547-56.
145. Lipinski MM, Jacks T. The retinoblastoma gene family in differentiation and development. *Oncogene* 1999;18(55):7873-82.
146. Jones DL, Munger K. Interactions of the human papillomavirus E7 protein with cell cycle regulators. *Seminars in cancer biology* 1996;7(6):327-37.

BASIC INFORMATION

Name	Yi-Hsin Lin
Sex	Female
Birth Date	May/28/1979
Birth Place	Tainan, Taiwan
Citizenship	Taiwan
Addresses & Phone No.	
Permanent	4F-1, No.32, Ln. 450, Sec. 5, Cheng-gong Rd, Neihu Dist. Taipei City, 114, Taiwan +886-2-2631-3917
Current	123 Dumbarton Rd. Apt. B, Baltimore, MD, 21212 +1-443-240-3747

EDUCATION

2017	Ph.D.	Pathobiology Program Johns Hopkins University School of Medicine Mentor: T.-C. Wu, M.D., Ph.D.
2004	M.D.	National Defense Medical Center, Taipei, Taiwan

PROFESSIONAL EXPERIENCE

2011-2012	Clinical Fellow	Department of Obstetrics & Gynecology Kaohsiung Armed Forces General Hospital, Taiwan
2010-2011	Chief Resident	Department of Obstetrics & Gynecology Tri-Service General Hospital, Taipei, Taiwan
2006-2010	Resident	Department of Obstetrics & Gynecology Tri-Service General Hospital, Taipei, Taiwan
2004-2006	Military medicine	First Lieutenant Rank, Military Officer Aviation & Special Warfare Command, Taiwan
2002-2004	Clinical rotation	Internship Tri-Service General Hospital, Taipei, Taiwan

CERTIFICATIONS AND LICENCESURE

2010	OB/GYN Physician Certificate, Taiwanese Board of Obstetrics & Gynecology
2004	Certificate of Medical Doctor, Taiwan

PROFESSIONAL AFFILIATION

2010-present	The Taiwan Association of Obstetrics and Gynecology
2004-present	Taiwan Medical Association

ACADEMIC APPOINTMENT

2011-present	Lecturer of Medicine, National Defense Medical Center, Taipei, Taiwan
2010-2011	Assistant of Medicine, National Defense Medical Center, Taipei, Taiwan

RESEARCH EXPERIENCE

2014-2016 PhD Candidate, Laboratory of Dr. T.-C, Wu, Johns Hopkins Medicine
Thesis Project: generation of a spontaneous HPV 16 E6/E7 expressing pre-clinical tumor model for therapeutic intervention

PUBLICATIONS

1. **Yi-Hsin Lin**, Yu-Chi Yeh, Chii-Ruey Tzeng, Wei-Jen Shang, Jah-Yao Liu, Chi-Huang Chen. Evaluating the effects of immunosuppression by in-vivo bioluminescence imaging after allotransplantation of ovarian grafts. *Reprod Biomed Online*. 2011 Feb;22(2):220-7. Epub 2010 Oct 31.
2. **Yi-Hsin Lin**, Rui-Lan Huang, Hung-Cheng Lai. Presacral teratoma in a Curarrino syndrome woman with an unreported insertion in MNX1 gene. *Taiwan J Obstet Gynecol*. 2011 Dec;50(4):512-4.
3. **Yi-Hsin Lin**, Fung-Wei Chang, and Chi-Huang Chen. Perimenopausal Amenorrhea with Cervical Atresia and Hematotrachelos. *J Med Sci* 2010;30(4):173-176
4. Chao-Yi Wu, Li-Hua Yang, Huang-Yu Yang, Jayne Knoff, Shiwen Peng, **Yi-Hsin Lin**, Chenguang Wang, Ronald D. Alvarez, Sara I. Pai, Richard B.S. Roden, Chien-Fu Hung, T-C Wu. Enhanced Cancer Radiotherapy through Immunosuppressive Stromal Cell Destruction in Tumors. *Clin Cancer Res*. 2014 Feb 1;20(3):644-57.

POSTER PRESENTATION

1. **Yi-Hsin Lin**, Wei-Shi Chang, Mu-Hsien Yu, Jah-Yao Liu. Cesarean section wound hemorrhage and disruption due to chronic disseminated intravascular coagulation: A case report. 46th Annual Meeting of Taiwan Association of Obstetrics and Gynecology.

2. **Yi-Hsin Lin**, Tzai-Guang Jau, Gwo-Jang Wu, Mu-Hsien Yu. Breast cancer metastasized to uterine myoma mimicking a simple cystic degeneration, 48th Annual Meeting of Taiwan Association of Obstetrics and Gynecology.
3. **Yi-Hsin Lin**, Chi-Huang Chen, Gwo-Jang Wu, Jah-Yao Liu, Chii-Ruey Tzeng. In vivo bioluminescence imaging of ovarian transplantation. 49th Annual Meeting of Taiwan Association of Obstetrics and Gynecology.
4. **Yi-Hsin Lin**, Feng-Sheng Jin, Tzai-Guang Jau, Gwo-Jang Wu, and Fung-Wei Chang. Ruptured angular pregnancy with impending hypovolemic shock, 50th Annual Meeting of Taiwan Association of Obstetrics and Gynecology.
5. **Yi-Hsin Lin**, Tae Heung Kang, Chien-Fu Hung, T-C Wu. Immunogenic antigens facilitate tumor control after chemotherapy. JHSOM 9th Annual Pathobiology Graduate Program Retreat
6. **Yi-Hsin Lin**, Chien-Fu Hung, T-C Wu. Generation of a Spontaneous HPV-16 E6/E7 Expressing Preclinical Tumor Model for Therapeutic Intervention JHSOM 11th Annual Pathobiology Graduate Program Retreat
7. **Yi-Hsin Lin**, Feng-Woei Tsay, Rosie Jiang, Chien-Fu Hung, T-C Wu. Generation of a Spontaneous HPV-16 E6/E7 Expressing Preclinical Tumor Model for Therapeutic Intervention. 18th Annual Department of Pathology Young Investigator's Day

SCHOLARSHIP

2012-1016 Full Tuition Scholarship for Studying Abroad, Ministry of National Defense, Taiwan